MicroRNA-mediated silencing of bovine NANOG and MBD3

A thesis submitted in partial fulfilment

of the requirements for the degree

of

Masters of Science (Research) in Biological Sciences

at

The University of Waikato

by

Brooke Carol Wilson

The University of Waikato
2015

THE UNIVERSITY OF
WAIKATO
Te Whare Wānanga o Waikato

Abstract

Embryonic stem cells (ESCs) are pluripotent due to their ability to differentiate into any cell type of the body, including functional gametes. These cells are also capable of infinite self-renewal and are highly receptive to genetic modification. The use of ESCs as a reproductive tool offers an exciting platform for farmers to efficiently amplify or introduce desirable agricultural traits within their herd. Unfortunately, all attempts to derive naive pluripotent ESCs from livestock animals have been unsuccessful. This is most likely attributed to a poor understanding of pluripotency specification in these animals. Nanog and Mbd3 are two proteins which are intimately involved in early embryonic development and pluripotency in the mouse. However, their specific function in livestock animals remains unknown. The primary aim of this research project was to determine the feasibility of using a microRNA-mediated silencing approach to knockdown these two proteins in a bovine model.

Three candidate microRNAs, designed for each gene transcript, were cloned into the BLOCK-iT™ pcDNA™6.2-GW/EmGFP-miR expression plasmid. Before application in an *in vivo* system, each microRNA was transiently screened *in vitro* to determine its specificity and knockdown potential. For screening purposes, various attempts were made to generate a stable bovine NANOG expression fibroblast line using an inducible piggyBac transposon expression system. However, stable integration rates were lower than expected and all surviving and overexpressing cell clones eventually entered into a non-proliferate state of cellular senescence. The knockdown potential of the NANOG microRNAs was eventually determined by transient cotransfection with a constitutively active NANOG expression plasmid into a bovine embryonic fibroblast line. All three NANOG-specific microRNAs were able to efficiently knockdown NANOG protein expression. The highest knockdown efficiency was 89% as quantified by immunocytochemistry. By contrast, a MBD3 knockdown effect was not visible after transient expression of the MBD3-specific microRNAs, likely due to the longevity of the MBD3 protein which has a half-life of around 48 hours.

The practicality of the BLOCK-iT™ microRNA expression system for functional gene analysis relies on its ability to generate stable knockdown cell lines which could then be used as donor cells for somatic cell nuclear transfer cloning and production of bovine knockdown embryos. Despite the slow proliferative nature of the stable transfectants and their frequent failure to expand during selection, we have been able to eventually generate GFP-microRNA expressing stable knockdown cell clones, suggesting that this system is still a feasible option for investigating the biological functions of NANOG and MBD3 in cattle.

Acknowledgements

The completion of this thesis would not have been possible without the immense support, guidance, and mentoring I received from the incredible Reproductive Technologies team at AgResearch Ruakura.

A special thank you to my AgResearch supervisor, Dr Björn Oback. Thank you for your continuous support and assistance throughout the project. Your eternal optimism and passion for research has encouraged me to persevere numerous times through the many obstacles encountered on this project. I am incredibly grateful for the opportunity to work within your stem cell research team and I would especially like to thank you for helping to develop my scientific and analytical skills. I am honoured to have been your student.

I also offer my sincerest gratitude to my university supervisor, Dr Linda Peters. Thank you for your steadfast support and commitment to this project. I appreciate your attention to detail and constructive feedback when reviewing my thesis.

To my lab mentors, specifically Dr Stefan Wagner, Andria Green, Pavla Turner, and Jing Wei Wei, thank you for your patience, your wisdom, and your positivity. I appreciate the time, the kindness, and the encouragement you continuously gave to me. It was a pleasure to have learnt from you all.

To my fellow lab buddies, thank you for all your encouragement and support. You made this experience for me so much more enjoyable and I will always look back on this time with fond memories.

Special thanks must also be given to my amazing mother who housed me, feed me, and encouraged me when I had a bad day. I thank you for your unconditional love and support throughout this journey.

I would also like to thank the University of Waikato, AgResearch, and the Agricultural Fieldays Committee for their financial support of this thesis. Thank you for believing in me and in realising the benefits stem cell research will have for the agricultural industry.

Table of Contents

List of Figures

List of Tables and Equations

List of Abbreviations

(v/v)	Volume per volume
(w/v)	Weight per volume
A	Absorbance
AI	Artificial insemination
BEFs	Bovine embryonic fibroblasts
BLAST	Basic local alignment search tool
BLG	B-lactoglobulin
bp	Base pair
cDNA	Complementary DNA
CFFs	Caprine fetal fibroblasts
ChIP	Chromatin immunoprecipitation
CMV	Cytomegalovirus
COGIV	Cycling of gametes *in vitro*
CP	Crossing point
CRISPR	Clustered regulatory interspaced short palindromic repeat
DEPC	Diethylpyrocarbonate
DMSO	Dimethyl sulfoxide
dNTP	Deoxyribonucleotide triphosphate
DOX	Doxycycline
dsRNA	Double-stranded RNA
EGTA	Ethylene glycol tetraacetic acid
ESCs	Embryonic stem cells
FCS	Fetal calf serum
GFP	Green fluorescent protein
h	Hour
Hdac	Histone deacetylase
HR	Homologous recombination
ICM	Inner cell mass
iPSCs	Induced pluripotent stem cell
IRES	Internal ribosome entry site
ITR	Inverted terminal repeat
IVP	*In vitro* production
kb	kilobase

LB	Luria-Bertani
LIF	Leukaemia inhibitory factor
LTR	Long terminal repeat
MBD3	Methyl binding domain protein 3
MEFs	Murine embryonic fibroblasts
$MgCl_2$	Magnesium Chloride
miRNA	microRNA
mRNA	Messenger RNA
NTC	Negative template control
NuRD	Nucleosome remodelling and deacetylation
Oct4	Octamer-binding transcription factor 4
Oligos	Oligonucleotides
ORF	Open reading frame
PB	piggyBac
PBase	piggyBac transposase
PBS	Phosphate buffered saline
PCR	Polymerase chain reaction
PFA	Paraformaldehyde
PGCs	Primordial germ cells
PTC	Positive template control
qPCR	Quantitative polymerase chain reaction
RFP	Red fluorescent protein
RISC	RNA induced silencing complex
RNAi	RNA interference
rpm	Revolutions per minute
RT	Reverse transcriptase
rtTA	Reverse tetracycline transactivator
SCNT	Somatic cell nuclear transfer
shRNA	Small hairpin RNA
siRNA	Small interfering RNA
SNP	Single nucleotide polymorphism
Sox2	Sex determining region Y box 2
TRE	Tetracycline response element
UTR	Untranslated region
UV	Ultraviolet
WR	Tryptophan repeat
XIST	X-inactive specific transcript

Introduction

By 2050, the human population is expected to exceed 9 billion (FAO, 2009). To feed such a population will require a 50% increase in food production from what is currently being achieved (FAO, 2009). In addition to meeting these demands, farmers will also have to deal with an increasing social pressure on environmental sustainability as well as resource limitations as expanding metropolitan areas begin to envelop surrounding pastoral land. Improving animal productivity is thus an important and immediate objective for the pastoral industry, as well as a pressing priority for governments around the world.

For centuries, farmers have been selectively breeding animals based on high productivity characteristics (Phillips, 2010). However, owing to the long gestation time of ruminants (150 – 280 days) and a prior lack of genetic understanding, productivity selection based on phenotypic observations was painstakingly slow and often unreliable (Hernandes Gifford & Gifford, 2013). In the last few decades, a number of molecular reproductive technologies such as artificial insemination (AI), *in vitro* production of embryos (IVP) and somatic cell nuclear transfer (SCNT) cloning have radically improved the speed of trait selection and revolutionised animal breeding strategies.

Whilst research has been directed into improving upon these existing molecular reproductive technologies, alternative avenues for accelerated breeding are also currently being explored. The generation of embryonic stem cells (ESCs) from mice in 1981 was a ground-breaking discovery in the scientific and medical field (Martin, 1981, Evans & Kaufman, 1981). In the decades that have followed, there has been immense interest and effort in deriving analogous cells from other mammalian species. The concept of using livestock-derived ESCs as a reproductive tool for accelerated breeding is now beginning to gather support within the agricultural community and may just be the next ‘big thing’ in reproductive technologies.

ESCs are considered the unicellular equivalent to a whole animal and are derived from early preimplantation embryos (Oback & Huang, 2014). These cells have two important hallmarks; firstly, they have the ability to self-renew indefinitely without karyotypic change allowing them to continually proliferate in culture, and secondly, they are capable of differentiating into any cell type found in the adult animal including functional gametes – a phenomenon known as pluripotency (Blair et al., 2011). These cells are also highly receptive to homologous recombination (HR), enabling precise genetic modification of the genome (Capecchi, 2005). Because of these properties, ESCs have radically transformed our understanding of mammalian gene function and are considered molecularly and functionally one of the best-defined cell types (Oback & Huang, 2014).

From an animal breeding perspective, ESCs have the ability to shift the initial stages of reproduction from the field to the laboratory and, in doing so, enable precise generation of genetically elite livestock animals. Currently, the conventional method of animal selection is based on genotyping the offspring after they are born (Oback & Huang, 2014). Under this system, there is no guarantee that the offspring will have inherited the desired traits of the parents. However, it is now becoming possible to apply genomic selection prior to birth, when the IVP embryo is only one week old (Fisher et al., 2012). At this stage, around 10 – 15 cells from the outer layer, the trophectoderm, can be removed and used for genome-wide single nucleotide polymorphism (SNP) analysis. Because the embryo is particularly amenable to alterations in cell number, it is not destroyed in the process (Tarkowski & Wroblewska, 1967).

After confirmation that the embryo is of high genetic merit, the farmer may decide to transfer the embryo into a receptive female, and in 40% of cases, that embryo will develop to term (Wells et al., 2003). Alternatively the farmer could instead choose to amplify the desirable genotype of that embryo by extracting its pluripotent cell population and generate an ESC line. The stem cell line could then serve as a reservoir for high quality genetics and, under certain conditions, a select portion of those ESCs could be molecularly cued to differentiate into a variety of cell types, most importantly gametes (Fig. 1) (Murray et al., 2013). The generation of fully functional gametes from pluripotent stem cells is known as

cycling of gametes *in vitro* (COGIV) and a proof of principle study has already been achieved in mice (Hayashi et al., 2012). In essence, farmers would have the opportunity to produce as many high quality animals as required, replacing those within the herd of average productivity.

Aside from the reproductive advantages ESCs offer, these cells are also highly efficient cellular vectors for genetic engineering, enabling genes of agricultural or medical value to be inserted into, or removed from the genome with much more precision and ease (Buecker et al., 2010). Combining ESC technology with transgenics would allow for the introduction of traits to improve not only productivity in livestock animals but also reproduction, animal health and feed conversion (Laible, 2009). From a biomedical perspective, livestock ESCs would be particular useful for biopharming applications. For example, using cattle as bioreactors for large scale production of biopharmaceutical proteins (Oback & Huang, 2014). Most importantly, the establishment of livestock ESC lines would help satisfy basic research interests enabling researchers to explore gene function and physiology in a larger mammalian model (Muñoz et al., 2008).

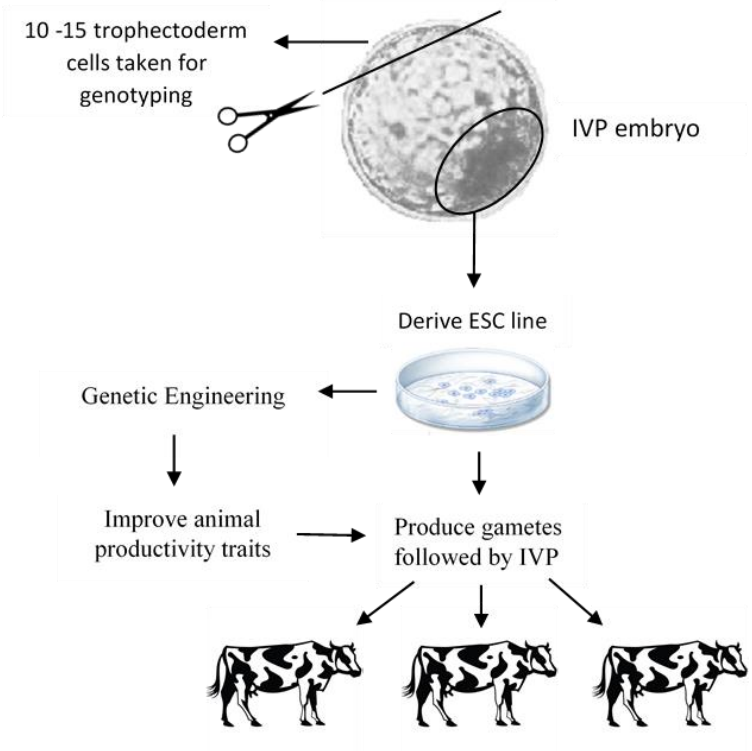

Fig. 1. Potential reproductive applications of livestock ESCs.

ESCs have the potential to revolutionise the pastoral industry and change the way farmers generate high-value farm animals. However, despite extensive research efforts, attempts to derive bona-fide ESCs in any mammal other than rodents has been unsuccessful. This is particularly surprising given that the basic course of embryonic development is highly conserved throughout mammalian species (Wolpert & Tickle, 2011). Derivation in domestic animals, such as cattle, is not without fruition and has yielded cells which resemble ESCs both in their morphology and molecular profile (Evans et al., 1990, Mitalipova et al., 2001). These ESC-like cells have also been reported in a number of other domestic species, including pigs (Li et al., 2003), goats (Keefer et al., 1996), sheep (Notarianni et al., 1991), and horses (Saito et al., 2002). However, unlike authentic ESCs, ESC-like cells from livestock animals lack the capacity for continual propagation and become senescent after several passages (Talbot & Blomberg, 2008). Furthermore, ESC-like cells are yet to fulfil the stringent requirements which functionally define naïve pluripotency, them being teratoma formation, contribution to chimeric embryos, in particular the germline, and tetraploid complementation (Oback & Huang, 2014).

Attempts to derive livestock ESCs have so far relied on what is known about embryonic development and pluripotency maintenance in mice. However, there are a number of important differences between mice and livestock animals with regard to early embryonic development and the timing of key events (Oback & Huang, 2014). Furthermore, the molecular mechanisms responsible for cell lineage segregation have also been found to subtly differ between species (Kirchhof et al., 2000, Kuijk et al., 2008). This could imply that the specification of the pluripotent cell population of the embryo is not evolutionary conserved and may explain why ESCs have failed to be captured in other animals. It seems that the mouse can no longer be used as a reliable model for ESC derivation in other mammals. Instead, it is imperative that more species-specific research is carried out to develop a better understanding of pluripotency regulation, specifically in livestock animals. This knowledge will likely assist in refining ESC derivation protocols and cell culture conditions which will hopefully eventuate in the establishment of authentic livestock ESC lines.

The aim of this this research project was to examine the function of two proteins, NANOG and MBD3, that have been implicated as playing vital roles in murine (mouse) embryonic development and pluripotency. Using cattle (*Bos taurus*) as a model organism, this research will provide the necessary cross-species comparison to validate whether these two proteins are also important for pluripotency regulation in livestock animals.

To appreciate the biological role of NANOG and MBD3, a brief overview of mammalian preimplantation development will firstly be provided in the literature review of this thesis followed by an explanation of how ESC are derived and maintained *in vitro*. The subsequent sections will then focus on what is already known about NANOG and MBD3 with regard to their biological functions in mice, highlighting any inconsistences or gaps within the literature that require further investigation. The technique of RNA interference will then be introduced including an explanation as to why it is the preferable method for functional gene analysis in livestock. The objectives of this research project will then be presented alongside an overview of the research strategy.

Chapter One: Literature Review

1.1 Preimplantation Development

In the mouse, fertilisation of an oocyte results in the formation of a single cell embryo, the zygote. Because the zygote has the capacity to give rise to the entire animal as well as all the supporting extraembryonic tissues it is said to possess totipotency (De Miguel et al., 2010). Approximately 36 hours after fertilisation, the zygote undergoes its first cleavage event where it divides in half to generate a 2-cell embryo (Cockburn & Rossant, 2010). From there, the embryo continues to undergo a series of divisions as it works its way along the oviduct towards the uterus. By the 8-cell stage, the embryo begins to compact into a tight ball of cells, known as the morula. As the morula grows in cell number, the first wave of lineage segregation commences, signalling the end of totipotency (Takaoka & Hamada, 2012). As the outer and inner cells of the embryo segregate, a blastocoel cavity develops and two separate cell populations become apparent; the trophectoderm and the inner cell mass (ICM). An embryo at this stage is referred to as a blastocyst and consists of around 100 cells (Cockburn & Rossant, 2010). During the blastocyst stage, a second lineage segregation event takes place within the ICM resulting in the formation of an apical layer of cells, the hypoblast, which overlay a solid sphere of cells known as the epiblast (Fig. 2) (Rossant & Tam, 2009).

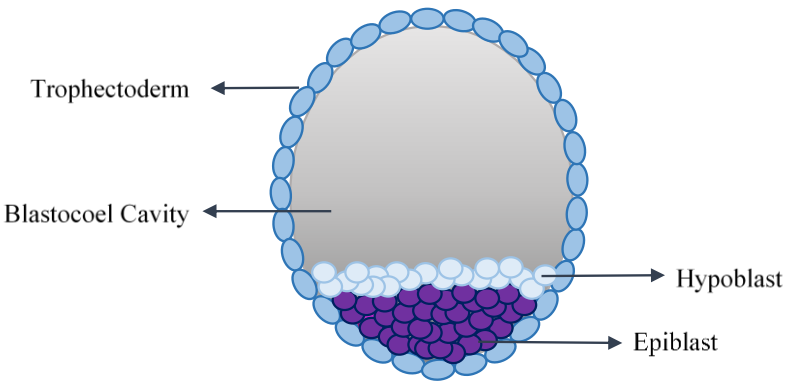

Fig. 2. Mammalian blastocyst after the second lineage segregation event. Three separate cell populations are apparent; the trophectoderm, hypoblast, and epiblast.

Of the three distinct cell populations now present within the blastocyst, only the epiblast will continue to develop the embryo. Although totipotency has been lost, the epiblast still possesses pluripotent cells. Following implantation, the epiblast will undergo gastrulation to generate the three embryonic germ layers (ectoderm, mesoderm, and endoderm) as well as the primordial germ cells (PGCs) (Oback & Huang, 2014). By contrast, the trophectoderm and hypoblast are not pluripotent and can only give rise to supporting extraembryonic tissues, such as the placenta and the yolk sac (Cockburn & Rossant, 2010).

Compared to the mouse, bovine (cattle) embryonic development generally follows the same chronological order of events, albeit at a slower pace. Because the gestation time of mice is only 20 days, development has to occur very quickly and as soon as the blastocyst has hatched from its zona pellucida casing, the murine embryo immediately begins to implant into the uterine wall (Rossant & Tam, 2009). By comparison, the cow which has a gestation time of 280 days, can have a much slower rate of embryonic development. Rather than implanting immediately after hatching, the bovine blastocyst instead elongates to form a long filamentous structure which allows it to efficiently exchange metabolites within the uterus (Blomberg et al., 2008). At the same time, gastrulation is also occurring – another important difference from the mouse development model. Only after the completion of gastrulation at around day 18-20 does the bovine embryo begin to attach, non-invasively, to the uterine wall (Vejlsted et al., 2006). This extended period of preimplantation development in cattle presents a significant challenge for ESC derivation and may offer an explanation as to why ESCs have not yet been captured in these animals.

1.2 ESC Derivation and Maintenance

Because of its pluripotent nature, the preimplantation epiblast tissue is the major derivation source for murine ESCs, although ESC lines have also been derived from morula stage embryos prior to lineage segregation (Eistetter, 1989, Strelchenko et al., 2004). To maintain murine ESCs *in vitro*, culture media is supplemented with the growth factors leukaemia inhibitory factor (LIF) and bone morphogenic protein (BMP4), which act via their respective signal transducers, STAT3 and SMAD proteins, to switch on a core set of pluripotency genes (Niwa

et al., 1998, Ying et al., 2003). Pluripotency promoting genes act to maintain the undifferentiated state by promoting self-renewal and inhibiting the expression of transcription factors which encourage differentiation (Boyer et al., 2005). In the mouse, three key transcription factors have emerged as being essential for early embryonic development and ESC identity and thus are considered the core regulators of the transcriptional pluripotency network (Nichols et al., 1998, Niwa et al., 2000, Mitsui et al., 2003, Chambers et al., 2003, Avillion et al., 2003, Masui et al., 2007, Kopp et al., 2008). They are Oct4, Sox2, and Nanog.

Unlike Oct4 and Sox2, Nanog expression within the embryo is exclusively confined to the epiblast, making it an ideal diagnostic marker for naïve pluripotency (Silva et al., 2009). In the mouse, the ideal time for deriving naïve ESCs is between days 3.5 and 4.5 when the expression of Nanog is high (Czechanski et al., 2014). Upregulation of Nanog during this time has been found to result in the reactivation of the paternal X chromosome within female epiblast cells (Silva et al., 2009). This reactivation event is critical for obtaining ground-state pluripotency and for allowing randomisation of the subsequent X chromosome inactivation event within the embryo proper (Silva et al., 2009). As such, high expression levels of Nanog, along with the presence of two active X chromosomes has become the most discriminatory marker for the naïve pluripotent state (Silva & Smith, 2008).

The analogous time point for deriving naïve pluripotent stem cells from bovine embryos is still yet to be determined. Preliminary research has shown that NANOG expression is significantly upregulated between day 7 and day 8 of bovine embryonic development. Whereas expression of *XIST*, the non-coding RNA molecule responsible for silencing the X chromosome (Ng et al., 2007), is concomitantly downregulated (AgResearch, unpublished data). These initial findings suggest that the transient naïve pluripotent cell population, capable of giving rise to authentic ESCs, may be present within the day 8 bovine blastocyst. However, a greater appreciation of NANOG's role in bovine embryonic development is still required. Results from such research will determine whether NANOG can also be used as a diagnostic marker for naïve pluripotency in

livestock which will likely assist in the ultimate goal of establishing authentic ESC lines for these animals.

1.3 The Naïve Pluripotency Marker, Nanog

Nanog is a unique homeodomain containing protein that was initially discovered during a polymerase chain reaction (PCR) screen of a murine ESC complementary DNA (cDNA) library (Wang et al., 2003). Subsequently, two separate research groups also identified the same gene via different methods, and renamed it Nanog, after the mythical Celtic land of the ever young, Tir Na Nog (Mitsui et al., 2003, Chambers et al., 2003). Functionally, both groups were able to show that among the different factors tested, Nanog was the only factor capable of maintaining the pluripotency of murine ESCs in culture devoid of LIF.

Structurally, Nanog is composed of three domains: an N-terminal domain, a homeodomain, and a C-terminal domain (Fig. 3) (Pan & Thomson, 2007). The C-terminal domain, which contains a well-conserved ten pentapeptide tryptophan repeat series, possesses the highest level of transcriptional activity (Pan & Pei, 2003, Oh et al., 2005). With regard to Nanog's unique homeodomain, there is very low sequence identity between mammalian, avian, and teleost orthologs. However, all of the different Nanog orthologs were still capable of regulating mouse Nanog target genes (Theunissen et al., 2011). Upon further analysis, it was discovered that this conserved function was attributable to just two adjacent amino acids within the DNA recognition helix of the homeodomain, tyrosine (Y) 42 and lysine (K) 43.

Fig. 3. Schematic showing the domain structure of Nanog. ND, N-terminal domain. HD, homeodomain. CD1, C-terminal domain 1. WR, trypotophan repeat series. CD2, C-terminal domain 2 (Adapted from Theunissen et al., 2011).

In mice, Nanog protein expression is first detected within the inner cells of the compacted morula and is restricted to the nucleus (Hatano et al., 2005). By the blastocyst stage, Nanog is exclusive to the ICM and is no longer detectable within the trophectoderm. As the blastocyst matures, Nanog expression becomes further confined to the epiblast and is subsequently absent from the hypoblast. Interestingly, numerous groups have reported a heterogeneous expression pattern of Nanog within epiblast cells, or their derived ESCs, with some cells having a higher expression level of Nanog than others (Singh et al., 2007, Toyooka et al., 2008, Abranches et al., 2014). Initially, researchers suspected that the high expressing Nanog cells may represent a distinct population of pluripotent cells. However, further evidence revealed that the heterogeneous expression observed was both reversible and stochastic in nature (Abranches et al., 2014). Consistent with a role in pluripotency, Nanog is subsequently downregulated following implantation but remains detectable within the primordial germ cells (PGCs). Additionally, the abundance of Nanog within ESCs is also rapidly downregulated upon differentiation with no protein detectable within differentiated cells.

1.3.1 Modulation of Nanog in Embryos and ESCs

Nanog's role in embryonic development and in stabilising ESC pluripotency has been investigated by a number of different research groups. In mice, *Nanog* knockout embryos (*Nanog*$^{-/-}$) were found to contain highly disorganised extraembryonic tissues and did not develop beyond implantation (Mitsui et al., 2003). These embryos lacked a functional epiblast cell population suggesting that Nanog is specifically required to demarcate and maintain the pluripotent epiblast. Interestingly, the hypoblast also failed to form within the mutant embryos which would suggest Nanog plays an additional role in potentiating the specification of the hypoblast. By contrast, mice heterozygous for *Nanog* (*Nanog*$^{+/-}$) were normal in gross appearance and were fertile. Because of the mutant epiblast, the researchers were unable to derive an ESC line from the *Nanog*$^{-/-}$ embryo. However, they were able to engineer *Nanog*$^{-/-}$ ESCs *in vitro* via gene targeting, but these cell quickly differentiated into extraembryonic endoderm.

A series of subsequent studies have further confirmed that a reduction in Nanog expression increases a cells propensity to differentiate (Chambers et al., 2007,

Hatano et al., 2005, Ivanova et al., 2006). *Nanog*$^{+/-}$ ESCs, which produce half the amount of Nanog compared with wild type ESCs, were found to readily differentiate into a variety of embryonic lineages including mesoderm, endoderm, and ectoderm (Hatano et al., 2005). Moreover, when exogenous Nanog was added to the *Nanog*$^{+/-}$ ESC cultures, the undifferentiated pluripotent state was successfully restored.

In contrast to earlier knockout studies (Mitsui et al., 2003, Hatano et al., 2005), Chambers et al. reported that *Nanog*$^{-/-}$ ESCs were still capable of infinite self-renewal despite being more prone to differentiation (Chambers et al., 2007). This would suggest that a reduction in Nanog does not strictly commit ESCs to differentiate. Furthermore, even though the *Nanog*$^{-/-}$ ESC colonies exhibited slower proliferation and contained prominent cytoplasmic protrusions, these cells were still capable of forming teratomas when transplanted under the mouse kidney capsule. The group also discovered a novel function of Nanog in PGC development as PGCs failed to mature upon reaching the genital ridge in Nanog$^{-/-}$ embryos. This would suggest that Nanog is specifically required to switch on the germ cell developmental program.

Culturing ESCs in the presence of retinoic acid can cause cells to differentiate. However, the differentiating effect of retinoic acid was found to be overcome by overexpression of Nanog (Loh et al., 2006). Based on this observation and the results of their own knockout studies, Chambers et al. have proposed a basic model explaining how Nanog acts to specify and maintain pluripotency (Fig. 4). The fluctuation of Nanog expression allows pluripotent stem cells to exist into two separate states. When Nanog expression is high, the cell is in a pristine naïve state of pluripotency and is unresponsive to differentiation cues. That same cell can then enter into a transient state of low Nanog expression where it exists in a 'primed' state of pluripotency. This low Nanog state provides the cell with the opportunity to respond to any intrinsic or extrinsic differentiation signals, also known as 'lineage priming'. However, this primed state of pluripotency is reversible and subsequent reversion to high Nanog levels brings the cell back to naïve pluripotency. When Nanog is completely absent, cell reversion is no longer possible but the cell can still self-renew assuming pluripotent promoting

conditions are maintained. By contrast, if Nanog is overexpressed, the low Nanog transitional state does not exist and the cells do not have the opportunity to respond to differentiation signals and thus exist in a continuous state of self-renewal.

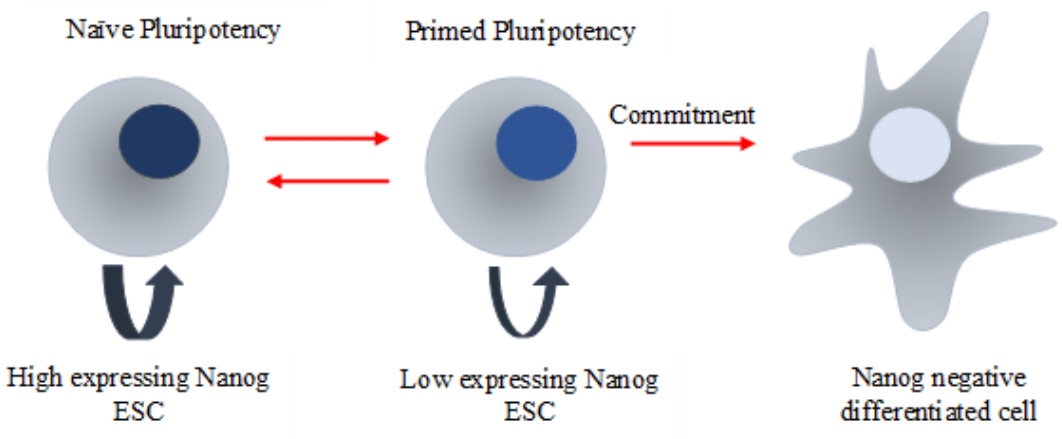

Fig. 4. Chambers et al. model of how Nanog acts to specify and maintain pluripotency. This model shows how Nanog expression levels dictate a cell's differentiation and self-renewal status. Curved arrows represent the potential for self-renewal (Adapted from Chambers et al., 2007)

Exactly how Nanog functions to regulate the pluripotent state is still under investigation. The combined use of chromatin immunoprecipitation (ChIP) and microarrays have been particularly helpful in unravelling the various gene targets of Nanog (Boyer et al., 2005, Loh et al., 2006). In mouse ESCs, Nanog was found to bind to 3006 different regions of DNA (Loh et al., 2006). Subsequent modulation of Nanog levels together with microarray expression profiling revealed that the major downstream targets activated by Nanog were associated with pluripotency and self-renewal processes (e.g. *Oct4, Sox2, FoxD3*). The majority of genes downregulated by Nanog were affiliated with lineage commitment, in particular transcription factors which induce differentiation into the three primary germ lineages (e.g. *Hoxb1, Pax6, Lhy5*).

Currently, it is still unclear how Nanog binding can activate some promoters whilst repress others, but it is likely additional co-factors are involved (Boyer et al., 2005). Indeed, Nanog binding has been found to facilitate the cooperative binding of additional pluripotency factors to the same target. For example, Nanog

binding to the *Xist* promoter results in exposure of the Oct4 and Sox2 binding motifs, allowing them to subsequently bind and act together to repress transcription (Navarro & Avner, 2009).

In comparison to murine Nanog, characterisation of bovine NANOG is still in its infancy. However, preliminary research does suggest that NANOG expression in cattle closely resembles that of the mouse model. On the mRNA level, *NANOG* was found to be restricted to the ICM in day 7 and day 8 bovine blastocysts (Harris et al., 2013, McLean et al., 2014). Similarly, the NANOG protein was found to be expressed initially within a few cells of the ICM before becoming restricted to the epiblast in day 8 blastocysts (Kuijk et al., 2012). By contrast, expression of NANOG in porcine (pig) embryos was not detectable until day 10 (Alberio et al., 2010) suggesting that subtle differences do exist even within livestock animals.

1.4 Mbd3 and the NuRD Complex

Whilst a lot of research has focused on the transcriptional network of pluripotency, considerably less attention has been paid to the epigenetic regulation of these factors. However, one epigenetic protein that has recently been making headlines in the stem cell community because of its influential role in lineage commitment and pluripotency is the methyl binding domain protein 3 (Mbd3). Not only has this protein been found to be essential for early embryonic development, it also seems to be intimately involved in the efficiency of induced pluripotent stem cell generation. The following section will summarise what is known about Mbd3 with regard to its structure and function in mice. A brief overview of induced pluripotent stem cells will then be provided highlighting the controversy as to Mbd3's involvement.

Mbd3 is an essential scaffold protein for the epigenetic repressor complex NuRD (nucleosome remodelling and histone deacetylation). Without Mbd3, the NuRD complex fails to assemble, resulting in embryonic lethality (Kaji et al., 2006). Mbd3 expression is strictly nuclear and is initially downregulated during embryo cleavage, but reappears at the morula stage where it continues to be expressed ubiquitously in all somatic tissues (Kaji et al., 2007). Mbd3 is part of a small

family of nuclear proteins, all of which contain a methyl-CpG binding domain. However, unlike other MBD proteins, Mbd3 does not bind directly to methylated DNA (Menafra & Stunnenberg, 2014).

NuRD is an abundant co-repressor complex that is broadly conserved throughout the animal kingdom (McDonel et al., 2008). Structurally, NuRD is composed of six core subunits, two of which possess enzymatic activity (Fig. 5). The Hdac1/2 subunit functions as a histone deacetylase while the Mi-2β subunit is involved in chromatin remodelling. Within the NuRD complex, Mbd3 is sometimes replaced by its related protein Mbd2. Mbd2, however, is not essential for embryonic development and is far less abundant (Hendrich et al., 2001)

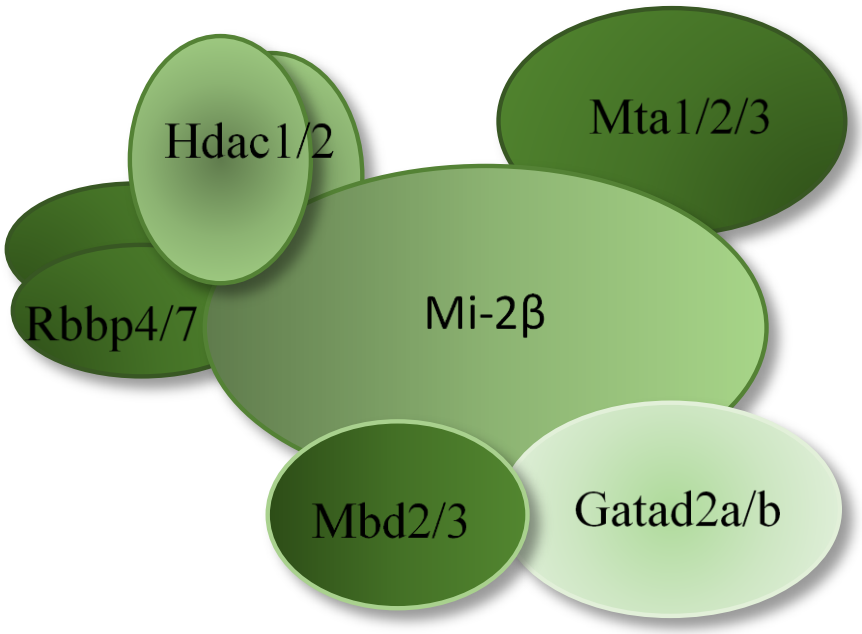

Fig. 5. Structure of the nucleosome remodelling and deacetylation (NuRD) complex. The NuRD complex is composed of six core subunits. The principle subunit is the Mi-2β chromatin remodelling subunit, which is complexed with a metastasis-associated protein (Mta1, Mta2 or Mta3) and a methyl binding domain protein (Mbd2 or Mbd3). NuRD also contains a histone deacetylase (Hdac) complex which consists of Hdac1, Hdac2, and retinoblastoma binding proteins (Rbbp) 4 and 7. Gata2a and Gata2b are also commonly detected in NuRD purifications. (Adapted from McDonel et al., 2008)

1.4.1 Function of the NuRD Complex

Any major change in gene expression, such as the switch between a pluripotent state and differentiated state, requires extensive epigenetic alterations (Liang & Zhang, 2013). In ESCs, the chromatin is largely in an open transcriptional state (euchromatin) which is what gives these cells their wide differentiation potential. In contrast, somatic cells which have already committed to a specific lineage, have much more condensed chromatin (heterochromatin) (Meshorer & Misteli, 2006).

The ATP-dependent chromatin remodelling complex NuRD is capable of regulating local changes in chromatin and therefore plays an important role in cell fate changes. Specifically, it functions as a transcriptional repressor, binding to methylated DNA sequences and mediating heterochromatin formation through histone modification (Luo et al., 2013).

Histones are nuclear proteins which wrap around DNA and package it into chromatin (Gelato & Fischle, 2008). Histones have a covalently modifiable N-terminal tail which can incur nine different post-translational modifications, most commonly, acetylation, methylation, and phosphorylation (Vinci, 2011). These modifications influence chromatin condensation and consequently DNA accessibility to transcription factors and DNA binding proteins. Histone acetylation on lysine residues is generally associated with transcriptional activation due to the acetyl groups' ability to neutralise the positively charged histones (Vinci, 2011). Consequently, the electrostatic bonding between histones and DNA is reduced and the chromatin can open up allowing transcription factors to gain access to their target sites.

The function of the histone deacetylase subunit of the NuRD complex, is to remove the acetyl groups from the histone proteins, and in doing so, return the chromatin back to a closed heterochromatin state. To gain access to the histone tail, the NuRD complex first has to remodel the chromatin, which is carried out by the Mi-2β subunit. The NuRD complex thus acts as a cohesive unit in repressing transcription, and is also known to cooperate with a number of additional repressor complexes (Reynolds et al., 2012b).

1.4.2 Modulation of Mbd3 in Embryos and ESCs

In murine embryos, Mbd3 was found to play a prominent role in regulating cell lineage specification (Kaji et al., 2007). By day 4.5, *Mbd3*$^{-/-}$ embryos morphologically resemble their wild-type counterparts, with clearly segregated trophectoderm, epiblast, and hypoblast tissue. However, following implantation, *Mbd3*$^{-/-}$ ICM cells fail to expand into late epiblast and continue to express the hypoblast marker, Gata4. Various other embryonic lineages, such as the extraembryonic ectoderm, and visceral endoderm, also fail to develop appropriately resulting in embryo death. Evidently, no ESC lines were derived from *Mbd3*$^{-/-}$ embryos suggesting Mbd3 is important for the proliferation of epiblast cells *in vitro*. However, *Mbd3*$^{-/-}$ ESCs could be generated by gene targeting, suggesting Mbd3 is not required for ESCs to self-renew. Genetic analysis of the mutant ICMs discovered several lineage-specific markers were significantly altered. Notably, Mbd3 deficiency resulted in the upregulation of germ cell markers, *Sohlh2* and *Daz1*, and a down regulation of the early embryonic *Pramel* gene family, whose exact function is still unknown (Kaji et al., 2007).

In vitro, *Mbd3*$^{-/-}$ ESCs were found to express higher levels of certain pluripotency genes. Interestingly, the core pluripotency factors, *Oct4*, *Sox2*, and *Nanog* were not affected (Kaji et al., 2006, Reynolds et al., 2012a). Upon LIF withdrawal, Mbd3 deficient ESCs fail to commit to differentiation and remain in a state of self-renewal (Reynolds et al., 2012a). However, subsequent treatment with retinoic acid did lead to cell differentiation suggesting Mbd3 does not completely prevent differentiation. It is likely that in the absence of Mbd3, expression of self-renewal factors can continue without inhibition by the NuRD complex. Therefore, when LIF is removed, which normally results in a loss of self-renewal, the higher expression of pluripotent genes allows Mbd3 deficient ESCs to retain their pluripotent state and continue to self-renew.

1.4.3 Mbd3's Role in Induced Pluripotent Stem Cell Generation

Less than a decade ago, the stem cell community was elated after it was discovered that differentiated somatic cells could be fully reprogrammed back to a stable pluripotent state (Takahashi & Yamanaka, 2006). Previously, this had only

been achieved by fusing somatic cells with pre-existing pluripotent cells (Tada et al., 2001, Cowan et al., 2005). In a ground-breaking study, Takahashi and Yamanaka analysed 24 candidate genes they suspected were capable of inducing pluripotency in somatic cells. By screening the individual candidates one by one, or in combination, they discovered that a quartet of factors, when retrovirally transduced into mouse embryonic fibroblasts (MEFs), were capable of generating what they refer to as induced pluripotent stem cells (iPSCs). These four factors were Oct4, Sox2, Klf4, and c-Myc, more commonly referred to as the OSKM factors. In recognition of his contribution to the scientific community, Yamanaka received the 2012 Nobel Prize in physiology or medicine.

Compared to ESCs, iPSCs have a remarkably similar gene expression profile, chromatin configuration, and likewise possess two active X chromosomes. In addition to inducing teratoma formation and generating germline competent chimeras (Takahashi & Yamanaka, 2006), iPSCs were also able to pass the most stringent assay for naïve pluripotency, that is, the generation of an embryo entirely derived from iPSCs (Boland et al., 2009, Zhao et al., 2009).

To generate iPSCs the differentiated cell must pass through two distinct phases of molecular reprogramming (Apostolou & Hochedlinger, 2013). Firstly, the somatic cell must switch off its current lineage-specific gene expression program, shedding its former cellular identity, resulting in the generation of a partially reprogrammed dedifferentiated pre-iPSC intermediate. To complete the reprogramming process, the cell then has to switch on its endogenous pluripotent gene network allowing it enter into a self-sustaining naïve pluripotent state. The OSKM factors are fundamental for initiating the first gene expression change. However, once the cell has dedifferentiated, and the endogenous pluripotency network activated, the cells no longer need to rely on the exogenous reprogramming factors which consequently become silenced (Takahashi & Yamanaka, 2006).

Unfortunately, the reprogramming process is very inefficient with anywhere between 0.1 and 10% of transfected cells successfully reprogramming to full pluripotency. The arrival at full pluripotency is typically determined by the

number of iPSC colonies formed that are positive for authentic pluripotency markers (e.g. Oct4 or Nanog). The stochastic nature of reprogramming is also a problem as cells proceed at different rates making the entire reprogramming process very difficult to monitor. Consequently, considerable research has been directed towards improving the efficiency of molecular reprogramming (De Miguel et al., 2010).

Recently, Abad et al., successfully generated a secondary expression system in which the *OSKM* transgenes were already stably integrated within the mouse's genome and could be switched on in an inducible manner (Abad et al., 2013). Administration of the antibiotic doxycycline was sufficient in activating ubiquitous expression of the transgenes. As expected, expression of *OSKM* throughout the animal resulted in the formation of multiple teratomas – a sign that reprogramming can occur *in situ*. The researchers then proceeded to isolate and characterize iPSCs from the bloodstream of the transgenic mice, which they found had a higher differentiation potential than *in vitro* produced iPSCs, capable of contributing to both embryonic and extraembryonic tissues in chimeras.

Using a similar secondary reprogramming system, a separate group set off to discover which molecular factors were responsible for blocking the efficient generation of iPSCs (Rais et al., 2013). Given that pluripotent cells possess relatively open chromatin (Meshorer & Misteli, 2006), and the recent finding that depletion of epigenetic repressors can improve reprogramming efficiencies (Luo et al., 2013), Dr Jacob Hanna and colleagues carried out a loss-of-function screen in mice to identify which candidate repressor complexes were hindering the reprogramming process. Remarkably, they found that inhibition of a single repressor protein, Mbd3, in embryonic fibroblasts led to an almost 100% reprogramming efficiency, compared to only 20% in wild-type cells. Moreover, reprogramming was synchronised and complete within one week of OSKM induction and *Mbd3* genetic depletion. The pluripotent potential of the *Mbd3*$^{-/-}$ iPSCs was validated by successful teratoma formation and generation of chimeric mice. On further analysis, Mbd3 was found to inhibit only the initial stage of reprogramming by binding, and presumably repressing, the OSKM factors. The authors describe the generation of iPSCs in the presence of Mbd3 like "driving a

car with the handbrake on." However, depleting cells of Mbd3 releases the brake and allows the cells to complete their reprogramming and arrive smoothly at their pluripotent destination.

The findings presented by Hanna's group have now been challenged by a separate research group led by Dr José Silva, who just recently published results which suggest that Mbd3 plays a facilitative role in molecular reprogramming (Dos Santos et al,, 2014). Using neural stem (NS) cells, the group generated a variety of *Mbd3* modulated cells lines, including a homozygous null line (*Mbd3*$^{-/-}$), a heterozygous line (*Mbd3*$^{fl/-}$) and a rescue cell line containing a *Mbd3* transgene (*Mbd3*$^{-/-:Mbd3}$). Because NS cells already express *Sox2*, the cell lines were transduced retrovirally with the remaining factors, *Oct4*, *Klf4*, and *c-Myc* to generate iPSCs. Coincidently, they discovered that *Mbd3* null cells produced fewer iPSC colonies than wild-type or rescue lines.

The apparent disagreement between these two studies is a major cause for concern. Differences in results could stem from the different reprogramming systems used to generate iPSCs, i.e. secondary system vs. retroviral induction. Furthermore, as the groups chose to focus on different cell types, any direct comparisons are difficult. It might be that Mbd3 simply behaves differently in a stem cell line (i.e. NS cells) as opposed to a somatic cell line (i.e. MEFs). Further research is clearly still required to determine the precise function of Mbd3 in molecular reprogramming and thus establish whether it plays an inhibitory or facilitative role in iPSC generation. If the removal of Mbd3 is indeed sufficient to overcome the reprogramming block in iPSCs, one would assume it plays a similar role *in vivo* (i.e. embryonic development). Therefore, it is theorised that removing Mbd3 during early embryonic development may prevent differentiation of the epiblast, maintaining the naïve pluripotent cell population for longer, and increasing the likelihood of deriving authentic pluripotent ESCs.

1.5 Research Rationale

ESC derivation has so far proven non-permissive for livestock animals, which may in part be due to a limited understanding of pluripotency specification in these animals. The core pluripotency factor Nanog, has been shown to play a

dominant role in orchestrating the pluripotency network alongside additional core factors, Oct4 and Sox2 in the mouse. Importantly, unlike Oct4 and Sox2, Nanog expression within the embryo is solely restricted to the epiblast, the population of cells from which naïve pluripotent cells can be derived. As such, the expression of Nanog within the early embryo is considered to be a key discriminatory marker of naïve pluripotency.

The function of NANOG in livestock animals, such as the cow, is still yet to be determined. At present, current livestock ESC derivation protocols are strongly based on what is known about pluripotency specification in rodents. However, development of the preimplantation embryo differs significantly between these two groups of animals particularly with regards to timing of key embryonic events. Therefore, it can be assumed that the specification and regulation of the transcriptional pluripotency network may also indeed differ between these animals. To validate NANOG as a core pluripotency factor in cattle, it's functionality in bovine embryos needs to be investigated.

Similarly, the epigenetic protein, MBD3, has yet to be studied in any livestock species. The discovery made by Hanna's team that removing Mbd3 can lead to synchronised and highly efficient conversion of MEFs to iPSCs is a dramatic new development for the iPSC community. However, contradictory evidence presented by Silva's team, who claim Mbd3 is required for efficient molecular reprogramming, has now called the protein's function into question. The murine embryo data does support a role of Mbd3/NuRD in developmental transitions suggesting that Mbd3 is an influential embryonic protein, particularly in regulating cell fate decisions. Because of its controversial role in molecular reprogramming and its necessity for embryonic development in mice, its function in cattle warrants particular attention.

1.6 Functional Study Approaches

Functional studies are often used to determine the precise molecular function of a gene in a given context. Although it might seem rather counterintuitive, one of the best ways of figuring out what a gene does is to monitor what happens when it is removed from an organism (Alberts et al., 2002). This approach is known as a

reverse genetic approach and typically involves the generation of knockout animals in which the protein-coding regions of a gene are mutated or deleted entirely such that it becomes inoperant (Laible & Alonso-González, 2009).

Gene knockouts rely on the natural phenomenon of homologous recombination (HR) in which similar regions of DNA can crossover when paired up next to each other. Taking advantage of this system, targeting vectors can be engineered to contain a mutated sequence of a target gene flanked by two stretches of homologous sequence. Consequently, when this vector is introduced into a cell it can undergo HR with the endogenous target sequence removing the functional copy of the gene.

In contrast to ESCs, the frequency of HR in primary somatic cells is very low. As such, the efficiency of gene knockout in farm animals, which do not yet have any established ESC lines, is also very low. Moreover, because of their long gestation time and small number of offspring, gene knockout in livestock animals is not a practical approach for investigating gene function. An alternative and simpler method, is to instead reduce the expression level of a gene via a technique known as RNA interference (RNAi).

1.6.1 RNA Interference

RNAi is a widespread natural phenomenon that has become a powerful new research tool for understanding gene function (Novena & Sharp, 2004). As its name suggests, RNAi involves the use of small double stranded RNA (dsRNA) molecules. Despite their small size, these dsRNA molecules can significantly knockdown the expression of a particular gene by simply preventing translation of complementary messenger RNA (mRNA) transcripts (Hammond, 2005). In nature, RNAi is commonly employed to combat viral infections, particularly in small eukaryotic organisms (Buchon & Vaury, 2006). RNAi is also involved in fine tuning gene expression for many important cell processes, such as cell growth and differentiation (Wilson & Dounda, 2013).

Like most phenomena in science, RNAi was initially stumbled upon by accident by several plant biologists in 1990 (Napoli et al., 1990, van der Krol et al., 1990).

In an attempt to deepen the purple colour of petunias, the researchers decided to introduce multiple copies of a transgene responsible for purple flower pigmentation. However, rather unexpectedly, the transgene did not give rise to darker purple flowers, but instead resulted in plants with white or patchy flowers. Unsure what to make of this peculiar observation, they hypothesised that the transgene must have somehow switched off both itself as well as the endogenous pigmentation gene. Subsequently, it was later discovered that multiple copy transgenes are capable of producing small amounts of dsRNA.

To confirm whether dsRNA was responsible for the dramatic gene knockdown observed by the plant biologists, two molecular scientists started researching the effect of dsRNA on nematodes. In a Nobel Prize winning experiment, Fire and Mello were able to show that injection of dsRNA molecules into *Caenorhabditis elegans* led to potent silencing of complementary gene transcripts (Fire et al., 1998). Not long after, numerous other researchers began reporting the occurrence of dsRNA-induced silencing in various other plants and animals and it was soon realised that this RNA phenomena was a broadly conserved mechanism for genome defence and regulation (Novena & Sharp, 2004). Exploiting this system, scientists now have the ability to artificially engineer dsRNA molecules which they can use either for therapeutics or for functional gene studies.

The RNAi pathway utilises various different forms of dsRNA molecules. The two most common forms are small interfering RNAs (siRNAs) and microRNAs (miRNA) which both originate from longer dsRNA precursors (Ketting, 2011). A siRNA is generally about 21-22 nucleotides in length and is commonly derived from an exogenous source, such as a virus. Biomedically, synthetic siRNAs have successfully been used to efficiently knockdown various target genes (Soutschek et al., 2004, George & Tsutsumi, 2007, Howard et al., 2008). However, because of their exogenous origin, their knockdown effect is only transient (Wilson & Dounda, 2013). By contrast, a miRNA, which is usually 19-25 nucleotides in length, is derived from the genome and thus can generate stable gene knockdown when used experimentally (Novina & Sharp, 2004).

The genesis of miRNAs begins in the nucleus with transcription of the primary miRNA transcript (pri-miRNA) by RNA polymerase II. The pri-miRNA is about 1000 nucleotides in length and because of its self-complementarity, it can fold over in the middle to base pair with itself, resulting in the formation of a hairpin structure (Saini et al., 2007).

A nuclear micro-processing enzyme, Drosha, then cleaves the pri-miRNA transcript to generate a 65-70 nucleotide precursor miRNA (pre-miRNA) (Kim & Kim, 2007). Subsequently, the pre-miRNA associates with the transport facilitators, Exportin 5 and RanGTP, allowing it to be exported out of the nucleus (Lund & Dahlberg, 2006).

Once in the cytoplasm, the pre-miRNA encounters a second enzyme, Dicer, which as its name suggests, cuts the pre-miRNA down to its mature miRNA form. Similarly, siRNA precursors are also processed by Dicer so that they are of appropriate size for loading onto an Argonaute protein. Argonaute proteins can associate with both miRNAs and siRNAs and preferentially select one strand of the duplex for binding. The selected RNA strand, known as the guide strand, specifically binds to the proteins PAZ and MID domains to generate a RNA-induced silencing complex (RISC) (MacRae et al., 2008). The other strand which does not get incorporated is consequently discarded (Wilson & Dounda, 2013).

The guide strand within the RISC is used as a template for recognising and binding complementary mRNA, typically within the 3' untranslated region (UTR) (Kim & Rossi, 2007). The level of complementarity between the guide strand and the target mRNA determines the subsequent silencing effect. If there is perfect complementarity, as is the case for most siRNAs, RISC binding will result in endonucleolytic cleavage, followed by mRNA degradation (Wilson & Dounda, 2013). However, if the binding is not 100% complementary, a common feature of miRNAs, cleavage does not occur and instead the binding of RISC to mRNA prevents translational machinery from binding so no protein is able to be produced (Fig. 6). RNAi is thus an effective post-transcriptional method for silencing gene expression, and therefore, widely used for investigating the molecular function of genes.

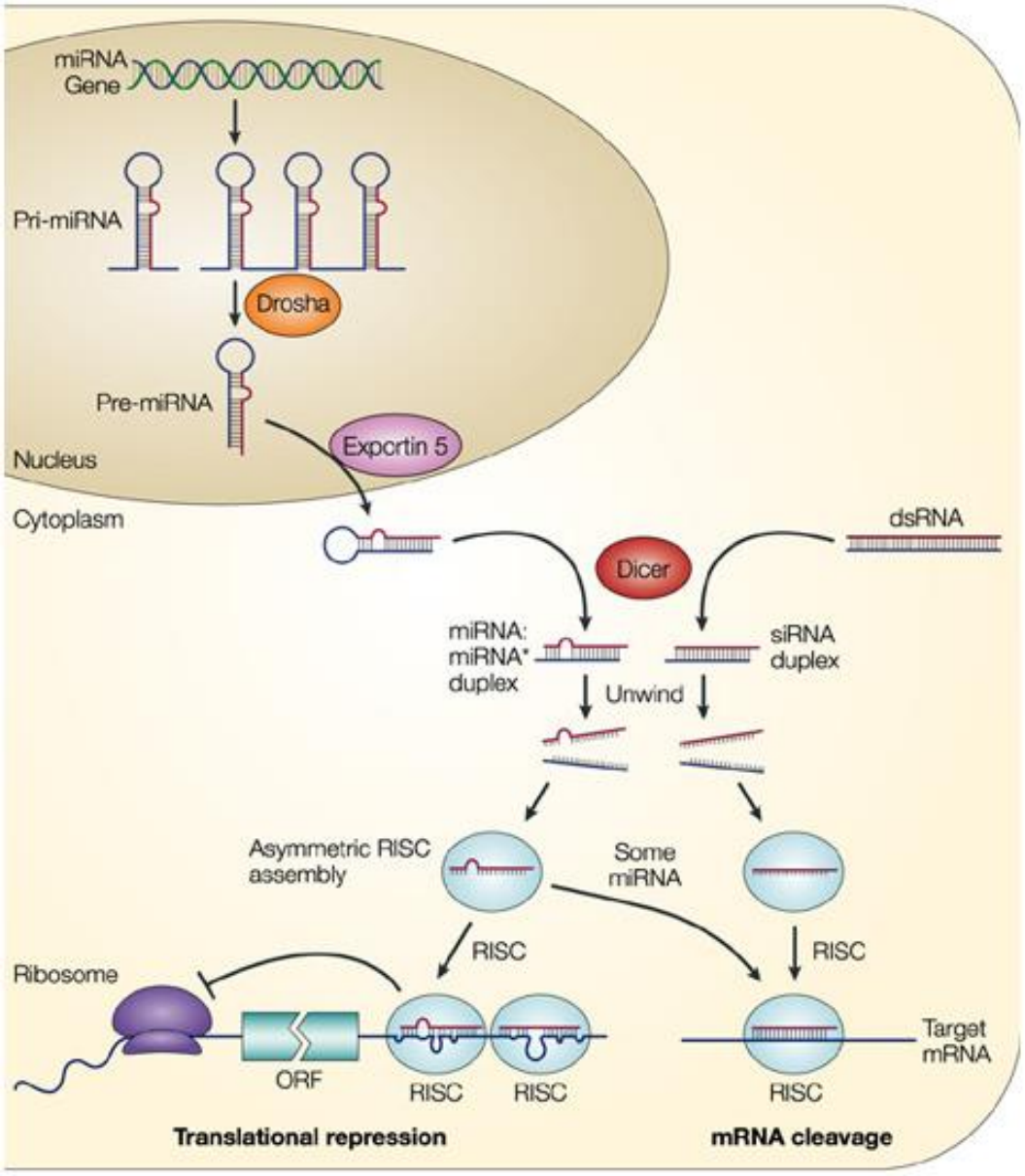

Fig. 6. Biogenesis and post-transcriptional silencing model of miRNA and siRNA. Endogenously expressed miRNAs are transcribed in the nucleus and processed by Drosha into pre-miRNAs before being transported into the cytoplasm via Exportin 5. In the cytoplasm, pre-miRNAs or long dsRNA molecules are processed by the enzyme dicer into their mature miRNA or siRNA form. Consequently, one strand of the duplex preferentially becomes incorporated into an RNA-induced silencing complex (RISC) which guides the complex towards the target mRNA. Binding of the RISC to the target mRNA can either result in translational repression or mRNA cleavage depending, in part, on the degree of sequence complementarity. ORF, open reading frame. (He & Hannon, 2004)

1.6.1.1 The BLOCK-iT™ Pol II miR RNAi Expression System

To experimentally introduce miRNAs into mammalian cells, numerous groups have developed vector-based expression systems which allow integration within the genome. For example, the BLOCK-iT™ Pol II miR RNAi expression system supplied by Invitrogen has been specifically designed for transient or stable expression of pre-miRNAs in mammalian cells. For simplicity, this will hereon be referred to as the BLOCK-iT™ miRNA expression kit. Using the online program, RNAi designer (Invitrogen), scientists can input the sequence of a gene they want to knockdown, and the software will design a variety of suitable pre-miRNA sequences. The engineered pre-miRNA sequences are modelled on the structure of an existing endogenously expressed murine miRNA, miR-155, and are designed to fully complement their target.

The pre-miRNA sequences can then be cloned into the 5699 bp pcDNA 6.2-GW/EmGFP-miR plasmid supplied by the BLOCK-iT™ kit (Fig. 7). This plasmid allows for dual expression of the pre-miRNA along with an emerald green fluorescent protein (EmGFP) marker enabling researchers to track expression levels. Relatively high expression levels of the plasmid is made possible by the constitutively active cytomegalovirus (CMV) promoter which is recognised by RNA Polymerase II. The plasmid also carries both a spectinomycin and blasticidin resistance gene to allow for prokaryotic and eukaryotic selection, respectively. Expression of the blasticidin resistance gene is driven by the synthetic EM7 promoter which is based on the bacteriophage T7 promoter. Following transfection of the miRNA expression plasmid into mammalian cells, the engineered pre-miRNAs get processed into mature miRNAs by the cell's own machinery, allowing them to enter into the RNAi pathway for direct target cleavage.

The BLOCK-IT™ miRNA expression kit also includes both a positive and negative pre-miRNA control. The negative miRNA control construct contains a pre-miRNA sequence that can form a hairpin structure and is also processed by the host cell's RNAi machinery. However, the mature form of the negative control miRNA has no target homology to any vertebrate gene and therefore is not predicted to cause any knockdown effect. The positive miRNA control supplied

by the kit is a pre-miRNA sequence for *lacZ* which requires cloning into the pcDNA 6.2-GW/EmGFP-miR vector. A *lacZ* reporter plasmid is also provided. The *lacZ* gene encodes for β-galactosidase, the enzyme responsible for hydrolysing lactose into glucose and galactose. β-galactosidase can also hydrolyse the lactose analog X-gal which, in addition to forming galactose, also forms an insoluble blue coloured product 5,5'-dibromo-4,4'-dichloro-indigo (Macgregor et al., 1991). The positive BLOCK-iT^{TM} control experiment can therefore be performed by cotransfecting the *lacZ* reporter plasmid alongside the *lacZ* miRNA plasmid and assaying for knockdown of β-galactosidase (Invitrogen, 2008).

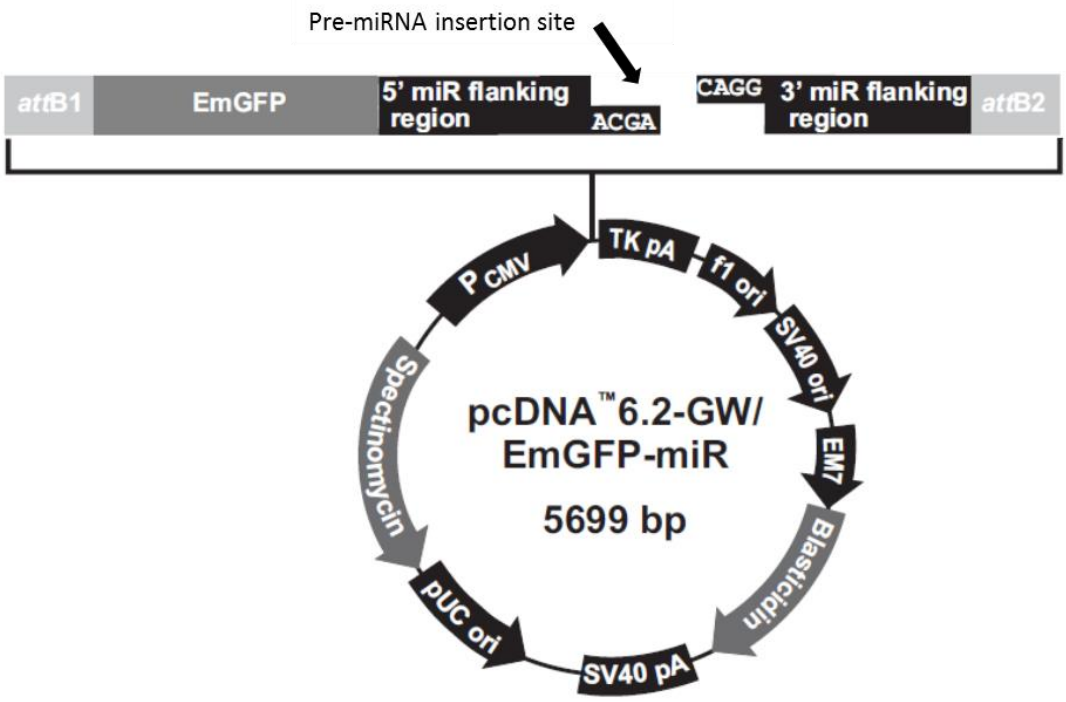

Fig. 7. Plasmid map of the BLOCK-iT^{TM} plasmid pcDNATM6.2-GW/EmGFP-miR used for miRNA expression (Invitrogen). Once ligated with the pre-miRNA, the total plasmid size is 5759 bp. Details: Cytomegalovirus **(**CMV) promoter (1–588), attB1 site (680-704), emerald green florescence protein (EmGFP) (713–1432), forward sequencing primer site (1409–1428), 5' miR flanking region (1492-1518), 3' miR flanking region (1519-1563), attB2 site (1592-1616), reverse sequencing primer site (1607-1626), TK polyadenylation signal (1645-1916), f1 origin (2028-2456), SV40 early promoter and origin (2483-2791), EM7 promoter (2846-2912), blasticidin resistance gene (2913-3311), SV40 polyadenylation signal (3469-3599), pUC origin (3737-4410), spectinomycin resistance gene (4480-5490), spectinomycin promoter (5491-5624).

1.6.2 Protein Overexpression

In parallel to loss-of-function approaches, such as RNAi, overexpression of a protein resulting in a gain-of-function can also be used to determine gene function. Overexpression studies are particularly useful when a gene is not usually expressed, or expressed at low levels. One way of increasing the expression of a gene is to introduce transgenic plasmids containing the gene of interest into the desired cell line. Once inside the cell, the plasmids gets processed by the host's transcription and translation machinery resulting in high expression levels of the gene product. If the plasmid integrates within a transcriptionally active region of the genome, it can maintain stable expression. The challenge of gene overexpression lies in maximising the number of plasmids which can enter into a cell and integrate within the genome without causing cellular stress and cell death. Recently, a transposon-based expression system was developed which takes advantage of the 'genome jumping' nature of transposable elements. This system, referred to as the piggyBac system, allows for high levels of plasmid integration and is described in the section below.

1.6.2.1 The Inducible PiggyBac Expression System.

The key component of the piggyBac expression system is the highly efficient host factor independent piggyBac transposase (PBase) plasmid, pCyL43. The PBase facilitates chromosomal integration of transposon-containing plasmids by recognising a pair of inverted terminal repeat sequences (ITRs) positioned either side of the donor DNA. The donor DNA is then integrated into random TTAA sites on the chromosomal DNA via a 'cut-and-paste' mechanism (Ding et al., 2005). As many as 15 copies of the plasmid can be randomly integrated throughout the genome within one cell (Wang et al., 2008).

In some instances, overexpression of a protein can lead to cell stress and poor cell growth (Palomares et al., 2004). To circumvent these issues a variety of inducible promoter expression systems have been developed (Gossen & Bujard, 1992, No et al., 1996, Fussenegger et al., 2000, Weber et al., 2004). In particular, the highly efficient piggyBac system has been modified to allow for inducible protein production (Li et al., 2013). The system relies on the PBase-mediated integration of two transposon-containing piggyBac plasmids. The first plasmid contains the

gene of interest and a puromycin resistance gene which are both under the control of a tetracycline response element (TRE) promoter.

The second plasmid carries the reverse tetracycline transactivator (rtTA) inducer which is constitutively expressed from a CMV promoter. In the presence of the antibiotic doxycycline, the rtTA undergoes a conformational change allowing it to bind to the TRE promoter and activate expression of the donor DNA. When doxycycline is removed, the rtTA can no longer bind and expression is suppressed (Fig. 8). Thus protein expression can be switched on or off by simply administering doxycycline to transfected cells.

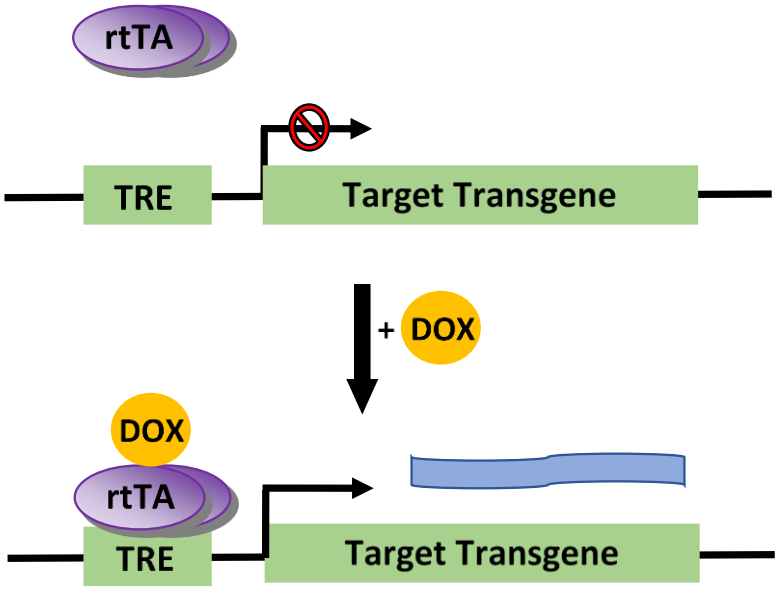

Fig. 8. The doxycycline-inducible expression system. When no doxycycline (DOX) is present, the reverse tetracycline transactivator (rtTA) cannot bind to the tetracycline response element (TRE) promoter, resulting in no transcription of the target transgene. Upon administration of DOX, the rtTA undergoes a conformational change allowing it to bind to the TRE and induce transcription of the target transgene.

1.7 Research Strategy and Objectives

The aim of this research project was to determine the feasibility of using the BLOCK-iT^{TM} miRNA expression system for knockdown of the pluripotency-related proteins NANOG and MBD3 in cattle. An outline of the research strategy and the specific objectives of this project are summarised below.

The first objective of this research project was to design a variety of different miRNA sequences that would be specific for either the *NANOG* or *MBD3* mRNA transcript. This design process was completed online using the BLOCK-iT™ RNAi designer tool (Invitrogen) and the sequences were then assembled into an expression plasmid using the BLOCK-iT™ miRNA expression kit.

Next, to determine the knockdown potential of the various designed miRNAs, the miRNA expression plasmids had to first be tested on somatic cell lines. For MBD3, which is ubiquitously expressed in somatic cells, miRNAs were tested using a standard bovine embryonic fibroblast (BEF) line. By contrast, NANOG is not expressed in somatic cell lines. Therefore, to test the knockdown potential of the NANOG miRNAs, a NANOG expressing somatic cell line had to first be generated. To generate this NANOG cell line, the inducible piggyBac expression system was used.

To establish which miRNA induced the most potent and specific knockdown, a robust screening assay for MBD3 and NANOG had to be developed. Knockdown assays were developed to detect the expression of the mRNA transcript as well as the protein for both NANOG and MBD3.

Additionally, the feasibility of generating a stable knockdown cell line was investigated with the future objective of being able to use such a line for producing donor cells for SCNT cloning followed by IVP of embryos. In this way, bovine embryos could be produced that would be deficient in either NANOG or MBD3 and thus the functionality of these proteins in early embryonic development and pluripotency could be determined.

Chapter Two: Methods

All incubation periods and centrifugations were carried out at room temperature unless stated otherwise. All glassware and plastic tubes were autoclaved (121ºC) prior to use. For mRNA work, filter pipette tips were used and water was treated with diethylpyrocarbonate (DEPC). Non-filtered pipette tips and milliQ water was used for all other research purposes at a quality of 18.2 MΩ ·cm. All solutions used for bacterial and mammalian cell culture were filter-sterilised and prepared under laminar flow. A detailed list of materials, including plasmids, sequences, equipment, software, and commonly used reagents can be found in the appendices.

2.1 Statement of Approval

This research project was granted Environmental Protection Authority (EPA) New Zealand approval under the Hazardous Substances and New Organisms (HZNO) Act 1998. The EPA approval number was GMOO5/ARR003. All cell culture work was carried out in a physical containment 2 (PC2) laboratory.

2.2 Generation of miRNA Expression Plasmids

2.2.2 miRNA Sequence Design

For RNAi-mediated knockdown of NANOG and MBD3, miRNAs were designed that specifically targeted either the *NANOG* or *MBD3* mRNA transcript, respectively. Using the National Center for Biotechnology Information (NCBI) nucleotide database, the *NANOG* and *MBD3* mRNA sequences were obtained and their accession numbers (*NANOG* = NM_001025344.1, *MBD3* = NM_001128505.1) were input into the online program, BLOCK-iT^{TM} RNAi designer (Invitrogen, USA). The program then used a proprietary algorithm to design miRNA sequences specific for each mRNA transcript. To avoid off-target effects, miRNAs were designed to specifically target the open reading frame (ORF) as opposed to the 3' or 5' untranslated regions (UTRs), a common target of endogenous miRNAs. The top three most highly ranked miRNA sequences for each gene were then screened against the entire bovine genome (Genbank

accession number: GCA_000003205.4) to confirm their specificity using NCBI's Basic Local Alignment Search Tool (BLAST). Three miRNA sequences for each gene were selected and ordered from Integrated DNA Technologies. The miRNA sequences can be found in Appendix II.

2.2.3 Assembly of miRNA Oligonucleotides

The miRNA sense and anti-sense oligonucleotides (oligos) arrived in a lyophilized state and were resuspended in DEPC-treated water to a final concentration of 1 mM. To generate miRNA expression plasmids, the BLOCK-iT^{TM} miRNA expression kit was used (Invitrogen, USA). Firstly, an annealing reaction was set up in a 600 µl Eppendorf tube and involved combining 1 µl from each miRNA oligo pair (sense and anti-sense) with 2 µl of 10x oligo annealing buffer and 16 µl of DEPC-treated water. To anneal the single-stranded miRNA oligo pairs, the annealing reaction was first incubated by placing on a 95^{0}C thermomixer for 4 minutes and then cooled down to room temperature for 10 minutes. Samples were centrifuged briefly for 5 seconds before removing 1 µl for a dilution series. The double-stranded (ds) oligo was firstly diluted 100-fold in DEPC-treated water (1 µl of 50 µM ds oligo in 99 µl of DEPC-treated water) to give a final concentration of 500 nm. After vortexing gently to mix, the reaction was then further diluted 50-fold in annealing buffer (1 µl of 500 nm ds oligo in 5 µl of 10x annealing buffer and 44 µl DEPC-treated water) to generate the 10 nM working concentration. All dilutions were stored at -20^{0}C.

2.2.4 Ligation of miRNA Oligonucleotides into the BLOCK-iT^{TM} Plasmid

The ds miRNA oligos were then ligated into the BLOCK-iT^{TM} plasmid pcDNA TM6.2-GW/EmGFP-miR using the BLOCK-iT^{TM} miRNA expression kit. To clone in the ds miRNA oligos, a 10 µl ligation reaction was prepared which included 2 µl of the linearized BLOCK-iT^{TM} expression plasmid (5 ng/µl), 1 µl of ds miRNA oligo (10 nM), 2 µl of 5x ligation buffer, 1 µl of T4 DNA ligase, and 4 µl of DEPC-treated water. The ligation reaction was mixed well by gently pipetting up and down then left to incubate for 5 minutes. In addition to the three miRNAs for each gene (*NANOG* and *MBD3*), a positive miRNA expression plasmid was also prepared using the *lacZ* ds miRNA oligo (10 nM) supplied by the BLOCK-iT^{TM} miRNA expression kit.

2.3 Generation of the PB-TRE-NANOG Plasmid

2.3.1 NANOG Fragment Design

Because the intended target of the NANOG miRNAs is endogenously expressed *NANOG* within bovine embryos, the *NANOG* expression plasmid had to contain a 100% identical mRNA sequence to the endogenous mRNA transcript. Using the NCBI database, the bovine *NANOG* mRNA sequence was obtained and the entire coding sequence was used to design a *NANOG* fragment for plasmid cloning. To assist with plasmid cloning, the *NANOG* coding sequence was flanked by a 5' SalI and 3' NotI restriction enzyme cut site, plus an additional three 'stuffer' nucleotides either side (see Appendix II for full sequence). The fragment was ordered using GeneArt Strings^{TM} DNA fragments (Life Technologies, USA) and was resuspended in DEPC-treated water to a final concentration of 20 ng/µl and then stored at -20^{o}C.

2.3.2 TOPO-TA Ligation

The TOPO-TA plasmid was used as an intermediary vector that the *NANOG* fragment was subcloned into for the purpose of cutting out again to generate 'sticky ends' either side of the fragment. To ligate the *NANOG* fragment into the TOPO-TA plasmid, 3' adenosine overhangs had to first be added on either side of the fragment. This was achieved by combining 0.5 µl of Faststart Taq DNA polymerase, 4 µl of Faststart 10x buffer, 0.5 µl of dATPs (10mM) with 5 µl milliQ water and placing on a 95^{0}C thermomixer for 3 minutes. After leaving on ice to cool for 60 seconds, 30 µl of *NANOG* fragment (600ng) was added to the reaction and left to incubate at 72^{0}C for 20 minutes. Following this, the TOPO-TA ligation reaction was prepared using the TOPO-TA cloning® kit (Invitrogen, USA) which included 0.5 µl of linearized TOPO-TA plasmid backbone, 1 µl of salt solution, 1 µl of milliQ water, and 0.5 µl of the 3' adenosine overhang *NANOG* fragment. A negative ligation control reaction, that did not contain the *NANOG* fragment, was also prepared. The reactions were vortexed briefly to mix, spun down, and then left to incubate for 3 hours.

2.3.3 Inducible PiggyBac Ligation

A ligation reaction was prepared by combining together 100 ng of linearized inducible piggyBac plasmid, PB-TRE (6.6 kb), 100 ng of 'sticky ends' *NANOG*

fragment (900 bp), 4 µl of 5x DNA ligation buffer, and 1 µl of T4 DNA ligase. A negative ligation control reaction was also prepared which did not contain any *NANOG* fragment. The ligation reactions were mixed gently by pipetting up and down and then left to incubate for 3 hours.

2.4 Generation of the CMV-NANOG Plasmid

In addition to the inducible PB-TRE-NANOG plasmid, a constitutively active CMV-NANOG plasmid was also generated. The commercial plasmid, pEGFP-N1 (4.7 kb) was digested with the restriction enzymes SalI and NotI (as described in section 2.8) to excise the 700 bp GFP fragment. The digest reaction was then run on an agarose gel (section 2.9) and the 4 kb CMV backbone fragment was excised and purified (section 2.10). Subsequently, a ligation reaction was prepared using 100 ng of CMV backbone, 100 ng of the 'sticky ends' *NANOG* fragment, 4 µl of 5x DNA ligation buffer, and 1 µl of T4 DNA ligase. The ligation reactions were mixed gently by pipetting up and down and then left to incubate for 3 hours.

2.5 Bacterial Culture and Transformation

2.5.1 Transforming Bacteria

To amplify plasmid copy numbers, plasmids were introduced into bacterial cells by transformation. Bacterial stocks containing 50 µl of One Shot® TOP10 competent *Escherichia coli* (Invitrogen, USA) were stored at -80ºC and were thawed on ice when required for transformation. To transform the bacteria, 2 µl of the ligation reaction was added to one vial of bacteria and allowed to incubate on ice for 30 minutes.

The bacterial cells were then heat shocked in a 42ºC water bath for 30 seconds and then immediately placed back on ice. Subsequently, the bacteria/DNA mixture was combined with 250 µl of SOC medium and left to incubate in a 37ºC water bath for 60 minutes. The transformed bacteria were then spread across a pre-warmed Luria-Bertani (LB) agar plate containing the appropriate antibiotic (Table 1) and placed upside down in the 37ºC Sanyo incubator overnight.

Table 1. Selection antibiotics for bacterial cell culture

Plasmid	Antibiotic	Source	Working Concentration
BLOCK-iT™	Spectinomycin	Sigma Aldrich, Switzerland	50 µg/ml
TOPO-TA-NANOG & CMV-NANOG	Kanamycin	Roche, Germany	25 µg/ml
PB-TRE-NANOG	Ampicillin	Applichem, USA	50 µg/ml

2.5.2 Selecting Bacterial Colonies

Transformed bacterial plates were checked for colony formation the following day. To validate that the bacterial clones contained the plasmid of interest, four random colonies were selected to be grown up for a miniprep plasmid isolation. The bacterial colonies were transferred individually (via a pipette tip) to a test tube containing 3 ml of LB broth and the appropriate antibiotic (Table 1). The bacterial cultures were placed in the Infors HT ecotron 37ºC incubator overnight on a moderate shake (150 rpm). If a larger quantity of bacteria was required (i.e. for a maxiprep), 1 ml of the overnight starter culture was transferred to a 1 L volumetric flask containing 100 ml LB broth with the appropriate antibiotic (Table 1) and cultured for a second night under the same conditions.

2.5.3 Glycerol Freezing

To preserve bacterial clones that contained a validated plasmid of interest, the bacterial culture was frozen down in a glycerol solution for long term storage. The glycerol stock was prepared by gently mixing 200 µl of glycerol (100%) with 200 µl of the overnight bacterial culture in a 1.5 ml Eppendorf tube. All bacterial glycerol stocks were stored at -80ºC.

2.6 Plasmid Preparation

2.6.1 Miniprep

For small scale plasmid isolation (10 µg), the PureLink® Quick Plasmid DNA Miniprep Kit (Invitrogen, USA) was used according to the manufacturer's instructions. Firstly, the overnight bacterial culture was harvested by centrifugation (8,000 x g, 2min). The bacterial pellet was then resuspended in 250

µl of resuspension buffer with RNase A. Subsequently, the bacteria was lysed by adding 250 µl of lysis buffer and mixed thoroughly by inverting five times. The lysis reaction was neutralised by adding 350 µl of precipitation buffer causing the denatured chromosomal DNA and proteins to precipitate. The lysate was then centrifuged (12,000 x g, 10min) and the resulting supernatant, containing the plasmid DNA, was poured into a spin column within a wash tube. To bind the plasmid DNA to the silica membrane, the spin column was centrifuged (12,000 x g, 1 min) and the flow through discarded. The column was then washed with 700 µl of wash buffer containing ethanol and centrifuged twice more (12,000 x g, 1min) discarding the flow through each time. The spin column was then placed into a sterile 1.5 ml recovery tube and 75 µl of TE buffer pH 8.0 was incubated on the membrane for 1 minute before centrifugation (12,000 x g, 2min) to elute the plasmid DNA. Plasmid DNA was stored at 4°C short term, or -20°C long term.

2.6.2 Maxiprep

For large scale plasmid isolation (600 µg), the PureLink® Quick Plasmid DNA Maxiprep Kit (Invitrogen, USA) was used according to the manufacturer's instructions. In brief, the 100 ml overnight bacterial culture was pelleted by centrifugation (5,000 x g, 10min, 4°C). The resulting supernatant was discarded and the bacterial pellet was completely resuspended in 10 ml of resuspension buffer with RNase. The bacteria was then lysed in 10 ml lysis buffer and gently inverted until homogenous. After a 5 minute incubation, 10 ml of precipitation buffer was added to neutralise the reaction. The solution was then poured into a HiPure filter maxi column containing a filtration cartridge that had already been equilibrated with 30 ml of equilibration buffer. After allowing the solution to flow through, the column was washed with 30 ml of wash buffer. The tank beneath the column was then replaced with a 50 ml polypropylene centrifuge tube and 15 ml of elution buffer was added to the column to elute the plasmid DNA. Subsequently, 10.5 ml of isopropanol was added to precipitate the DNA which was then centrifuged (20,000 x g, 30min, 4°C). The supernatant was discarded and the DNA pellet was washed in 5 ml of 70% ethanol before being spun again (20,000 x g, 10min, 4°C). Excess ethanol was removed and the DNA pellet was left to air dry for 10 minutes before dissolving in 200 µl TE buffer. The maxiprep solution was transferred to a sterile 1.5 ml Eppendorf tube and stored at -20°C.

2.7 Plasmid Quantification

The Nanodrop Spectrophotometer ND-1000 (Thermo Scientific, USA) was used to measure the concentration of plasmid DNA. The machine was first calibrated with water and then blanked with the solution used to resuspend the DNA. Plasmid DNA was measured by light absorbance (A) at 260 nm using a 1 µl sample to give a final concentration in ng/µl. The purity of the DNA was assessed by dividing its A value at 260 nm by its A value at 280 nm. An A_{260}/A_{280} ratio between 1.8 and 2.0 was considered to be of good purity for further use.

2.8 Restriction Digestion

To ensure plasmid DNA contained the target insert, it was digested with the appropriate restriction enzyme (Table 2). All restriction enzymes and buffers were supplied by New England BioLabs (USA). As a general rule, 1 µg of DNA was used per 1 unit of restriction enzyme in the specified 10x digest buffer, with a total reaction volume of 20 µl. The reaction was left to incubate in a 37°C water bath for 1 hour before being loaded onto a 1% agarose gel.

Table 2. Restriction enzymes and buffers

Restriction Enzyme	Digest Buffer	Cut Site
MscI	10x NEB buffer 4	TGG^CCA
NotI (HF)	10x cut smart buffer	GC^GGCCGC
SalI (HF)	10x cut smart buffer	G^TCGAC

2.9 Gel Electrophoresis

Agarose gel electrophoresis was used to separate and analyse fragments of DNA by size. To separate fragments greater than 200 bp, a 1% agarose gel was used. To prepare the gel, 0.8 g of UltraPure™ agarose powder was combined with 80 ml of 1x TAE buffer and heated in the microwave for approximately 60 seconds until completely dissolved. Once the solution had cooled down, 8 µl of SYBR® Safe was mixed in to enable DNA to be visualised under UV light. The gel mix was poured into a taped gel cast with the appropriate sample comb inserted and left for 15 minutes to solidify. Once solid, the gel was placed into an electrophoresis tank containing 1x TAE buffer and the sample comb was gently removed. To determine the molecular size of the DNA fragments, 8 µl of 1 kb+ DNA ladder was loaded into the first well using a pipette. On a strip of parafilmM®, 8 µl of

DNA sample was mixed with 2 µl of 5x DNA loading dye and subsequently loaded into the adjacent wells. The electrophoresis chamber was then connected to the power unit and run at a constant voltage of 100V until the loading dye had run approximately two thirds of the way down the gel. The gel was then removed from the gel cast and visualised on the BioRad Gel Doc UV Imager and analysed using Quantity One software (BioRad, USA).

2.10 Gel Extraction and Purification

The Wizard® SV Gel and PCR Clean-Up System Kit (Promega, USA) was used to extract and purify DNA from an agarose gel. Firstly, the gel was transferred to an ultraviolet (UV) light box and exposed briefly to identify the desired band which was quickly excised using a sterile scalpel blade. The isolated gel piece was then weighed and placed into a 1.5 ml Eppendorf tube. To solubilise the agarose, an equal volume of membrane binding solution was added to the tube which was placed on a 60ºC thermomixer for approximately 10 minutes. Once dissolved, the solution was poured into a SV mini column and left to incubate for 1 minute so that the DNA could bind to the column membrane. The mini column was then spun on max speed (14,000 x g, 1min) and the resulting flow through was discarded. Subsequently, the column was washed twice with wash buffer to remove any residual salts or impurities within the membrane. The first wash involved adding 700 µl of wash buffer followed by centrifugation at max speed for 1 minute. Whereas, the second wash step used 500 µl and was centrifuged on max speed for 5 minutes. After discarding the flow through, the column was then spun dry (14,000 x g, 1min) to remove any excess ethanol leftover from the wash steps. To elute the DNA, the column was placed within a 1.5 ml Eppendorf tube and incubated with 50 µl of nuclease-free water for 1 minute before being spun at max speed (14,000 x g, 1 min). The resulting flow through containing the purified DNA of interest was then measured by the Nanodrop and stored at -20ºC.

2.11 DNA Sequencing

2.11.1 Sequencing Preparation

To verify that the target insert had not undergone any point mutations during the plasmid preparation steps, plasmid DNA was sent to Massey Genome Service, New Zealand for sequencing. Each sequencing reaction was made up to a final

volume of 20 µl and contained 300 ng of plasmid DNA and 4 pM of forward and/or reverse sequencing primer (Table 3).

Table 3. DNA sequencing primers

Primer Name	Sequence (5'-3')
BLOCK-IT™	F: GGCATGGACGAGCTGTACAA R: CTCTAGATCAACCACTTTGT
M13	F: CCCAGTCACGACGTTGTAAAACG R: AGCGGATAACAATTTCACACAGG
NANOG + RE	F: ATTGTCGACATGAGTGTGGGCCCAGCTT R: ACAGCCTGAAGATTTGTAAGCGGCCGCATA

2.11.2 Sequencing Analysis

Sequencing results were opened and analysed using the bioinformatics software Geneious, version 7 (Biomatter Ltd, New Zealand). Any mismatches in sequence were investigated further by analysing the chromatogram using the program Chromas Lite, version 2.01 (Technekysium, Australia). Any plasmid that did contain a mutation was discarded and not used for transfection experiments.

2.12 Mammalian Cell Culture

To prevent contamination with bacteria, fungi, mycoplasma, or other cell lines, mammalian cell culture work was carried out under sterile laminar flow hoods that were routinely wiped before and after use with 70% ethanol. Bovine cell lines and HeLa cells were cultured in 5% CO_2 water jacketed incubators set at 38.5°C or 37°C, respectively. Base media was prepared when required and consisted of DMEM/F12 + glutamax media (GIBCO, USA) supplemented with 10% fetal calf serum (FCS). Base media, phosphate buffered saline (PBS), 0.25% trypsin, and TrypLE™ Express were always pre-warmed to 37°C just prior to use.

2.12.1 Thawing Cells

Frozen aliquots of cells were stored in cryovials in a liquid nitrogen tank (-196°C). When required, a cryovial containing the desired cell line was transferred directly from liquid nitrogen to the 37°C water bath and thawed until only a small ice clump was remaining. Thawed cells were then gently added to a 15 ml Falcon tube containing 9 ml of pre-warmed base media and pelleted by centrifugation (1,000 rpm, 3 min) on the Biofuge fresco (Heraeus, Germany). The supernatant

was aspirated and the cell pellet was gently resuspended in the appropriate volume of base media before transferring to the appropriate tissue culture dish.

2.12.2 Cell Count

Cell counts were performed to gain an estimate on the number of cells suspended in base media to ensure seeding was done at the optimal density. To perform a cell count, the suspended cell solution was mixed gently to prevent cells settling at the bottom of the tube. Two 10 µl aliquots were then taken and loaded either side of a hematocytometer. Under the Nikon light microscope, cells within the 5 counting squares were counted and the total concentration of cells was calculated using Equation 1.

Equation 1. Estimation of cell concentration using a hematocytometer

$$\frac{\text{no. of cells counted}}{5} \times \text{total vol of cell suspension (ml)} \times 10{,}000 = \text{total no. of cells}$$

2.12.3 Passaging Cells

Cells were passaged during the log phase of growth from dishes that were around 70 - 90% confluent. Base media was aspirated and cells were washed briefly in PBS to remove any residual dead cells. To lift off adherent cell cultures, a minimal layer of 0.25% trypsin was added to just cover the tissue culture plate which was then left to incubate at 37ºC for 3 to 5 minutes. After checking under the microscope that the cells had detached from the surface, cell clumps were broken up by gently pipetting the cell solution up and down. The resuspended cells were then transferred to a 15 ml Falcon tube and 9 ml of fresh base media was gently mixed in to deactivate the trypsin. Two 10 µl aliquots were then taken and loaded either side of a haemocytometer for a cell count. Meanwhile, the trypsinised cells were pelleted by centrifugation (1,000 rpm, 3 min) and the resulting supernatant was removed by aspiration. Finally, the cell pellet was resuspended in the appropriate volume of base media and seeded onto fresh culture dishes.

2.12.4 Freezing Cells

To keep the passage number of cells low, cultures that were no longer immediately required were frozen down and stored in liquid nitrogen. Prior to freezing, a cryoprotectant solution was prepared which consisted of FCS + 20% DMSO. Cells were harvested in 0.25% trypsin and diluted in 9 ml of base media. A cell count was performed while the cells were pelleted by centrifugation (1,000 rpm, 3 min). The cell pellet was then resuspended in base media to a concentration of 2 x 10^6 cells per ml. An equal volume of cryoprotectant solution was then added slowly to avoid chemical shock bringing the concentration down to 1 x 10^6 cells per ml. The cell solution was then split across the required number of cryovials, typically in 1 ml aliquots. Cryovials were placed in a Mr Frosty™ freezing container filled with 100% isopropanol and placed at -80°C to begin the slow freezing process of -1 degree per minute. The next day, cryovials were transferred directly into liquid nitrogen for long term storage.

2.13 Transfection of Mammalian Cells

Transfection is the process by which plasmid DNA is introduced into eukaryotic cells. The majority of plasmid DNA will remain within the cytoplasm and will only be expressed a few days before being degraded or diluted by cell division (Recillas-Targa, 2006). However, a small percentage of plasmids will integrate into the host genome allowing stable expression assuming it has integrated into a transcriptionally active region (Kim & Eberwine, 2010).

2.13.1 Lipofectamine® LTX

Lipofectamine® LTX is a lipid-based transfection protocol that can generate relatively high transfection efficiencies whilst also being gentle on the cells (Invitrogen, USA). The cationic lipid reagent LTX supplied by the kit spontaneously forms condensed lipid complexes with DNA by binding to the negatively charged phosphate backbone. The complexes are then believed to interact with the cell membrane allowing for endocytosis and subsequent release within the cytoplasm (Chesnoy & Huang, 2000).

The number of cells required for transfection varied depending on the subsequent cell analysis. Similarly, the Lipofectamine® reagent volumes also varied

depending on the number of cells being transfected. The appropriate reagent volumes per culture dish size are represented in Table 4.

Table 4. Lipofectamine® LTX component amounts for different size culture dishes

Component	96-well	4-well	12-well	3 cm	6 cm	10 cm
Adherent cells	1 x 10^4	1 x 10^5	2 x 10^5	5 x 10^5	2 x 10^6	4 x 10^6
Opti-MEM medium	17.5 µl	100 µl	200 µl	500 µl	1 ml	3 ml
Plasmid DNA	0.1 µg	0.5 µg	1 µg	2.5 µg	5 µg	15 µg
PLUS™ reagent	0.1 µl	0.5 µl	1 µl	2.5 µl	5 µl	15 µl
Lipofectamine® LTX	0.3 µl	1.25 µl	2.5 µl	6.25 µl	12.5 µl	37.5 µl

The day before transfection, cells were seeded onto the required number of culture dishes so that they would be around 60-80% confluent at the time of transfection. The following day, base media was refreshed on each culture dish. To prepare the lipid complexes for transfection, plasmid DNA was firstly added to a 1.5 ml Eppendorf tube and diluted with opti-MEM reduced serum media. To boost transfection efficiencies, the diluted DNA solution was then gently mixed with the PLUS™ reagent and left to incubate for 5 minutes. Subsequently, DNA-lipid complexes were formed by mixing in the specified volume of LTX reagent and incubating for 30 minutes. After the incubation, the newly formed DNA-lipid complexes were added dropwise to the appropriate culture dish which were swirled gently before placing back into the respective incubator to culture for 24 hours.

2.13.2 Neon™ Electroporation

Neon™ electroporation is an alternative transfection protocol which can generate even higher transfection efficiencies than Lipofectamine® LTX but at a cost of reduced cell viability (Invitrogen, USA). Cells to be transfected are resuspended in a conductive solution which is then submitted to a brief electrical pulse. At the optimal voltage, this electrical pulse disturbs the phospholipid bilayer of the membrane causing temporary pores to form. Plasmid DNA is then presumed to be driven through the pores and into the cytoplasm via an electrostatic attraction (Shigekawa & Dower, 1998).

Similarly to the Lipofectamine® LTX protocol, the Neon™ electroporation protocol required cells to be 70-90% confluent on the day of transfection. Cells were washed briefly in PBS and trypsinised in 0.25% trypsin for 3 minutes at 37ºC. The trypsin/cell solution was then transferred to a 15 ml Falcon tube and diluted in base media to 10 ml. Two 10 µl aliquots were then taken for a cell count whilst cells were pelleted by centrifugation (1,000 rpm, 3min). The resulting supernatant was aspirated away and the cell pellet was washed in 10 ml of PBS. At this point, 1 x 10^6 cells were transferred to a separate 15 ml Falcon tube, pelleted, resuspended in 5 ml media, and seeded onto a 6cm 0.1% gelatin coated culture dish containing 3 round 0.78 cm^2 glass coverslips. These cells were then left to culture in the bovine incubator and acted as the non-transfected control. Meanwhile, the remaining cells in PBS were pelleted, and then resuspended in Neon™ R buffer at a density of 1.0 x 10^7 cells/ml.

To transfect 1 million cells, 100 µl of resuspended cell solution was transferred to a 1.5 ml Eppendorf tube containing 5 µg of plasmid DNA and stored on ice. Using Neon™ 100µl pipette tips, the DNA/cell solution was carefully pipetted up making sure no air bubbles formed as this can cause arcing during electroporation. The Neon™ pipette was then inserted vertically into the Neon™ pipette station. To initiate electroporation, the appropriate electroporation protocol was selected on the Neon™ machine (Table 5). Once complete, the Neon™ pipette was removed from the Neon™ pipette station and the cell solution was immediately transferred to a 6 cm 0.1% gelatin coated culture dish containing pre-warmed base media and three glass coverslips. Transfected cells were then left to culture in the appropriate incubator for 24 hours.

Table 5. Neon™ electroporation protocols

Protocol	Pulse Voltage	Pulse Width	Pulse Number
Bovine Cells	1500 V	20 ms	1
HeLa Cells	1005 V	35 ms	2

2.14 Generation of Clonal Mammalian Cell Lines

Approximately 48 hours post-transfection, base media was refreshed on all culture dishes and the appropriate selection antibiotic was added (Table 6). Selection media was refreshed every 48 hours and selection plates were monitored daily for

colony formation. A non-transfected control dish or the pMAX dish was used as a negative selection control. Cell colonies were typically picked 8 – 10 days into selection. Colonies were chosen only if they contained dividing cells and were far enough away from neighbouring cell colonies. After marking the cell colonies with ink on the Nikon light microscope, base media was removed and the dishes were washed twice with PBS to remove any residual dead cells. Cloning rings coated on the base with Vaseline were then placed over top of each marked colony and 40 µl of TrypLE^{TM} Express, a synthetic gentler alternative to trypsin, was added inside and incubated for 3 minutes at 37^{0}C. The selection dishes were then gently smacked down on the bench to help dislodge any cells still attached. The TrypLE^{TM} Express was then diluted in 100 µl of base media and pipetted up and down 5 times before transferring to a 0.1% gelatin-coated 48-well plate containing an additional 400 µl of base media supplemented with the selection antibiotic.

Table 6. Selection antibiotics for mammalian cell culture

Plasmid	Antibiotic	Source	Working Conc
BLOCK-iT^{TM}	Blasticidin	Invitrogen, USA	10 µg/ml
PB-TRE-NANOG	Puromycin	Sigma Aldrich, Switzerland	1 µg/ml

Cell clones were then left to culture in the appropriate incubator until they reached 80% confluence, at which point they were passaged onto a 12-well plate. Clones were sequentially passaged onto larger culture dishes until they reached 80% confluence on a 3 cm culture dish. At this point cells were harvested for characterisation of transgene expression and freezing.

2.15 RNA Extraction

The ZyGEM (New Zealand) RNA extraction kit, *RNA*Gem Tissue, was used to rapidly isolate total RNA from mammalian cell cultures. Mammalian cells were harvested and resuspended in 50 µl of *RNA*GEM master mix solution composed of 1 µl *RNA*Gem, 5 µl SILVER buffer and 44 µl of DEPC-treated water. Once resuspended, the solution was transferred to a 1.5ml Eppendorf tube, vortexed briefly and spun down in a minicentrifuge. The reaction was then incubated for 10 minutes at 75°C to activate the enzyme, *RNA*Gem. Afterwards, the reaction was

placed back on ice and 2 µl of DNase in 5 µl of DNase buffer was added to the reaction, vortexed briefly and spun down. To activate the DNase, the reaction was incubated at 37ºC for 5 minutes followed by 5 minutes at 75ºC to deactivate the enzyme. After placing back onto ice, 5.7 µl of TE buffer was added to the reaction and spun down. A 9 µl aliquot of reaction mix was then taken for cDNA synthesis while the remaining RNA reaction was stored at -80ºC.

2.16 Complementary DNA Synthesis

To analyse mRNA expression, mRNA had to first be converted to cDNA. The reaction was prepared by adding 1 µl of dNTP mix and 0.5 µl of random hexamer primers to 9 µl of the RNA extract. The reaction was then incubated at 65ºC for 5 minutes to denature secondary RNA structures before plunging into ice for 1 minute to allow the random hexamer primers to bind. Meanwhile, a cDNA master mix was prepared which was composed of 4 µl First-Strand 5x buffer buffer, 4 µl of $MgCl_2$, 1 µl of RNaseOUT™, and 1 µl of SuperScript™ III reverse transcriptase (RT). The cDNA master mix was then added to the reaction mix, vortexed briefly and spun down. A RT negative reaction was also prepared in which 1 µl of DEPC-treated water was added in place of SuperScript™ III RT. The reactions were then placed into the Eppendorf mastercycler gradient PCR machine and run on the cDNA synthesis program (25ºC 10 min, 50ºC 50 min, 80ºC 5 min, hold at 4ºC). Once complete, cDNA samples were stored at -20ºC.

2.17 Messenger RNA Quantification

2.17.1 Primer Design

Primers that were used to amplify the gene of interest were designed using the NCBI nucleotide database (Table 7). Where possible, primers were designed under the following criteria; i) product length between 170 – 230 nucleotides, ii) a melting temperature (Tm) between 57 and 63ºC, and iii) spans exon-exon junctions. Selected primer pairs were ordered from Integrated DNA Technologies and arrived in a lyophilized state. After a brief spin down, primers were resuspended in DEPC-treated water to a stock concentration of 1mM. To form a 10µM working concentration, 1 µl of forward and 1 µl of reverse primer was combined with 198 µl of DEPC-treated water. Working concentrations of primers were stored at -20ºC while primer stocks were kept at -80ºC.

Table 7. PCR primers

Primer	Sequence (5'-3')	Tm (^{0}C)	Amplicon Size (bp)
18S	F: GACTCATTGGCCCTGTAATTGGAATGAGTC R: GCTGCTGGCACCAGACTTG	80	87
GFP	F: CCGACCACATGAAGCAGCACGAC R: TCACGAACTCCAGCAGGACCAT	87	449
MBD3	F: GCACGGGCAAGATGCTAATG R: TCGCTCTTCACCTTGTTGCT	86	184
NANOG	F: CACCCATGCCTGAAGAAAGT R: TGCATTTGCTGGAGACTGAG	83	295

2.17.2 Standard Curve Generation

To enable relative mRNA quantification, standard curves for primer pairs had to first be generated. This involved preparing a series of log dilutions (1 to 1/1,000,000) using a purified gel extract of the gene of interest. A quantitative PCR reaction was prepared and run as described in section 2.17.3 using 2 µl of the serial dilution as the template The lower dilutions (1/10 to 1/1000) were run in triplicate while the higher dilutions (1/10,000 to 1/1,000,000) were run in quadruplicate to account for sensitivity bias. Standard curve information was exported and graphed in Microsoft Excel. A standard curve was only used for quantification equations of cDNA sample reactions if it had an amplification efficiency between 1.8 and 2.

2.17.3 Quantitative PCR

Quantitative PCR (qPCR) was used to quantify gene expression, in particular to assay for *NANOG* or *MBD3* mRNA knockdown. Reactions were prepared in LightCycler® glass capillaries with a total volume of 10 µl. The required number of capillaries were first arranged in a capillary box using sterile tweezers and left to chill at 4^{o}C while the reaction master mix was prepared. All reagents were thawed on ice and spun down briefly using a minicentrifuge. The Takara Bio SYBR® Ex Taq qPCR master mix was used for mRNA quantification and included the fluorescent DNA intercalating reagent, SYBR® green I.

The reaction master mix consisted of 5 µl of Takara master mix, 0.8 µl of combined forward & reverse primer (10µM), and 2.2 µl of DEPC-treated water,

per sample. After vortexing to mix and a brief spin down, 8 µl of reaction master mix was added to the pre-chilled glass capillaries followed by 2 µl of the respective cDNA sample. The capillaries were then sealed carefully using the capping device.

Alongside the cDNA samples, a positive template control (PTC) and a negative template control (NTC) were also set up to account for reaction success and contamination, respectively. The NTC contained 2 µl of DEPC-treated water in place of cDNA, while the PTC contained a 1/100 dilution of a purified gel extract of the gene of interest. Additionally, the RT negative was also included in each run to ensure there was no genomic DNA contamination from the cDNA synthesis reaction.

The reaction capillaries were then gently slotted into a capillary carousel and spun down using the LC Carousel Centrifuge 2.0 (3,000g, 10 sec). Any volume discrepancies were taken note of before fitting the carousel in the LightCycler machine. Using LightCycler® software, the reaction template described in Table 8 was selected.

Table 8. LightCycler® reaction template for qPCR

Step	**Temperature (^{o}C)**	**Duration**	**Cycle**
Denaturation	95	10 min	1
Amplification & Quantification	95	20 sec	45
	60	20 sec	
	72	20 sec	
Melting Curve	95	2 min	1
Cooling	4	Hold	1

Afterwards, results were analysed using LightCycler® software (Roche, Germany). A melting curve analysis was performed to verify product identity. Different primers produce different size amplicons with a varying GC content and therefore melt at a specific temperature. The NTC was not expected to produce a melting peak as it did not contain any cDNA template for the primers to amplify.

If the NTC did contain a melting peak it was either due to primer dimer formation or genomic DNA contamination and qPCR results were consequently discarded.

Each cDNA sample was given a crossing point (CP) value which corresponded to the cycling number at which they passed the threshold level of fluorescence. CP values were exported to Microsoft Excel and relative concentrations were calculated using Equation 2. The value from this equation was then divided by the relative concentration of the housekeeping gene, *18S*, to give the relative ratio.

Equation 2. How to calculate the relative concentration of the gene of interest based on the standard curve. Slope and y intercept values were taken from the primers' standard curve equation.

$$\text{Relative concentration} = e^{(-(\text{CP value} - \text{slope})/\text{y intercept})}$$

2.18 Immunocytochemistry

Immunocytochemistry (ICC) was used to detect protein on a single cell level. Cells that were cultured on round 0.78cm^2 glass coverslips were placed, using fine sterile tweezers, individually into fresh 4-well plates containing PBS. After removing the PBS by aspiration, cell were fixed in a 4% paraformaldehyde (PFA) solution for 15 minutes and then washed three times in PBS. Each wash step was carried out for 5 minutes. Cells were then incubated in quench solution for 10 minutes to minimise autofluorescence, washed once in PBS, and then permeabilised in 0.1% Triton-X for 10 minutes. After washing another two times in PBS, cells were incubated in the appropriate blocking solution for 60 minutes. Blocking solution depended on the host animal the secondary antibody was raised in and was either 5% donkey or 5% goat serum in PBS.

During blocking, wet chambers were assembled by placing a moistened circular piece of filter paper into a 10 cm Petri dish and layering on top a cut of parafilmM®. The required amount of primary antibody dilution was then prepared using blocking solution as the diluent (Table 7). Subsequently, 50 µl drops of primary antibody dilution were placed on top of the parafilmM®, ensuring there was one drop per coverslip. One coverslip per treatment was reserved as a negative immunofluorescence control. Negative controls were assigned their own

wet chamber containing 50 µl drops of blocking solution without primary antibody. After the blocking incubation, coverslips were picked up using fine tweezers and flipped on top of the primary antibody/blocking solution drops. The wet chambers were then gently sealed shut with parafilmM® and left to incubate for 60 minutes, or alternatively, at 4°C overnight.

Afterwards, coverslips were flipped cell side up into a fresh Petri dish and washed three times in PBS to remove any unbound primary antibody. During the washes, the secondary antibody/Hoechst dilution was prepared. Secondary antibodies were diluted as specified in Table 9 in blocking solution while the Hoechst 33342 nuclear stain was diluted to a working concentration of 5 µg/ml. The parafilmM® on the wet chambers was replaced and 50 µl drops of the secondary/Hoechst dilution were added on top, including on the negative coverslip dish. Coverslips were then gently flipped onto the drops and left to incubate for 60 minute under a sheet of tinfoil due to light sensitivity. Following this, coverslips were removed from the wet chamber and washed cell side up in a fresh Petri dish three times with PBS and once with distilled water. Coverslips were then mounted onto frosted glass slides (Labserv, Ireland) using 5 µl of ProLong® Diamond antifade mounting medium and left to set at 4°C for at least 30 minutes.

Table 9. Primary and secondary antibodies used for ICC

	Dilution	Source	Catalog#
Primary antibodies			
Mouse monoclonal anti-NANOG	1:100	eBioscience (USA)	14-5768
Rabbit polyclonal anti-NANOG	1:200	Peprotech (USA)	500-P236
Rabbit monoclonal anti-MBD3	1:250	Abcam (England)	EPR9913
Secondary antibodies			
AlexaFluor® 568 donkey anti-mouse IgG	1:1000	Invitrogen (USA)	A-10037
AlexaFluor® 488 donkey anti-rabbit IgG	1:1000	Invitrogen (USA)	A-21206
AlexaFluor® 568 goat anti-rabbit IgG	1:2000	Invitrogen (USA)	A-11036

Slides were visualised on the Olympus BX50 fluorescent microscope. The Hoechst stain was made visible by excitement at 405 nm (the blue channel), while red or green fluorophore-conjugated antibodies were visualised at 568 nm or 488

nm (red or green channel, respectively). Black and white images were captured by the inbuilt Spot RT3 camera, adjusting exposure times using the Spot Basic software (Spot Imaging Solutions, USA). Images were artificially coloured using the program, Image J (National Institute of Health, USA).

2.19 X-Gal Staining

X-Gal staining was used for the *lacZ* miRNA positive control experiment. To enhance the staining intensity, wash and fixing solutions were supplemented with 2mM magnesium chloride ($MgCl_2$) and 5 mM ethylene glycol tetraacetic acid (EGTA). Magnesium (Mg^{2+}) is a cofactor for the enzyme, β-galactosidase and EGTA specifically chelates calcium ions (Ca^{2+}) which would compete with Mg^{2+} for the active centre of the enzyme. In preparation for X-Gal staining, round 0.78 cm^2 glass coverslips were removed from culture dishes and placed individually into a 4-well plate containing the PBS wash solution. After a 5 minute PBS wash, cells were fixed with 4% PFA fixing solution for 15 minutes. Afterwards, cells were washed a further two times in PBS. During the washes, the staining solution was warmed to 37^0C and then used to dilute the 20x X-Gal stock to a working concentration of 1 mg/ml. The X-Gal staining solution was then incubated on the coverslips for 24 hours at 37^0C.

Afterwards, coverslips were washed once with PBS and then incubated for 6 minutes with Hoechst 33342 nuclear stain (5 µg/ml) under tinfoil. The coverslips when then washed a further two times in PBS and once in distilled water before being mounted onto frosted glass slides using 5 µl of Prolong® Diamond antifade mounting media. Glass slides were visualised on the Olympus fluorescent microscope, using the bright field to visualise blue β-galactosidase positive cells and the blue channel to visualise total cell nuclei (Hoechst stain). *LacZ* knockdown was indirectly assessed by calculating the proportion of cells that were positive for β-galactosidase.

2.20 Statistical Analyses

Protein and mRNA results were imported onto Microsoft Excel for data analysis. Replicate samples were averaged and standard deviation and standard error of the mean were calculated. Significance testing was performed using the Student's T test with $p < 0.05$ indicating significance.

Chapter Three: Results

3.1 Generation of miRNA Expression Plasmids

Specific miRNA sequences targeting either bovine NANOG or MBD3 were designed using Invitrogen's online tool, RNAi designer. For each gene, the top three most highly ranked miRNA sequences were selected and screened against the entire bovine genome. Screening confirmed that the miRNA were specific for their target as there was no sequence homology to any additional gene regions.

The BLOCK-iT^{TM} miRNA expression kit, was used to generate the miRNA expression plasmids. The miRNA sequence oligos were ligated into the BLOCK-iT^{TM} plasmid pcDNA TM6.2-GW/EmGFP-miR. The ligation reactions were then immediately used to transform bacteria which were cultured overnight under spectinomycin selection. The transformed bacterial plates were checked for colony formation the following day. Transformation was successful with over 100 colonies present on each plate and no colonies present on the negative control plate. Three to four bacterial clones were then randomly selected from each miRNA plate and were grown up overnight for a miniprep plasmid isolation.

The miRNA expression constructs contain two unique MscI restriction sites, one within the plasmid backbone and one within the miRNA loop (Fig. 9A). To validate that the transformants contained the miRNA insert, plasmid minipreps were digested with the restriction enzyme MscI and then visualised by gel electrophoresis. A positive ligation was determined by the presence of two bands, one at 1.4 kb and one at 4.3 kb. All bacterial clones gave two bands at the expected molecular size (Fig. 9B).

To ensure that none of the miRNA oligos had undergone any mutations during the preparatory reactions that could affect their specificity, plasmid minipreps (Fig. 8B 1-26) were sent to Massey Genome Service for DNA sequencing using the sequencing primers provided by the BLOCK-IT^{TM} kit. Sequencing results were analysed using the bioinformatics software Geneious which confirmed that all of

the miRNA constructs remained unchanged from the original miRNA sequence. Subsequently, one validated bacterial clone for each miRNA was then grown up for a plasmid maxiprep to ensure a large quantity of plasmid was available for mammalian cell transfections.

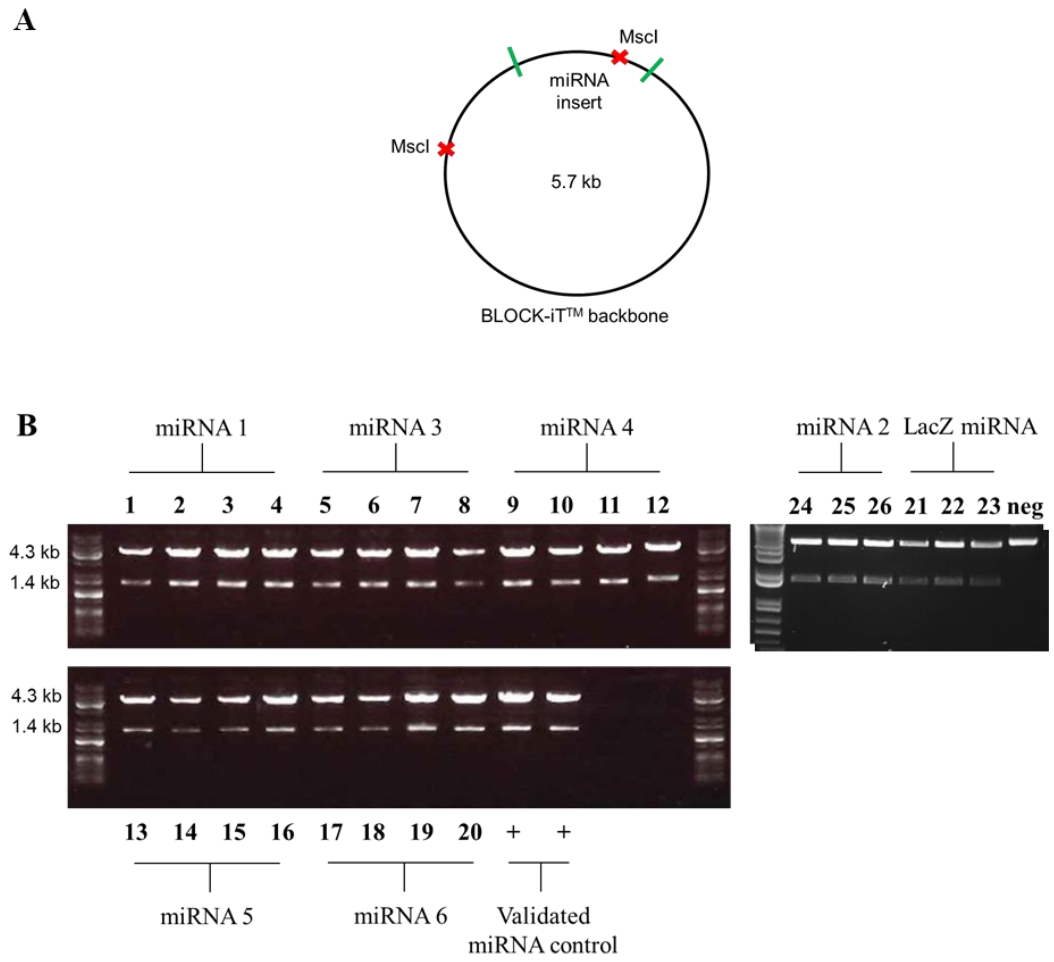

Fig. 9. MscI restriction digestion of the miRNA expression plasmids. A. Schematic representation of the BLOCK-iT™ expression plasmid showing the approximate positions of the MscI restriction enzyme cut sites. **B.** Gel electropherograms documenting the DNA fragments present after miRNA plasmids were digested with the restriction enzyme MscI. Two previously validated miRNA plasmids were used as positive controls for the restriction digest while an undigested miRNA plasmid was used as the negative restriction digest control ('neg').

3.2 Generation of an Inducible NANOG Expression Plasmid

NANOG expression is limited to the early preimplantation embryo. Therefore, a cell culture system had to first be engineered to express NANOG in order to evaluate the knockdown potential of the three NANOG miRNAs.

In our laboratory, a NANOG overexpressing bovine fetal fibroblast line, EOG-TET-NANOG, had already been engineered and was initially selected for screening the *NANOG* miRNAs. However, after several transient knockdown attempts which failed to show a reduction in NANOG protein or mRNA expression (data not shown), we discovered that the *NANOG* transgene within the line had been extensively codon-optimised during synthesis. Using Geneious pairwise alignment, the codon-optimised *NANOG* transgene was found to be only 77% identical to the endogenous sequence of *NANOG*. Furthermore, none of the three NANOG miRNAs were able to correctly align with the codon-optimised *NANOG* transgene. Because of the degree of codon optimisation, the bovine overexpressing NANOG line could no longer be used for miRNA screening purposes and a new NANOG expressing cell line was prepared.

The new *NANOG* transgene was designed using GeneArt Strings^{TM} DNA fragment (Life Technologies, USA) and consisted of the entire endogenous coding sequence for bovine *NANOG* flanked by a 5' SalI and 3' NotI restriction enzyme cut site to facilitate cloning into the inducible piggyBac expression plasmid.

3.2.1 TOPO-TA Plasmid Cloning and Validation

Before the *NANOG* fragment could be ligated into the inducible piggyBac expression plasmid, PB-TRE, it was first cloned into the intermediary plasmid, TOPO-TA. Bacteria transformed with the TOPO-NANOG ligation reaction were cultured overnight under kanamycin selection. The following day, many colonies were present on the positive transformation plate. Four colonies were selected at random to be cultured on for a plasmid miniprep.

To confirm that the bacterial clones contained the *NANOG* fragment, each plasmid miniprep was digested with the restriction enzymes SalI and NotI and the

resulting DNA fragments were visualised by gel electrophoresis. A positive ligation should result in three DNA fragments; one at 4 kb (TOPO backbone), one at 900 bp (*NANOG* fragment) and a smaller fragment of about 35 bp (Fig. 10A). The smallest fragment, which is due to a NotI site within the TOPO backbone, is too small to be detected on the agarose gel. Of the four bacterial clones, only one had correctly ligated the *NANOG* fragment (Fig. 10B). The validated miniprep (miniprep 30) was then sent away for DNA sequencing using M13 forward and reverse sequencing primers. Sequencing results confirmed that the *NANOG* insert remained unchanged from the original sequence.

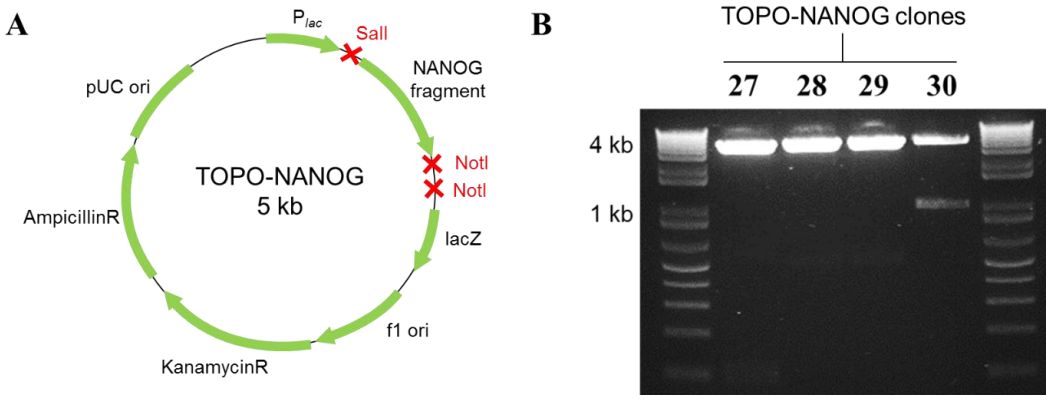

Fig. 10. SalI/NotI restriction digestion of the TOPO-NANOG plasmid. A. Schematic representation of the TOPO-NANOG plasmid showing the approximate positions of the SalI and NotI restriction enzyme cut sites. **B.** Gel electropherogram of a SalI/NotI restriction digestion showing that only one of the four bacterial TOPO-NANOG clones had correctly ligated the *NANOG* plasmid.

3.2.2 PB-TRE Plasmid Cloning and Validation

After excising the *NANOG* fragment from the TOPO-TA plasmid with restriction enzymes, the fragment now had the required SalI and NotI sticky ends required for cloning into the inducible PB-TRE plasmid. To isolate the *NANOG* fragment, the remaining digest reaction was run on an agarose gel. Adjacent to the DNA ladder, was a *NANOG* indicator lane. This lane contained only 5 µl of the digest reaction and was used to indicate where the *NANOG* fragment would be located. The adjacent three wells were filled with the remaining digest reaction and, to avoid DNA damage, these lanes were not exposed to UV. Thus, the 900 bp band in the indicator lane was excised using a scalpel blade and used to guide the excision of the 900 bp *NANOG* fragment from the unexposed lanes.

The unexposed *NANOG* fragment was extracted from the gel and quantified using the Nanodrop. The fragment was then ligated into the PB-TRE plasmid and transformed bacteria were cultured overnight under ampicillin selection. Transformation plates were checked for colony formation the following day and hundreds of colonies were present on the positive transformation plate. Six colonies were then randomly selected to be grown up for a plasmid miniprep.

Plasmid validation was performed by digesting the plasmid minipreps with SalI and NotI. Positive clones should give rise to bands of 6.6 kb (PB-TRE backbone) and 900 bp (*NANOG* fragment) (Fig. 11A). Five of the six bacterial clones exhibited the expected pattern of bands confirming they had correctly ligated the *NANOG* fragment (Fig. 11B 32-36). In addition, two plasmid minipreps (32 and 33) were selected for DNA sequencing. Sequencing results confirmed that the *NANOG* fragment had not undergone any mutations during the preparatory reactions. One of the validated bacterial clones was then grown up for a plasmid maxiprep ensuring a large volume of plasmid was available for transfection experiments.

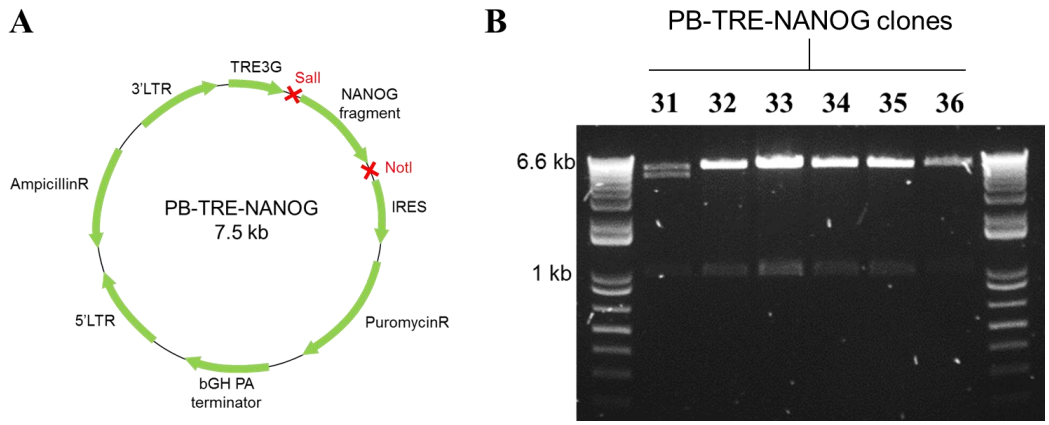

Fig. 11. **SalI/NotI restriction digestion of the PB-TRE-NANOG plasmid. A.** Schematic representation of the PB-TRE-NANOG plasmid showing the approximate position of the SalI and NotI restriction enzyme cut sites. **B.** Gel electropherogram showing the result of a SalI/NotI restriction digestion on PB-TRE-NANOG bacterial clones. All six bacterial clones gave rise to two bands, one at 6.6 kb (PB-TRE backbone) and one at 900 bp (*NANOG* fragment).

3.3 Generation of a NANOG Expressing Cell Line

3.3.1 Bovine NANOG Cell Line

Transfection of EF5-TET Cells with PB-TRE-NANOG

The bovine EF5-TET line was selected for transfection of the NANOG expression plasmid because it already contained the rtTA transgene required for inducible expression. Using the Lipofectamine® LTX protocol, approximately 1 x 10^6 passage 4 EF5-TET cells were cotransfected with 15 µg of PB-TRE-NANOG and 3 µg of the PBase plasmid, pCyL43. As a positive transfection control, 1 x 10^4 EF5-TET cells were transfected with 1 µg of the GFP plasmid, pMAX. All EF5-TET cells were induced with 2 µg/µl of doxycycline just prior to transfection. The following day, the pMAX dish was visualised on the EVOS fluorescent microscope which confirmed around a 30% transfection efficiency. The transfection efficiency of the PB-TRE-NANOG dish could not be determined as the plasmid did not contain a fluorescent marker. The cells transfected with the *NANOG* plasmid were then split across three new 10 cm tissue culture dishes at a density of 2 x 10^5 cells per dish. The pMAX dish was passaged onto a 6 cm tissue culture dish at a cell density of 2 x 10^4.

Subcloning of EF5-TET Cells

Approximately 48 hours post-transfection, base media and doxycycline were refreshed on all dishes and the selection antibiotic, puromycin, was added at a concentration of 1 µg/ml. These media conditions were refreshed every 48 hours and selection plates were monitored daily for colony formation. After 8 days of puromycin selection, 28 distinct cell colonies on the PB-TRE-NANOG plates were ready for transfer to individual wells. By contrast, all cells on the negative selection plate pMAX had died within 4 days of selection.

Cell clones were individually grown up continually in the presence of doxycycline and puromycin. Of the 28 colonies initially seeded onto a 48-well plate, 22 were passaged up onto 12-well plates and then 19 of those were passaged up to 6-well plates. However, the majority of cell clones which were seeded onto a 6-well plate flattened out, grew large processes, and stopped dividing. Only seven cell clones were able to grow to about 50% confluence on the 6-well plate at which point

they were harvested for NANOG expression analysis. Approximately 1 x 10^4 cells were taken for RNA extraction and cDNA synthesis. Another 1 x 10^4 cells were seeded onto a 4-well plate containing glass coverslips, and the remaining cells were cryopreserved across three cryovials.

Validation of EF5-TET NANOG Clones

To validate that the surviving clones expressed and produced NANOG, cells that had been seeded onto glass coverslips were stained for NANOG via ICC. Cells were blocked in 5% donkey serum and incubated with the Peprotech polyclonal rabbit NANOG antibody and the green AlexaFluor® donkey anti-rabbit 488 secondary antibody. NANOG expression in the seven different NANOG clones was compared to a non-transfected EF5-TET control sample which did not express any NANOG. All seven NANOG clones (A4, A6, A8, B8, C1, C8, D1) were positive for NANOG expression which was nuclear in localisation but absent within the nucleoli (Fig. 12). Intensity of fluorescence was not measured directly but all seven clones had similar NANOG staining intensities. Importantly, the negative ICC control and the non-transfected EF5-TET cells were both negative for NANOG expression.

The cDNA samples from the NANOG clones were then assayed for *NANOG* mRNA expression by qPCR. Relative *NANOG* concentration values were divided by their respective *18S* values to give the relative ratio. A non-transfected EF5-TET cDNA sample was used as a baseline comparison. Six out of the seven NANOG clones were found to have a significantly higher expression of *NANOG* compared to the EF5-TET parental line (Fig. 13). NANOG clone D1 had the largest fold difference in *NANOG* expression (67 fold), followed by A4 (59 fold), B8 (48.4 fold), and A8 (37 fold). The three remaining NANOG clones, C1, C8, and A6, had only slight fold differences in *NANOG* expression (5, 2 and 1.4 fold, respectively).

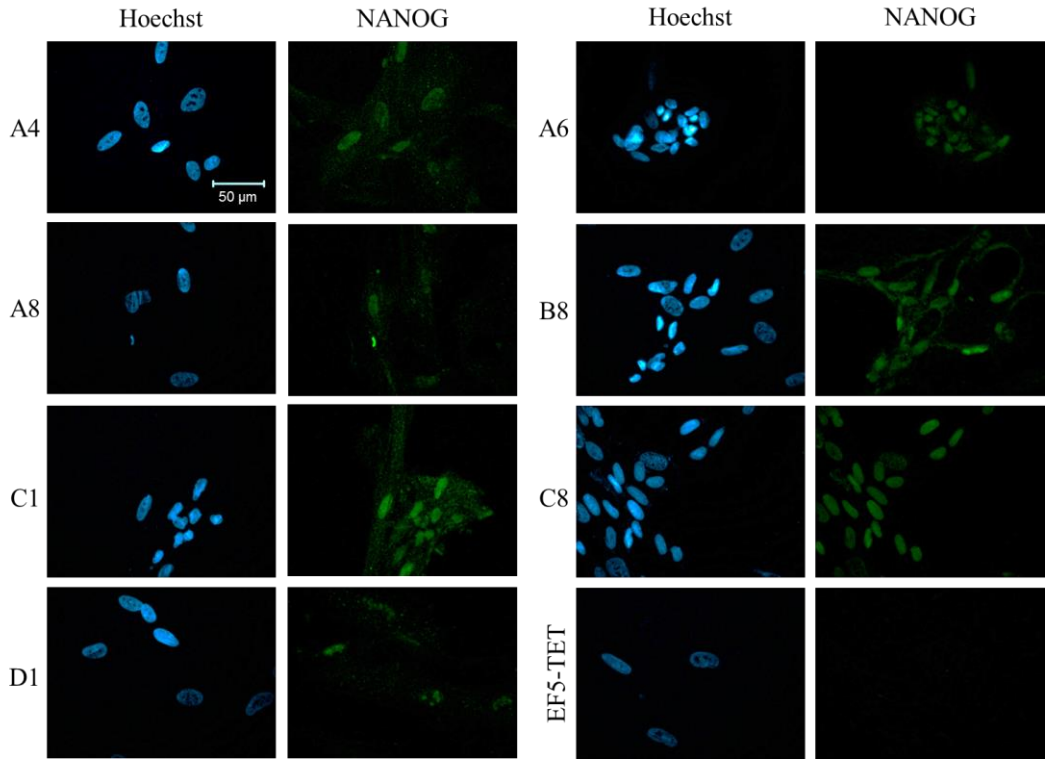

Fig. 12. ICC staining for NANOG on seven stably transfected EF5-TET clones. Black and white images were captured using the Olympus fluorescent microscope and were pseudo-coloured using ImageJ. Scale bar = 50 µm

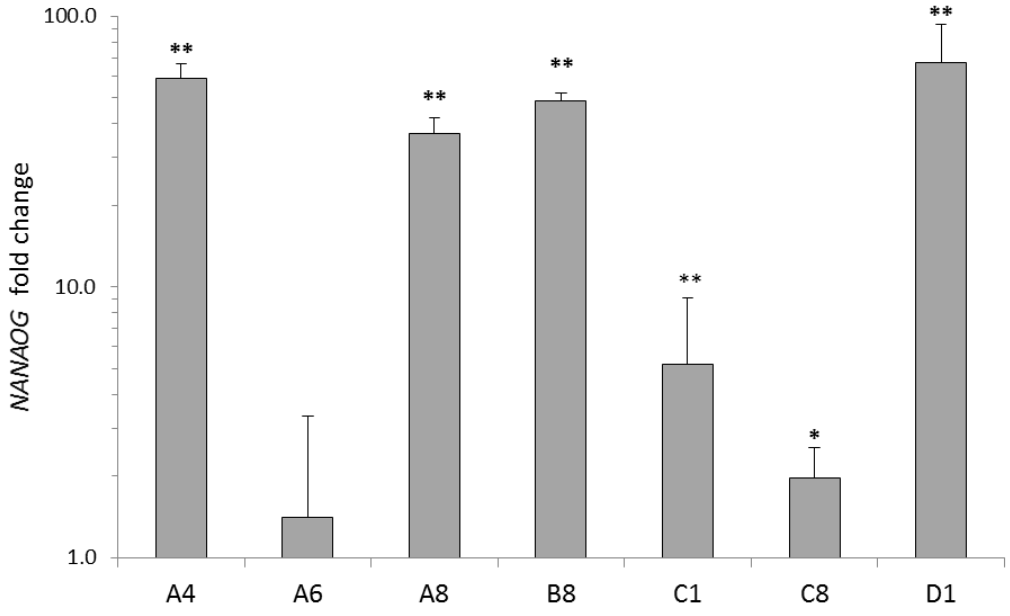

Fig. 13. Quantification of *NANOG* mRNA expression in seven stably transfected EF5-TET clones. *NANOG* expression represents the fold difference over the parental cell line, EF5-TET. Error bars based on SEM for technical triplicates, *P < 0.05, ** P < 0.01

Immortalisation of EF5-TET NANOG Clones

To further characterise the NANOG clones, one cryovial from each NANOG-expressing clone was thawed and seeded onto a 96-well 0.1% gelatin-coated culture plate containing 2 µg/µl of doxycycline. It soon became clear that the NANOG clones had reached their Hayflick (cycling) limit and had begun to enter cellular senescence. In an attempt to preserve the NANOG clones and direct them to divide again, they were transfected with the oncogene plasmid pC-MYC using the Lipofectamine® LTX protocol. Just like the PB-TRE-NANOG plasmid, pC-MYC also contains a TRE promoter and administration of doxycycline is required for the rtTA to activate expression of the *C-MYC* transgene as well as a monomeric (m) red fluorescent protein (RFP) reporter (mCherry).

The NANOG clones had been cultured in doxycycline for a period of three days prior to pC-MYC transfection. Additionally, three adjacent wells were each seeded with 1 x 10^4 EF5-TET cells to act as transfection controls. All seven NANOG clone wells and the first EF5-TET well were transfected with pC-MYC in the presence of 2 µg/µl doxycycline. The remaining two EF5-TET wells were not induced with doxycycline and were transfected with either pC-MYC or the GFP plasmid, pMAX.

The culture plate was analysed 24 hours post-transfection using the EVOS fluorescent microscope. The pMAX control well revealed that the transfection reaction had been successful with an efficiency of approximately 30%. Similarly, the EF5-TET well transfected with pC-MYC in the presence of doxycycline contained a number of RFP positive cells, with an estimated transfection efficiency of 30%. As expected, the non-doxycycline induced EF5-TET well contained no cells positive for RFP. Despite doxycycline-induction, no RFP positive cells were detected in any of the NANOG clone wells after transfection with pC-MYC (Fig. 14). Cells were continually monitored for two weeks following transfection but no cell growth was observed for the NANOG clones.

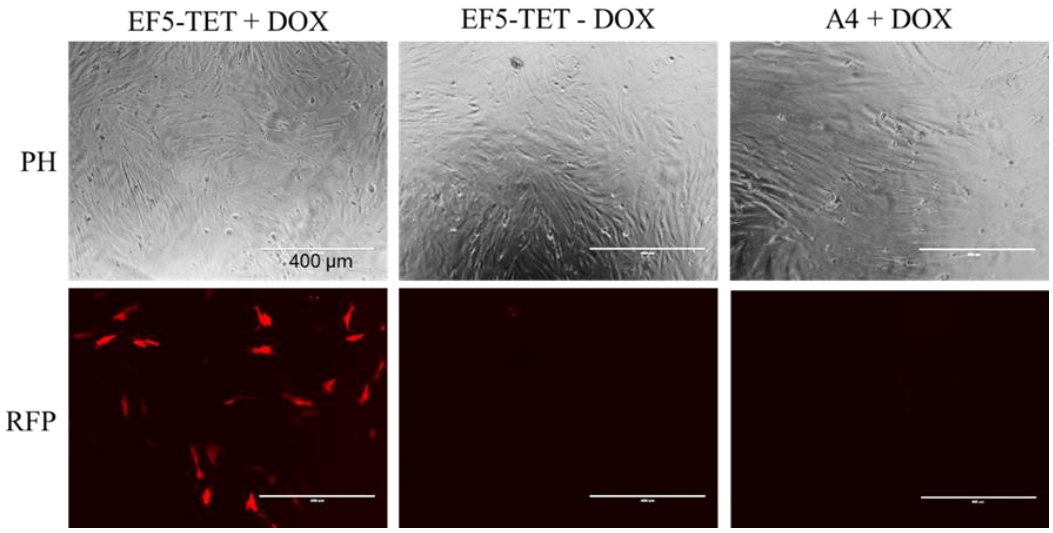

Fig. 14. Transfection efficiencies 24 hours after transfection of EF5-TET clones and EF5-TET controls with pC-MYC. Transfection performed using Lipofectamine® LTX. EF5-TET controls included a + DOX (2 µg/µl doxycycline) and – DOX (no doxycycline) group. Transfection efficiency was determined by the approximate proportion of RFP positive cells per field of view. All EF5-TET clones were negative for RFP as shown in the A4 + DOX column. Images were captured on the EVOS fluorescent microscope. PH = phase contrast. RFP = red fluorescent protein. Scale bar = 400 µm

3.3.2 HeLa NANOG Cell Line

Transfection of HeLa Cells with PB-TRE-NANOG and PB-CAG-rtTA

To circumvent issues with cellular senescence, the PB-TRE-NANOG expression plasmid was instead transfected into the immortalised human cancer cell line HeLa. Unlike the transgenic EF5-TET line, HeLa cells did not already contain the rtTA which meant a triple transfection was required. Approximately 2 x 10^6 HeLa cells were transfected with PB-TRE-NANOG (7.5 kb), PB-CAG-rtTA (7 kb), and pCyL43 (4 kb) at either an 8:1:1 or 5:4:1 molar ratio. To boost transfection efficiencies, the Neon™ electroporation protocol was used over the less efficient Lipofectamine® LTX method. A positive transfection control was also included by transfecting 1 x 10^5 cells with 0.5 µg of pMAX. Transfected cells were induced 2 hours post electroporation with 2 µg/µl of doxycycline to switch on expression of the PB-TRE-NANOG transgenes which also included the puromycin resistance gene. The following day (24 h post-transfection) the pMAX dish was analysed

under the EVOS fluorescent microscope which revealed a high transfection efficiency of around 70%. The transfection efficiency of the triple transfected HeLa dishes could not be determined due to the lack of a fluorescent reporter. Consistent with previous electroporation experiments, a high cell death rate of around 50% was observed. Transfected cells were subsequently split 1 to 4 onto fresh culture dishes and continually cultured in the presence of doxycycline.

Subcloning of HeLa Cells

Puromycin selection was initiated 48 hours post-transfection at a concentration of 1 µg/ml. HeLa cells were spread thin across the culture plate but mitotically dividing cells were still visible. Selection media, which was also supplemented with doxycycline, was replenished every 48 hours. After eight days under selection, one small HeLa colony was discovered on one of the 5:4:1 transfection plate, and 3 very small colonies (<10 cells) were discovered on the 8:1:1 transfection plates. On the 12^{th} day of selection, all four colonies were transferred to a 96-well 0.1% gelatin coated plate and continually cultured in the presence of puromycin and doxycycline. The three small colonies from the 8:1:1 plates did not grow after replating and underwent apoptosis. By contrast, the larger HeLa colony continued to grow, albeit at a slow pace, filling up a 10 cm culture dish after two weeks in individual culture.

Validation of the Puromycin Resistant HeLa Clone

The 10 cm puromycin resistant HeLa clone was harvested and 1 x 10^4 cells were taken for RNA extraction and cDNA synthesis while 1 x 10^5 were seeded onto a 3 cm culture dish containing glass coverslips. The remaining cells were frozen across three cryovials. The HeLa cells were fixed with 4% PFA on the glass coverslips and ICC was performed using the Peprotech rabbit polyclonal NANOG antibody and the AlexaFluor® 488 donkey anti-rabbit secondary antibody. A non-transfected HeLa control was included for baseline comparisons as well as a negative ICC control. Both the non-transfected HeLa control and the puromycin resistant HeLa clone were not positive for NANOG expression (data not shown). In agreement with the protein data, no NANOG expression was detectable by qPCR analysis of the HeLa clone cDNA sample suggesting that although the cells were puromycin resistant, they were not expressing the NANOG transgene.

3.4 miRNA-mediated Knockdown of NANOG

3.4.1 Generation of a Constitutive NANOG Expression Plasmid

For simplicity, a constitutive NANOG expression plasmid was prepared as a replacement for the inducible PB-TRE-NANOG plasmid. The *NANOG* fragment that was initially ligated into the PB-TRE plasmid, was ligated into a linearized CMV plasmid derived from pEGFP-N1 (Fig. 15A) and used to transform bacteria which were cultured overnight under kanamycin selection. Transformation was successful with hundreds of colonies present on the positive plate, of which, four were randomly selected to be grown up for a miniprep. A SalI/NotI restriction digest on the four minipreps revealed that all four clones had correctly ligated the *NANOG* expression plasmid giving the expected pattern of bands; one at 3.9 kb (CMV backbone) and one at 900 bp (*NANOG* fragment) (Fig. 15B).

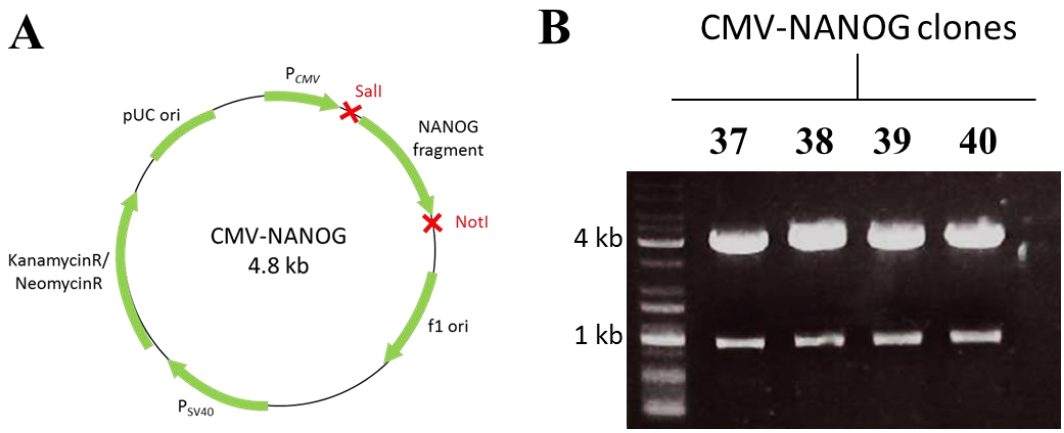

Fig. 15. SalI/NotI restriction digestion of the CMV-NANOG plasmid. A. Schematic representation of the CMV-NANOG plasmid showing the approximate position of the SalI and NotI restriction enzyme cut sites. **B.** Gel electropherogram of a SalI/NotI restriction digestion showing that all four bacterial CMV-NANOG clones had correctly ligated the *NANOG* plasmid.

To validate the CMV-NANOG plasmid for NANOG expression, one of the minipreps (miniprep 38) was transfected using the Lipofectamine® LTX protocol into a 3 cm dish of passage 5 BEFs. The following day, glass coverslips were removed from the culture dish and ICC was performed using the eBioscience mouse monoclonal NANOG antibody and the red Alexafluor® donkey anti-mouse secondary antibody (Fig. 16). The NANOG stain was specific and nuclear

localised. A non-transfected control remained negative for NANOG expression as did the negative ICC control. Transfection efficiency, based on the number of NANOG positive cells, was estimated to be around 35%. The validated miniprep was then used for all subsequent transfection experiments.

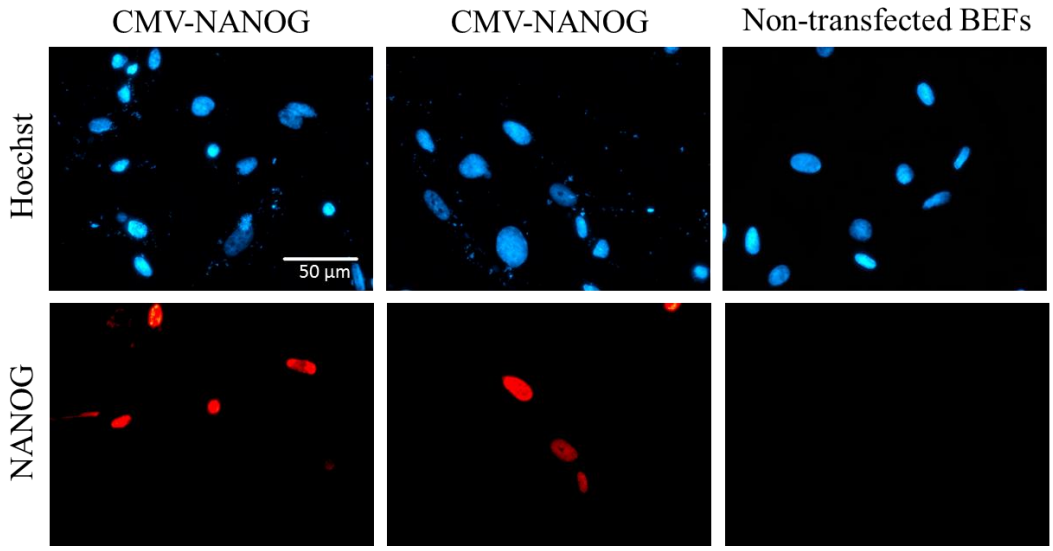

Fig. 16. ICC staining for NANOG after transient transfection with the CMV-NANOG plasmid. Black and white images were captured using the Olympus fluorescent microscope and were pseudo-coloured using ImageJ. Scale bar = 50 µm

3.4.2 Cotransfection of BEFs with CMV-NANOG and NANOG miRNAs

To determine the knockdown potential of the NANOG miRNAs, a cotransfection approach was undertaken whereby each miRNA was cotransfected into BEFs along with the NANOG expression plasmid, CMV-NANOG. Two days prior to transfection, passage five BEFs were thawed and seeded on 12-well plates containing round glass coverslips. On the day of transfection, cells were about 80% confluent. The Lipofectamine® LTX protocol was used to cotransfect the CMV-NANOG plasmid with the miRNA plasmids at a 1:1 molar ratio. To determine efficiency and specificity of knockdown, the negative miRNA plasmid and the pMAX plasmid, respectively, were cotransfected with CMV-NANOG. A non-transfected control was also included. Each transfection experiment was performed in triplicate.

Cells were visualised on the EVOS fluorescent microscope 24 hours after transfection. Transfection efficiencies, based on the number of GFP positive cells,

varied between the miRNA plasmids and were around 15 – 30%. Subsequently, coverslips were removed from each treatment well and ICC was performed using the eBioscience mouse monoclonal NANOG antibody and the red Alexafluor® donkey anti-mouse IgG secondary antibody (Fig. 17). As expected, not every cells which was took in the miRNA plasmid also took in the CMV-NANOG plasmid. On the negative miRNA control coverslips, an average of 40% of GFP positive cells were also positive for NANOG. To quantify NANOG knockdown, ten photos were taken from random fields of view for each coverslip. The number of GFP positive cells that were also positive for NANOG was then counted and divided by the total number of GFP positive cells. Proportions for each NANOG miRNA coverslip were normalised on the negative miRNA control proportion to account for the fact that not all cells would have taken in both plasmids.

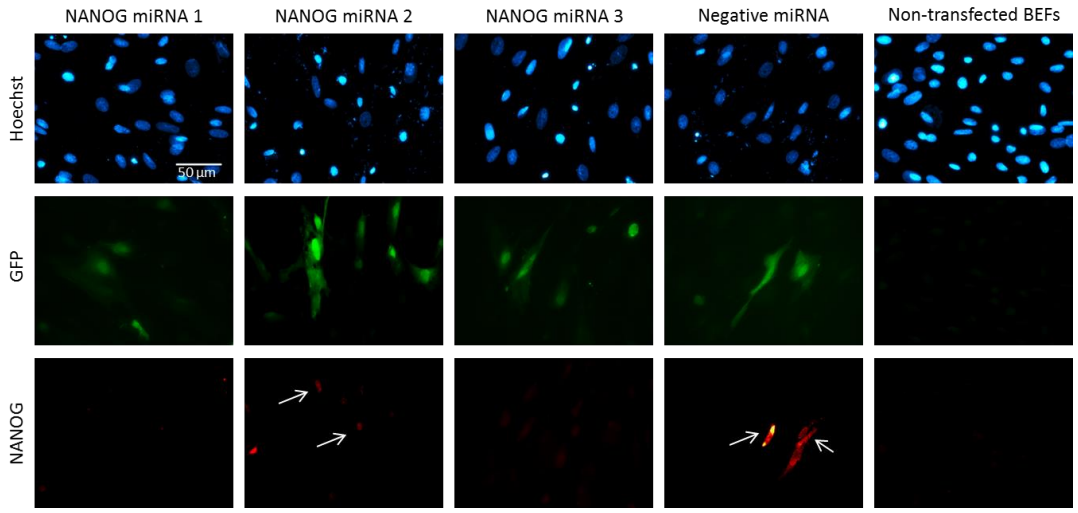

Fig. 17. ICC staining for NANOG after transient cotransfection of BEFs with CMV-NANOG and NANOG miRNAs. White arrows indicate NANOG positive cells which are also positive for GFP. Black and white images were captured on the Olympus fluorescent microscope and were pseudo-coloured on ImageJ. Scale bar = 50 µm.

The knockdown efficiencies for each miRNA were then determined which revealed all three NANOG miRNAs had a significant knockdown effect on bovine NANOG (Fig. 18). On average, miRNA 3 had the highest knockdown efficiency of 89.1% ($P = 0.0007$), followed by miRNA 2 with an 87.3% knockdown ($P = 0.0029$), and miRNA 1 with an 80.1% knockdown ($P = 0.0014$). Although significantly different from the negative miRNA control, the three

miRNAs were not significantly different from each other suggesting any of the three could be used for targeting endogenous NANOG in bovine embryos. The knockdown effect exhibited by the NANOG miRNAs was also found to be specific as the negative miRNA control exhibited no reduction in NANOG expression when compared to the pMAX transfected control (data not shown).

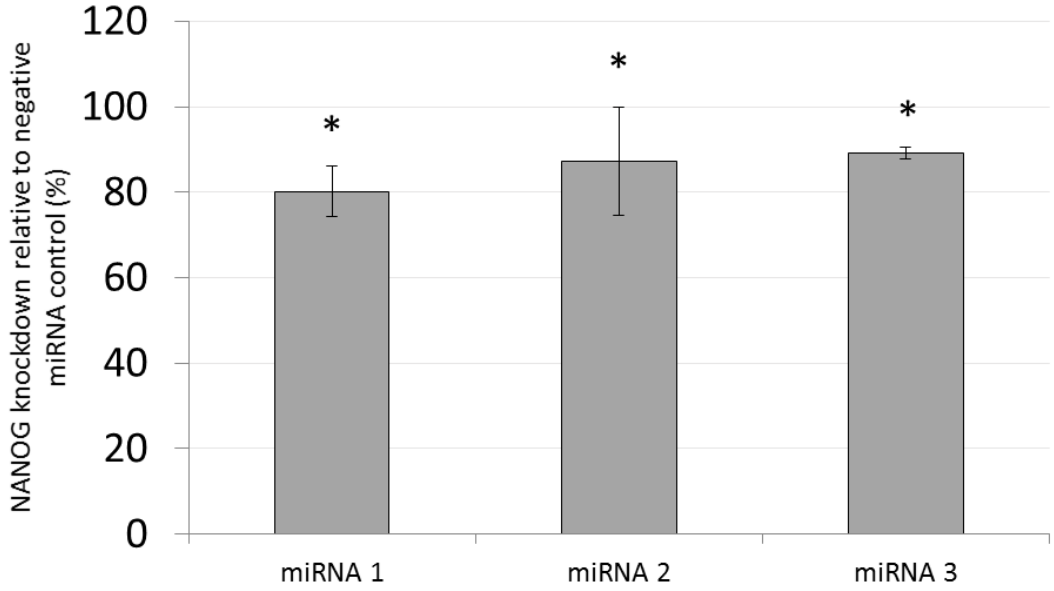

Fig. 18. Percentage of NANOG knockdown in BEFs transiently cotransfected with CMV-NANOG and NANOG miRNAs. Knockdown percentage of the NANOG miRNAs is expressed relative to the negative miRNA control. Error bars based on SEM for biological replicates (n = 3), *P < 0.05

The remaining cells from the transient cotransfection experiments were harvested for RNA extraction, followed by cDNA synthesis. The expression of *NANOG* and *GFP* was then investigated by qPCR. To account for differences in transfection efficiencies, *NANOG* expression levels were normalised on *GFP* expression. Compared to the negative miRNA control, *NANOG* expression levels appeared slightly reduced in the NANOG miRNA treated samples but these reductions were not found to be significant (miRNA 1, P = 0.18; miRNA 2, P = 0.32; miRNA 3, P = 0.45) (Fig. 19).

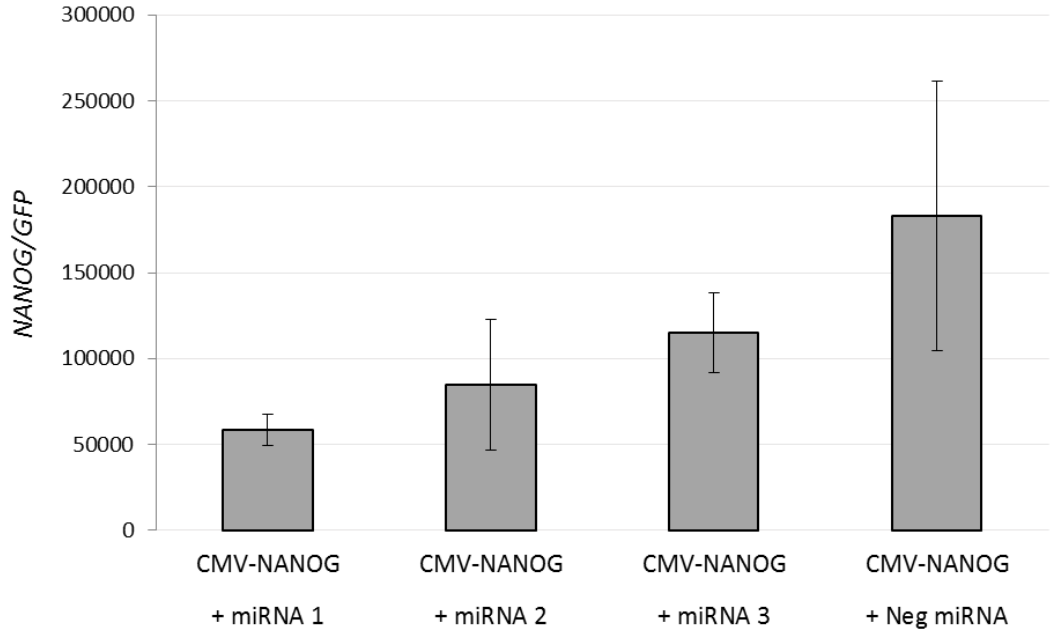

Fig. 19. Relative *NANOG* expression in BEFs transiently cotransfected with CMV-NANOG and NANOG miRNAs. *NANOG* expression normalised against *GFP* expression. Neg miRNA = Negative miRNA. Error bars based on the SEM for biological replicates (n = 3).

3.5 miRNA-mediated Knockdown of MBD3

3.5.1 Transient Knockdown in BEFs

A transient (24 h) MBD3 knockdown experiment was performed in BEFs to obtain a quick estimation of which miRNA plasmid had the most potent knockdown potential. Each MBD3 miRNA plasmid, as well as the negative miRNA control plasmid were individually transfected into 1 x 10^6 BEF cells via Neon^{TM} electroporation. After 24 hours, cells were visualised on the EVOS fluorescent microscope. Phase contrast images were taken to document cell density while GFP images were captured in the green fluorescent channel to estimate the transfection efficiency. Cell viability was found to be severely compromised by the transfection protocol with approximately 50% cell death. Transfection efficiency, based on the number of GFP positive cells, was also lower than expected at approximately 20%. The experiment was repeated twice more in BEFs using the Lipofectamine® LTX protocol which did not compromise cell viability. Cells were transfected in a 24-well format. Transfection efficiencies

were similar to the initial Neon™ electroporation transfection and ranged between 30 – 35%.

Knockdown potential was determined by ICC and qPCR analysis. Surprisingly, no difference in MBD3 protein expression was observed between cells transfected with either one of the MBD3 miRNA plasmids or the negative miRNA control plasmid (Fig. 20). The MBD3 stain was found to be almost entirely nuclear specific. Focusing specifically on cells with the highest GFP intensity (i.e. should be highly expressing the MBD3 miRNA), there was no difference in intensity of MBD3 compared to cells which were not GFP positive (i.e. were not expressing the MBD3 miRNA plasmid).

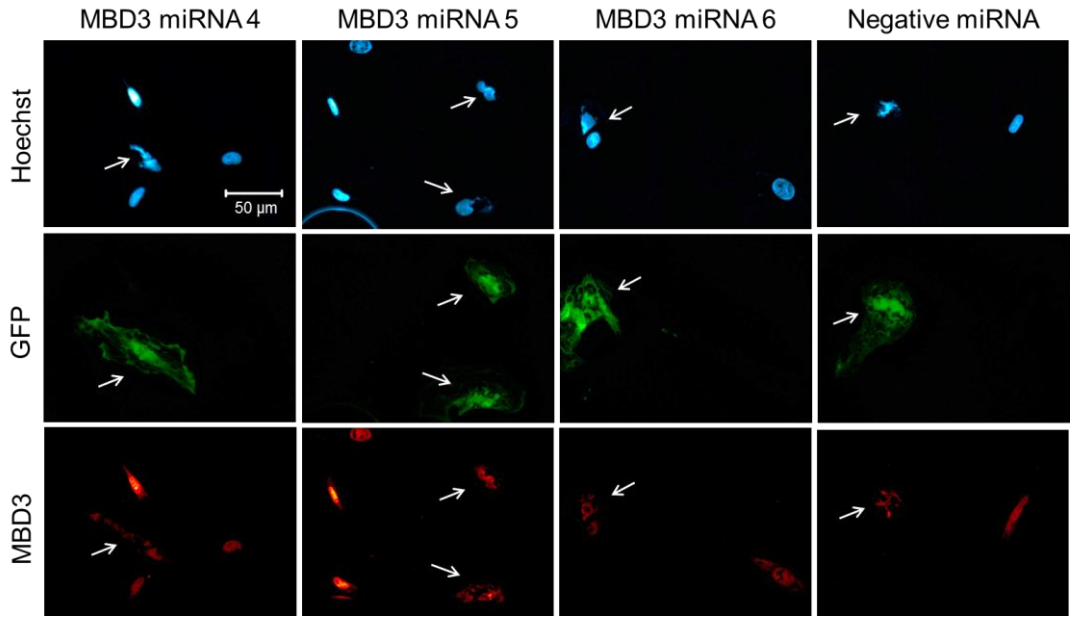

Fig. 20. ICC staining for MBD3 after transient transfection of BEFs with MBD3 miRNAs. ICC staining for MBD3 focusing on cells which have a high GFP expression. White arrows identify the oddly shaped nuclei of the GFP expressing cells. Black and white images were captured on the Olympus fluorescent microscope and were pseudo-coloured using ImageJ.

Interestingly, cells which were GFP positive exhibited oddly shaped nuclei. This unusual artefact was observed not only in the MBD3 miRNA transfected cells but also in cells transfected with the negative miRNA control. This would suggest that an abnormally shaped nucleus was related in some part to the BLOCK-iT™ miRNA expression plasmid rather than a specific effect of MBD3 knockdown. In

agreement with the protein data, no significant *MBD3* knockdown was observed on the mRNA level (Fig. 21).

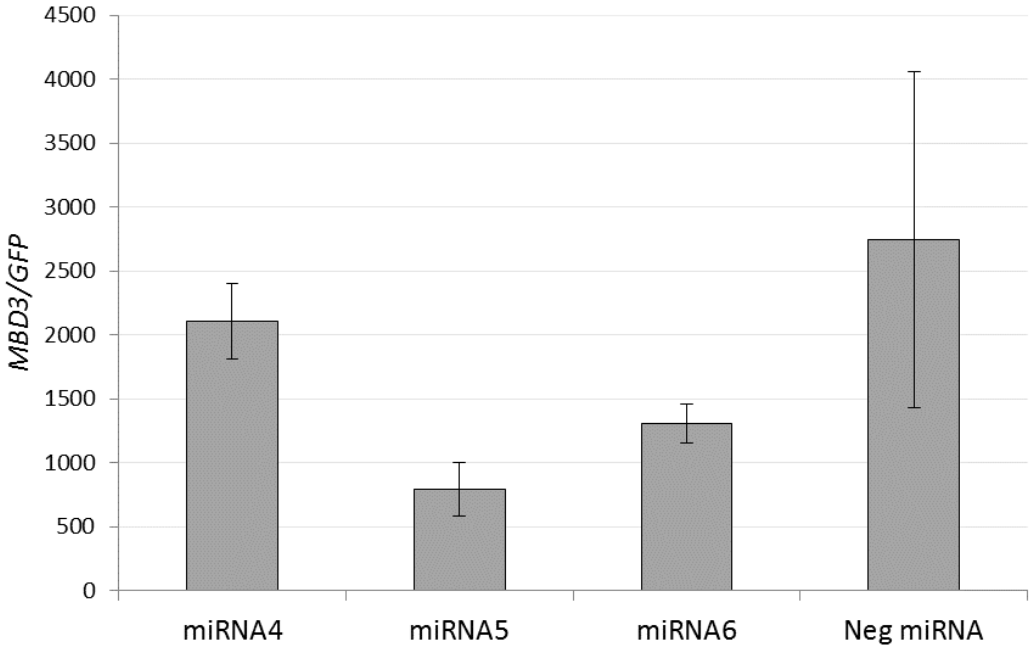

Fig. 21. Relative *MBD3* expression in BEFs transiently transfected with MBD3 miRNAs. *MBD3* expression normalised against *GFP* expression. Neg miRNA = Negative miRNA**.** Error bars based on SEM for biological replicates (n = 3).

3.5.2 MBD3 Half-Life Experiment

In an attempt to explain why no miRNA-mediated knockdown of MBD3 was observed after 24 hours, an experiment was designed to determine the protein half-life of MBD3. Approximately 5 x 10^5 passage 9 BEFs were thawed and seeded onto a 6 cm culture dish containing 12 round glass coverslips. The following day, cells were treated with 10 µg/ml cycloheximide to inhibit protein translation. Two coverslip were removed just prior to act as the negative ICC control and the 0 hour (h) protein control (t_0). The other coverslips were then removed at the following time points: 6 h, 12 h, 24 h, 36 h, 48 h, 63 h, 72 h, 88 h, 96 h, 112 h. To maintain the level of cycloheximide, base media and cycloheximide were replaced at the 63h time point.

Once removed, coverslips were fixed with 4% PFA for 15 minutes, washed three times with PBS and then stored at 4^0C. After all coverslips had been fixed, the presence of MBD3 was assessed by ICC (Fig. 22). Expression of the MBD3

protein could still be detected even after 112 h of inhibiting protein synthesis. MBD3 expression was consistently nuclear in localisation and its staining intensity was reduced the longer protein translation was inhibited.

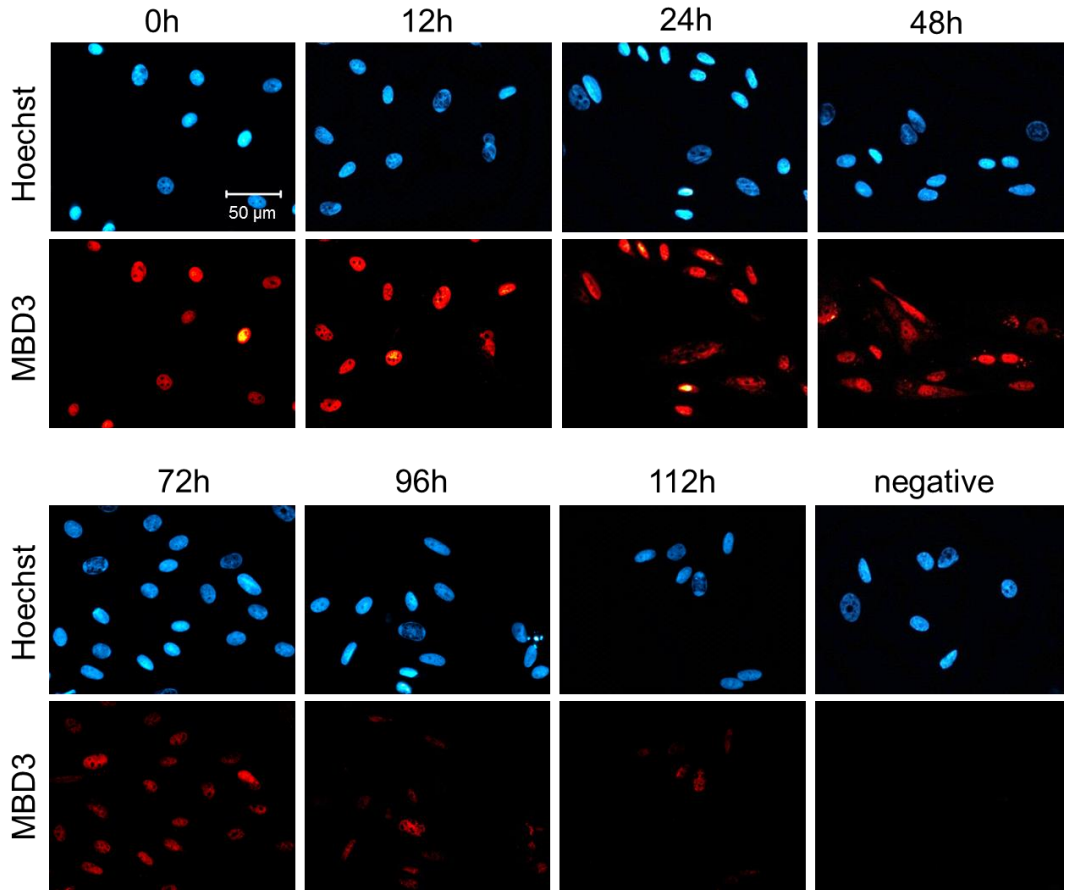

Fig. 22. ICC staining for MBD3 on cells exposed to cycloheximide for 0 – 112 hours. Black and white images were captured using the Olympus fluorescent microscope and were pseudo-coloured using ImageJ. Scale bar = 50 µm

To determine the half-life of the protein, ICC images were opened on ImageJ and the area and pixel-intensity (PI) of ten nuclei from each time point were measured. The PI measurements were then subtracted by the average of three background PI measurements taken from random background positions. The adjusted PI measurements were then normalised against their respective area measurement. For each time point, the ten normalised PI measurements were averaged and then expressed as a fold change over the t_0 measurement (Fig. 23). The linear regression estimated the half-life of MBD3 to be approximately 48 hours.

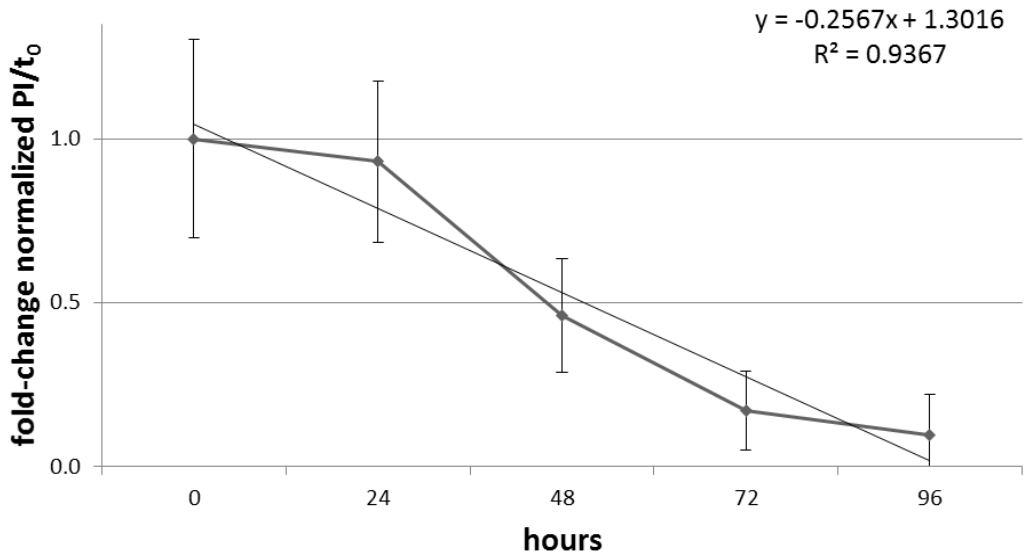

Fig. 23. MBD3 half-life estimate. Nuclei from cells treated with the protein translation inhibitor cycloheximide for 0 to 96 h were quantified for MBD3 expression by measuring their pixel-intensity (PI) from ICC images on ImageJ. PI values for 24, 48, 72, and 96 h time points were normalised on nuclei area are expressed as a fold-change over the 0 h time point (t_o). A linear regression trendline has been plotted and the equation and correlation coefficient (R^2) are displayed. Error bars represent SEM for biological replicates (N=10).

3.6 Stable Knockdown of NANOG and MBD3

3.6.1 Blasticidin Kill Experiment

The practicality of the BLOCK-iT^{TM} miRNA expression system for embryo research relies on its ability to generate stable knockdown cell lines which can then be used for SCNT. To select for stable transfectants that had integrated the miRNA plasmid into the genome, the optimal concentration of blasticidin for selection in bovine cells had to first be determined.

A previous experiment had already shown that 5 µg/ml of blasticidin was sufficient to kill 100% of BEFs within a week (data not shown). To determine the optimal concentration for the EF5-TET bovine line, $1x10^6$ EF5-TET cells were thawed and split across a 6-well plate. The following day, an image was captured on the EVOS fluorescent microscope to document cell density. Thereafter, cells were treated with either 0, 2, 4, 6, 8, or 10 µg/ml of blasticidin. Selection media was refreshed every 48 hours and photos were captured every day to qualitatively document the rate of cell death (Fig. 24)

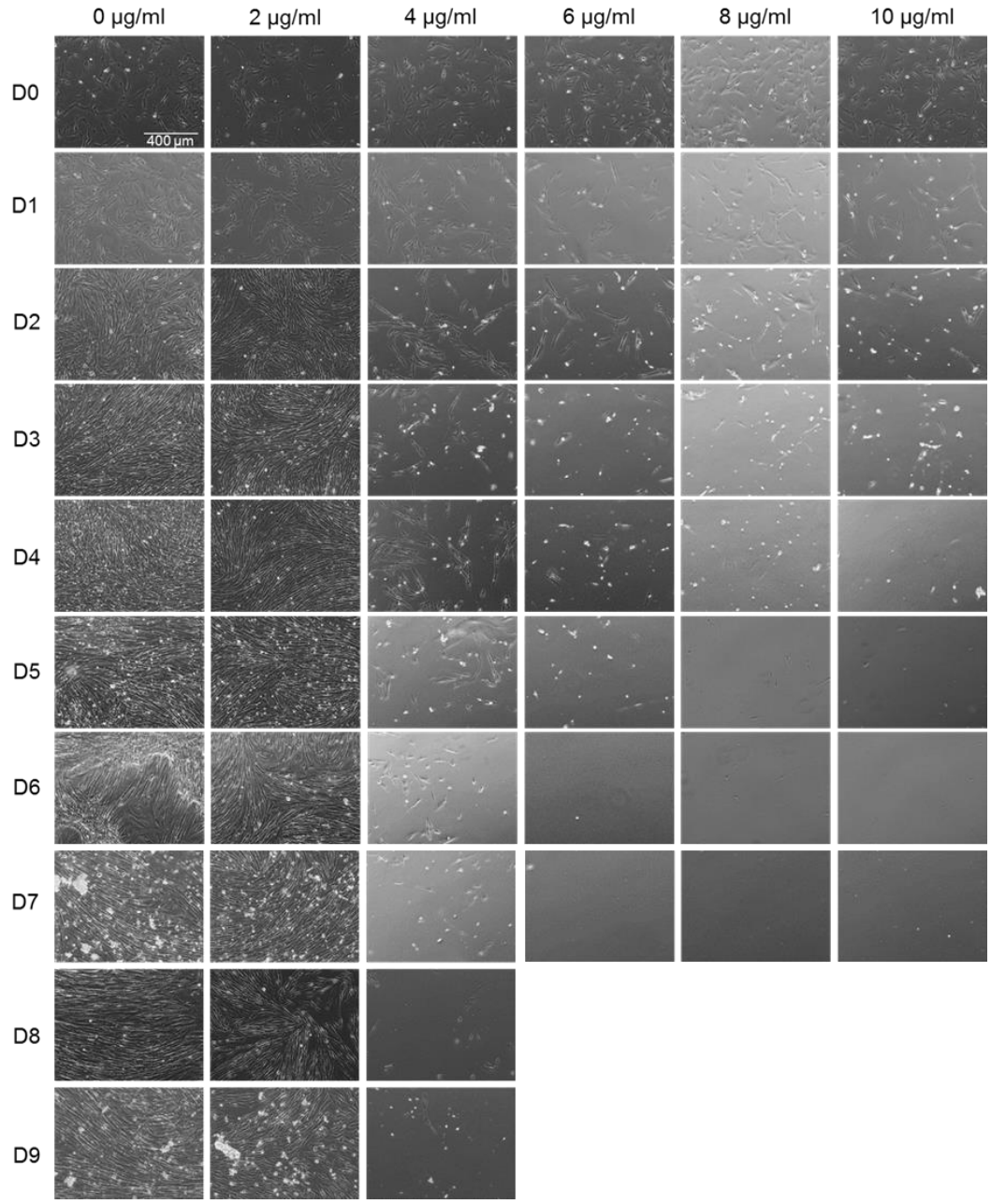

Fig. 24. The effect of various concentrations of blasticidin on EF5-TET cells. Phase contrast images were captured daily on the EVOS fluorescent microscope for up to 9 days. Blasticidin selection media was added on Day 0 (D0) and was refreshed every 48 hours. Scale bar = 400 µm

After 48 hours, cells treated with either 6, 8, or 10 µg/ml of blasticidin looked stressed and had begun detaching from the adherent culture plate. By the sixth day of selection, all of these cells had died. By contrast, cell death took slightly longer in the 4 µg/ml blasticidin treatment well, taking 10 days to achieve complete cell death. A blasticidin concentration of 2 µg/ml resulted in a minimal amount of cell

death, with cells growing to confluence within 48 hours. Likewise, cells not treated with blasticidin remained viable and continued to grow until they reached confluence.

3.6.2 Short-Term Blasticidin Selection

The first attempt to generate stable knockdown transfectants was carried out on BEFs. Approximately 2 x 10^6 passage 5 BEFs were thawed and seeded onto 10 wells of a 12-well plate. Once cells had reached 80% confluence, they were transfected using the Lipofectamine® LTX protocol. The first six wells were transfected with either one of the NANOG or MBD3 miRNA plasmids, while the remaining four wells served as controls; one was transfected with the negative miRNA control plasmid, another with the positive *lacZ* miRNA plasmid, one with the GFP plasmid, pMAX, and one well was left as a non-transfected control.

Transfection efficiencies after 24 hours varied between the different miRNA plasmids but were estimated to be between 20 – 30%. The same day, cells were passaged and split 1 to 6 onto fresh culture dishes ensuring cells would be spread thin for selection. Blasticidin selection was initiated 48 hours post-transfection to enable cells which had stably integrated the miRNA plasmid to be selected. Blasticidin was added to base media at a concentration of 10 µg/ml. Selection media was refreshed every 48 hours and cells were checked routinely for colony formation.

Unexpectedly, BEFs transfected with the miRNA plasmids continued to grow under selection suggesting these cells were expressing the blasticidin resistance gene encoded on the BLOCK-iT^{TM} plasmid. However, these cells were not positive for GFP expression. Moreover, the few cells that were GFP positive appeared not to have divided as no GFP expressing doublets were observed. By the eighth day of selection, these non-fluorescent cells had reached complete confluence. By contrast, the non-transfected cells and cells transfected with pMAX had all died within a few days of blasticidin selection.

As selection of clonal lines seemed no longer possible, the blasticidin resistant cells were harvested for RNA extraction followed by cDNA synthesis. To

determine whether the blasticidin resistant cells from the miRNA transfected dishes were also expressing the miRNA plasmid, despite not being GFP positive, a qPCR assay was performed. Because the miRNA could not be detected directly, the cDNA samples were analysed for *MBD3* and *GFP* expression. The qPCR assay revealed that there was no significant difference in *MBD3* expression levels between cells transfected with the negative miRNA control plasmid and any of the MBD3 miRNA transfected cells (Fig. 25). As expected, *GFP* expression was not detectable in any of the treatment cells.

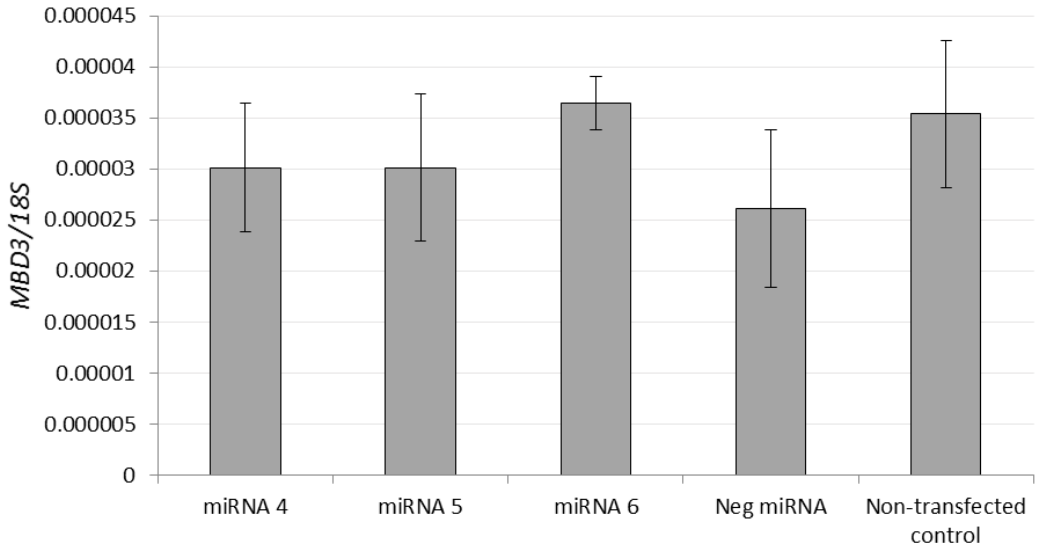

Fig. 25. Relative *MBD3* expression in BEFs stably transfected with MBD3 miRNAs. BEFs were harvested for RNA extraction and cDNA synthesis after reaching confluence on day 8 of blasticidin selection. *MBD3* expression normalised against the housekeeping gene *18S*. Neg miRNA = Negative miRNA. Error bars based on the SEM for technical triplicates.

Two more attempts were made to generate stable knockdown cell lines this time using a different bovine cell line, EF5-TET. The miRNA plasmids were transfected into EF5-TET cells firstly using the Lipofectamine® LTX protocol and, on a separate attempt, using the Neon™ electroporation protocol. Included each time was a pMAX transfection control and a non-transfected EF5-TET control. Consistent with the previous BEF experiment, all control cells died within a few days of blasticidin selection while the miRNA transfected cells grew to complete confluence by the eighth day of selection. Once again, the majority of these cells were not positive for GFP expression.

3.6.3 Long-Term Blasticidin Selection

Out of curiosity, a final stable knockdown experiment was conducted with the intention of applying blasticidin selection for a longer period of time. Approximately, 2 x 10^6 passage 6 BEFs were seeded across 10 wells of a 12-well plate and transfected as described in the first BEF experiment using Lipofectamine® LTX. The following day, cells were visualised on the EVOS fluorescent microscope. Phase contrast images revealed that the cells had reached 100% confluence. Transfection efficiency was estimated to be about 30 - 40%. Each treatment well was then passaged and 2 x 10^5 cells were seeded onto a 10 cm tissue culture dish.

Blasticidin selection was initiated 48 hours post-transfection at a concentration of 10 µg/ml (Fig. 26A). Selection media was refreshed every 48 hours for up to three weeks. Images were captured on the EVOS fluorescent microscope every two days to document cell density and GFP expression. After four days in selection, the pMAX transfected cells and the non-transfected cells had all died. By contrast, cells in the miRNA transfected dishes had minimal amounts of cell death with the population of non-fluorescent cells continuing to divide. By the eighth day of blasticidin selection, the GFP positive cells in the miRNA transfected dishes had still not proliferated and had become completely overgrown by non-fluorescent blasticidin resistant cells (Fig. 26B).

Approximately three days after reaching 100% confluence, the non-fluorescent population of cells started to die. As the non-fluorescent cells detached from the culture dish, the GFP positive cells suddenly begun to proliferate. By the 20th day of blasticidin selection, distinct cell colonies were apparent, of which 70% were positive for GFP expression (Fig. 26C). Colonies were transferred the following day to a 48-well plate for expansion as well as onto an 8-well chamber for characterisation. A total of 22 cell colonies were successfully transferred; eight for NANOG miRNA 1, three for NANOG miRNA 2, six for NANOG miRNA 3, and five for MBD3 miRNA 4. Due to bacterial contamination of the *lacZ* miRNA, negative miRNA, and MBD3 miRNA 5 and miRNA 6 plates earlier on in selection, no cell colonies were obtained for these plasmids. After transfer to

individual culture, the cell clones failed to proliferate, with all clones entering into a state of cellular senescence.

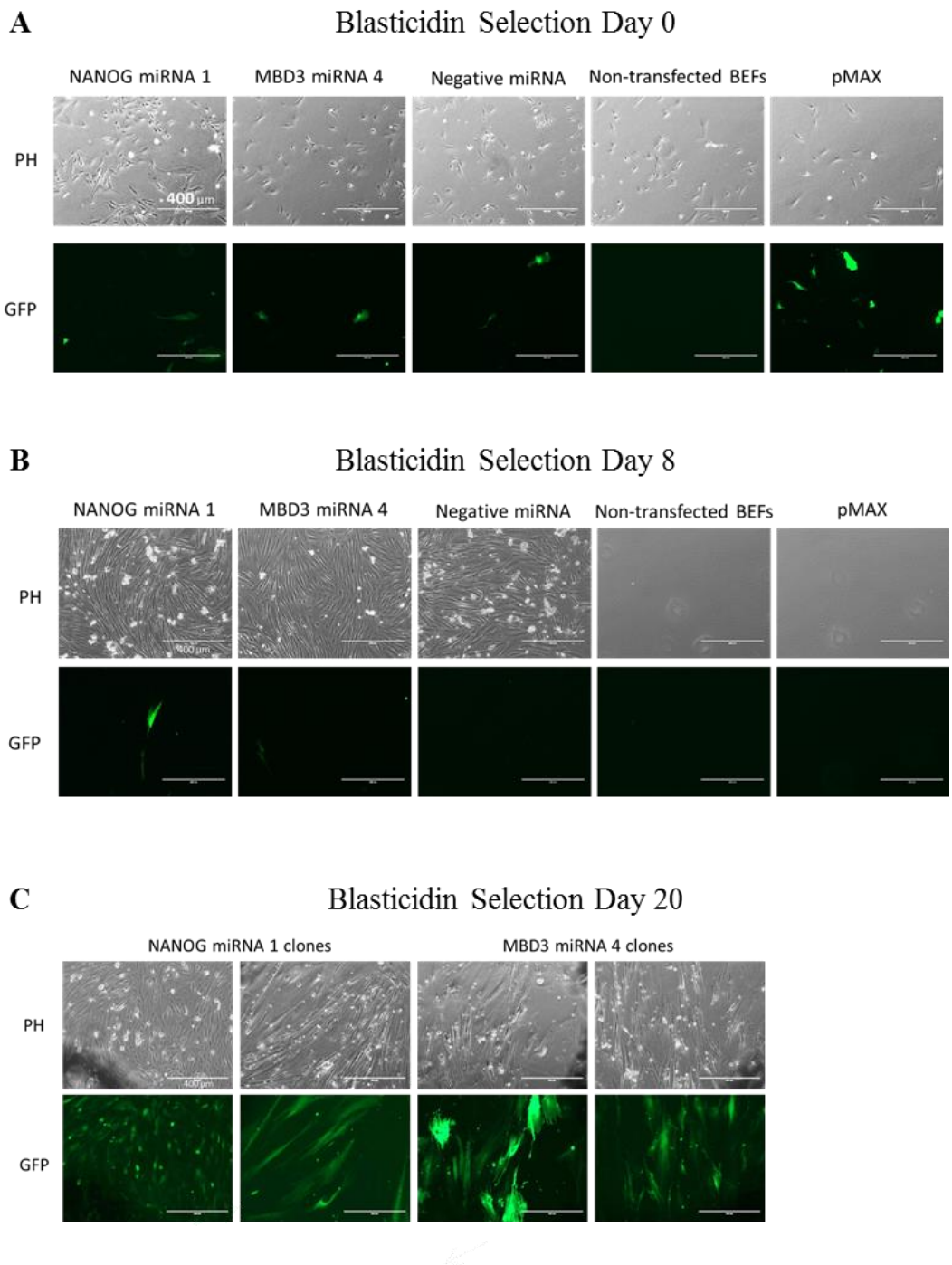

Fig. 26. Blasticidin selection in BEFs transfected with either NANOG, MBD3, or control miRNA plasmids. Images were captured on the EVOS fluorescent microscope. Scale bar = 400 µm. **A**. Initial seeding density and GFP expression at the initiation of blasticidin selection (day 0), 48 hours post-transfection. **B**. Seeding density and GFP expression on day 8 of blasticidin selection. **C**. GFP positive clonal populations after 20 days of blasticidin selection.

3.7 BLOCK-iT™ Positive Control Experiment: LacZ Knockdown

The *lacZ* miRNA plasmid supplied by the BLOCK-IT™ miRNA expression kit was used as a positive control for RNAi mediated knockdown. In preparation for the positive control experiment, the bovine commercial cell line CCL44 was seeded onto three wells of a 6-well tissue culture plate. Each well contained three coverslips. Once the cells had grown to about 70% confluence, they were transfected according to the Lipofectamine® LTX protocol. The first two wells were cotransfected with the *lacZ* reporter plasmid and either the *lacZ* miRNA or the negative miRNA control plasmid at a 1 to 6 molar ratio. The third well served as the non-transfected control. Coverslips were removed from culture dishes the following day for X-Gal staining.

Cells positive for β-galactosidase were visualised under bright field while total cell nuclei were visualised under the blue immunofluorescence channel using the Olympus fluorescent microscope. Knockdown quantification was performed by calculating the proportion of cells that were blue and thus positive for β-galactosidase. About 8% of cells cotransfected with the *lacZ* reporter and the negative miRNA plasmid were positive for β-galactosidase, indicative of a low transfection efficiency. By contrast, no β-galactosidase positive cells were present in cells transfected with the *lacZ* reporter and *lacZ* miRNA plasmid suggesting a complete knockdown. As expected, the non-transfected control cells were also negative for β-galactosidase expression.

Chapter Four: Discussion

The primary aim of this research project was to determine the feasibility of using a miRNA-based RNAi approach to knockdown NANOG and MBD3 in a bovine model. Using the BLOCK-iT^{TM} miRNA expression system, we constructed three miRNA constructs designed to target different regions of either the *NANOG* or *MBD3* transcript. *In vitro* screening of the miRNAs to determine their potency revealed that all three NANOG miRNAs were capable of significantly knocking down NANOG expression by as much as 89%. The knockdown potential of the MBD3 miRNAs is still yet to be determined due to the longevity of the MBD3 protein which complicates transient miRNA expression analysis. Various attempts were made to derive stable NANOG or MBD3 knockdown cell lines. However, stable transfectants that were GFP positive were slow to proliferate and failed to expand after transfer to individual culture. This meant that no stable knockdown lines were established that could be used for SCNT.

Our results are particularly disappointing given that the BLOCK-iT^{TM} miRNA expression system has previously been demonstrated to be an effective tool for silencing genes in livestock. In 2012, a separate group within our research organisation, AgResearch, used this miRNA system to successfully target and silence the major milk allergen, β-lactoglobulin (BLG) in cattle (Jabed et al., 2012). An *in vitro* screening system was first established by cotransfecting COS-7 cells with a bovine BLG plasmid and one of ten miRNA expression plasmids designed using RNAi designer. To account for differences in transfection efficiency, the expression of BLG was normalised against the expression of GFP encoded on the miRNA plasmid. BLG expression from cells cotransfected with bovine BLG and a scrambled miRNA control was used for baseline comparisons to determine the knockdown efficiency of each BLG-specific miRNA plasmid. Of the 10 miRNAs tested, eight showed BLG knockdown efficiencies greater than 70%, with the most efficient miRNA achieving a knockdown of 97%. To determine the efficiency of miRNA-mediated BLG knockdown *in vivo*, the group carried out SCNT cloning using a bovine fetal fibroblast line engineered to

express the most efficient BLG targeting miRNA. Of the 57 cloned embryos transferred into recipient cows, one resulted in the birth of a live female calf. After hormonally inducing her into lactation at 7 months of age, the milk of the transgenic calf was analysed by Western blot for BLG protein expression. With no detectable levels of BLG, and a higher overall level of casein proteins, the group concluded that targeted miRNA expression is an effective strategy for modifying milk composition and other important livestock traits.

The BLOCK-iT^{TM} miRNA expression system has also just recently been used to knockdown the skeletal muscle growth factor, myostatin in caprine fetal fibroblasts (CFFs) (Zhong et al., 2014). Natural mutations in the *myostatin* gene often result in a double muscling phenotype, a desirable trait for the agricultural industry (Bellinge et al., 2005). A previous knockdown attempt in cattle using integrating small hairpin RNA (shRNA) plasmids resulted in only slightly reduced myostatin levels in one of five transgenic calves (Tessanne et al., 2012). In an attempt to improve the efficiency of RNAi-mediated myostatin knockdown, a separate research team instead selected the BLOCK-iT^{TM} miRNA expression system to reduce myostatin levels in a caprine (goat) model (Zhong et al., 2014). Preliminary *in vitro* results have shown that the targeting miRNA plasmids can achieve transient knockdown efficiencies between 71-84% in CFFs when compared to non-transfected controls. However, their negative miRNA control plasmid also achieved a similar transient knockdown. This suggests that the reduction in myostatin was not a miRNA-specific response, but rather due to an elicitation of an immune response within the CFF as characterised by an increase in interferon gene expression. Stable knockdown attempts, resulted in a lower immune response but knockdown efficiency of myostatin was reduced to 31% compared to non-transfected controls. Importantly, neither Jabed et al. nor Zhong et al. reported any issues generating stable knockdown cell lines suggesting that the slow-proliferative nature of GFP positive cells is a phenomenon unique to our system.

4.1 Objective One: Design and Generation of the miRNA Constructs

The design of a miRNA is fundamental to its specificity and knockdown potential. Unfortunately, even when using established RNAi design software, there is no

guarantee that a particular miRNA will specifically and efficiently knockdown its respective mRNA target. For these reasons, researchers often design multiple miRNA molecules to target various different regions of the same mRNA transcript. *In vitro* screening is then applied to identify which miRNA has the most potent and specific knockdown potential before moving on to the *in vivo* model.

To knockdown the expression of bovine NANOG and MBD3, three miRNAs specific for each gene transcript were designed using Invitrogen's RNAi designer. During the design process, the target binding region as well as the GC content were taken into consideration. All three of the miRNAs for each gene were designed to target the ORF as opposed to the 3' or 5' UTRs. This decision to target the ORF was based on the assumption that UTR-binding proteins could potentially interfere with RISC binding and thus negatively impair miRNA activity. Furthermore, it was also assumed that UTR targeting might result in more off-target effects as UTR sequences can be similar across different mRNA transcripts (Jabed et al., 2012).

Based on Invitrogen's recommendation, NANOG- and MBD3-specific miRNAs were designed to have a GC content between 35 – 55%. Too high of a GC content is thought to negatively impair RNAi activity by slowing down helicase's ability to unwind the double-stranded miRNA duplexes during RISC assembly (Chan et al., 2009). In addition, due to their potential to hyperstack into agglomerates and thus inhibit miRNA-mediated silencing, strings of more than three Gs or Cs in a row were also avoided (Kumar & Clarke, 2007).

Another important criteria of miRNA design is specificity. To avoid any off-target effects, the designed miRNAs were screened against the entire bovine genome using BLAST which confirmed their specificity for either *NANOG* or *MBD3* with no homology to any additional gene transcripts. Another cause of off-target effects, as mentioned earlier in the myostatin knockdown study, is the unwanted elicitation of an immune response caused by activation of Toll-like receptors. The triggering of an immune reaction in response to the miRNA construct or its delivery vehicle can result in global degradation of total mRNA as well as protein

translation inhibition (Singh et al., 2011). To minimise the elicitation of an immune response, we opted to use Invitrogen's BLOCK-iT^{TM} expression system which allows for transfectional entry into mammalian cells. By comparison, viral transduction of the miRNA construct is more likely to trigger an immune reaction and thus lead to more off-target effects complicating knockdown analyses (Azzam & Dom, 2004). Conscious of the immune response observed by Zhang et al. with their myostatin miRNAs, we made sure we always included a non-transfected control to compare to cells transfected with the negative miRNA plasmid. In doing so, we were able to verify that protein knockdown was not due to any non-specific effects.

4.2 Objective Two: Evaluation of miRNA Knockdown Potential

After construction of the various miRNA plasmids targeting either the *NANOG* or *MBD3* transcript, the next objective was to identify which one had the most potent and specific knockdown potential.

4.2.1 NANOG Knockdown

Expression of NANOG is confined to only a subset of cells within the ICM of the early embryo. Testing miRNA-mediated knockdown using IVP embryos or their isolated ICM cultures would have been very labour intensive and costly as the number of NANOG expressing cells within these systems are limited. Therefore, a large number of biological samples would have been required. Furthermore, the most effective method of delivering the BLOCK-iT^{TM} miRNA plasmids would have been to microinject them into one-cell embryos. However, NANOG is not expressed until day 7 in bovine blastocysts, at which point the injected miRNAs would have degraded. Therefore, to develop a robust screening assay for validating the activity of the NANOG miRNAs, a NANOG expressing cell line was required.

In contrast to the cotransfection approach used by Jabed et al. who transiently transfected in a BLG expression plasmid alongside one of their BLG-specific miRNA plasmids, we decided it would be 'cleaner' to first generate a stably transfected NANOG cell line. Our intention was to use the NANOG expressing

cell line to evaluate the activity of the three NANOG miRNAs ensuring an equal 'playing field' for knockdown.

Previously our laboratory had successfully generated a bovine NANOG overexpressing fibroblast line that was doxycycline-inducible. This cell line, EOG-TET-NANOG, was initially selected for screening the NANOG miRNAs. However, we discovered that the *NANOG* transgene within this line had been extensively codon optimised during synthesis. Codon optimisation is typically performed when designing transgenes for protein production as it allows for uncommon and inefficiently translated codons to be replaced by the most efficient codon. In this way, protein translation can be significantly enhanced (Burgess-Brown et al., 2008). Despite the amino acid sequence remaining unchanged, the nucleotide sequence can be significantly altered, as was the case for the codon optimised *NANOG* transgene within EOG-TET-NANOG. As the NANOG miRNAs were designed against the endogenous *NANOG* transcript, we presumed and later confirmed that they were unable to target the codon-optimised *NANOG* transgene. Therefore, a second NANOG expressing cell line had to be generated for screening purposes.

To circumvent the issues of cellular stress and poor cell growth that occur from protein overexpression, we decided to use the highly efficient doxycycline-inducible piggyBac expression system (Li et al., 2013). This was the first time, to our knowledge, that this inducible piggyBac system has been used in a bovine model. However, piggyBac plasmids containing doxycycline-inducible transgenes have been shown to be an efficient strategy for modifying gene expression in various other animal cell types, including mice (Cardiñanos & Bradly, 2007, Tsukiyama et al., 2011), human (Saridey et al., 2009, Wang et al., 2011), and chicken (Glover et al., 2013).

The EF5-TET bovine embryonic fibroblast cell line was initially selected for transfection of the PB-TRE-NANOG plasmid because it had already been engineered to express the rtTA required for activation of the TRE promoter. The PBase plasmid, pCyL43, was cotransfected with the PB-TRE-NANOG into low passage EF5-TET cells at a 1 to 5 molar ratio respectively. Too high of a

concentration of the PBase plasmid is known to be detrimental to transgenic delivery due to its ability to re-excise the already integrated transposon based transgenes from the host's genome (Wang et al., 2008). In addition, the lingering of the PBase can also evoke an immune response, preventing efficient integration of the transgenes (Chakraborty et al., 2014). Previous piggyBac experiments using the EF5-TET line had revealed that a 1 to 5 molar ratio of transposase to transposon was optimal for efficient transgene delivery resulting in high integration rates eliminating the need to select for stable transfectants (Andria Green, personal communication, 2014).

Unfortunately, we were unable to replicate such efficient integrative transfection results when using the PB-TRE-NANOG plasmid. Of the one million EF5-TET cells transfected, only 28 puromycin resistant cell clones were selected, and many of them did not continue to grow during expansion. During the NANOG validation experiments, we discovered that there was a disagreement between the protein and mRNA data. Of the seven clones that grew to the validation stage, six showed a significantly elevated expression of *NANOG* mRNA compared to a non-transfected EF5-TET control. Four clones exhibited a high expression level of *NANOG* which was between 37 – 67 fold higher than the control, while the other three had only marginal differences in *NANOG* expression (between 1.5 – 5 fold). However, on the protein level, all seven clones were positive for NANOG with no detectable differences in ICC staining intensity between the clones.

To characterise the NANOG clones, the ICC protein assay was selected as it allowed us to detect NANOG expression on the single cell level. However, quantification via ICC is difficult requiring numerous cell images to be assessed for pixel-intensity differences. Ideally, it would have been better to analyse NANOG expression by Western blot which would have made it easier to quantify and compare protein expression between the clones. Unfortunately, the 34 kDa NANOG protein is notoriously difficult to visualise on a Western blot as it fragments easily resulting in multiple bands. In our laboratory, previous Western blot attempts to stain for NANOG using eight different commercial antibodies and various protein lysates have been unsuccessful (Bjorn Oback, personal

communication, 2014). For these reasons, we had to rely on ICC data to validate protein expression.

One big limitation for cell research in animals which do not yet have established ESC lines is cellular senescence. Normal somatic cells have a finite lifespan and will only divide a certain number of times before entering into cellular senescence – a metabolically active state where the cell can no longer proliferate. This division limit is more commonly referred to as a cell's Hayflick limit (Hayflick & Moorhead, 1961). Hayflick limits vary between different cell types and for many primary bovine fibroblast lines, the Hayflick limits have yet to be accurately determined. Unfortunately, even though we initially transfected low passage EF5-TETs, all seven of our NANOG expressing clones failed to proliferate after the validation experiments, with all entering into a state of cellular senescence.

In an attempt to override the cellular senescent state, a transformation experiment was performed using the oncogene *c-myc* plasmid. The *c-myc* gene encodes a transcription factor that is known to play a prominent role in regulating cell cycle progression. Specifically, it has been found to upregulate various cyclin proteins and ribosomal components encouraging cell growth and proliferation (Henriksson & Luscher, 1996, Prall et al., 1998). In addition c-myc is capable of inducing the expression of telomerase reverse transcriptase (TERT), a catalytic subunit of the enzyme telomerase which maintains telomeric length, enabling cells to continually divide (Gil et al., 2005). Testament to its role in cell proliferation, many cancers have been found to harbour mutations in the *c-myc* gene resulting in its constitutive expression (Dhang, 1999). Taking advantage of these properties, numerous researchers have discovered that mammalian cells, including bovine cells, can be transformed into an immortalised state by simple transfection of a c-myc transgene (Drissi et al., 2001, Gil et al., 2005, Bi et al., 2007). Importantly, c-myc transfected cells have been shown to maintain a normal karyotype ensuring the properties of the cell are not significantly altered (Gil et al., 2005). However, once a cell has already entered into senescence, it is particularly difficult to transform due to the much lower transfection efficiency (Di Micco et al., 2006). This would explain why we did not detect any RFP signal following transfection of the RFP-containing C-MYC plasmid into the senescent NANOG cell clones.

By contrast, transfection of the non-senescent EF5-TET control cells was successful with a transfection efficiency of around 30%. This suggests that lipid-based plasmid delivery is not an effective strategy for immortalising already senescent cells. An alternative approach to immortalise the NANOG clones is to use a lentivirus to deliver the *C-MYC* transgene as lentiviral vectors are capable of efficiently integrating into non-dividing cells (Naldini et al., 1996). A separate approach that does not require immortalisation, would be to try and rejuvenate the cell clones by using them as donor cells for SCNT cloning and then recovering the embryos at around D45 of embryonic development. Due to time constraints and the high risk of transgene silencing that accompanies SCNT, this approach was not pursued.

To avoid issues with cellular senescence, we decided to transfect PB-TRE-NANOG into an already immortalised cell line. The human cervical cancer cell line HeLa was selected because of its robust proliferation. However, the HeLa line did not already contain the rtTA transgene which meant a triple transfection of all three piggyBac plasmids was required. An electroporation-based transfection method was used due to its ability to achieve higher transfection efficiencies than lipid-based transfection approaches. Unfortunately, the lack of a fluorescent reporter plasmid meant that there was no way of initially assessing transfection efficiency. Instead, we had to rely on cells being puromycin resistant as a proxy for determining which cells had integrated both plasmids. As it turned out, this was not a reliable strategy as one HeLa clone spontaneously developed resistance to puromycin and was later confirmed to be negative for NANOG expression.

Similar to the EF5-TET transfection, the integrative efficiency of the inducible piggyBac plasmids, PB-TRE-NANOG and PB-CAG-rtTA in HeLa cells was extremely low, despite the inclusion of the PBase plasmid. A total of four million cells were transfected with all three plasmids but no NANOG expressing cell clones were produced. This suggests that our inducible piggyBac expression system, which has previously been shown to be highly efficient, was not working as expected. Because the EF5-TET experiment had resulted in some positive NANOG clones, it suggested that perhaps the PB-CAG-rtTA plasmid was at fault. However, two other attempts substituting the PB-CAG-rtTA plasmid with a

commercial non-transposon containing rtTA plasmid, EF1α-Tet3G, also did not result in any NANOG positive HeLa clones (data not shown) and so ultimately the inducible piggyBac system was abandoned and its inefficiency remains unresolved.

For simplicity, we then decided to return to the co-transfection approach used by Jabed et al., to determine the knockdown efficiencies of their BLG-specific miRNAs. A constitutive NANOG expression plasmid was prepared and was validated for NANOG expression by ICC following transient transfection into a BEF cell line. Because the half-life of the NANOG protein is two hours, transient (24 h) miRNA expression should result in a detectable knockdown effect. Therefore, transient knockdown experiments were performed by cotransfecting the CMV-NANOG plasmid alongside either one of the three NANOG-specific or control miRNA plasmids. ICC analysis was performed and knockdown potential was assessed by calculating the proportion of GFP positive cells that were also positive for NANOG. However, not every cell that took in the miRNA plasmid also took in the CMV-NANOG plasmid. To account for this, *NANOG* miRNA proportions were normalised against the proportions calculated from the negative miRNA control. Although not an ideal screening system, the protein knockdown assay revealed that all three NANOG miRNAs had significantly knockdown NANOG expression. Of the three miRNA plasmids, miRNA 3 was found to have the highest knockdown efficiency at 89.1%, closely followed by miRNA 2 on 87.3% and then miRNA 1 with 80.1%. When the negative miRNA control was compared to the pMAX transfection control, no knockdown effect was observed suggesting that the NANOG knockdown exhibited by the NANOG miRNAs was a specific effect and not the result of an immune response. These results suggest that either one of the NANOG miRNA plasmids would be a good candidate for future *in vivo* experiments.

On the mRNA level, there was no significant difference in *NANOG* expression between the various NANOG-specific and control miRNAs. This is not surprising given the high background nature that accompanies a transient cotransfection approach. To improve the sensitivity of the qPCR assay would require a significant increase in transfection efficiency. For the qPCR assay to be

informative, Invitrogen recommend transfection efficiencies upwards of 70% (Invitrogen Tech Support, personal communication, 2014). A number of factors are known to influence transfection efficiency including plasmid size and purity, plasmid form (linearised vs. circular), promoter choice and delivery vehicle (Colosimo et al., 2000). One method used to improve transfection efficiencies, which we did not pursue, is to subject transfected cells to a 10% glycerol (v/v) shock 20 minutes post-transfection for 3 minutes. Glycerol is known to disturb the endosome membrane and thus facilitate DNA release within the cell (Zauner et al., 1997). By including the glycerol treatment, Jabed et al. were able to enhance the lipid-based transfection efficiency of their COS7 cells from 35 to 76% (Jabed et al., 2012). However, other researchers have reported no difference in transfection efficiency with additional glycerol treatment (Campeau et al., 2001).

4.2.2 MBD3 Knockdown

Unlike NANOG, MBD3 is ubiquitously expressed. Therefore, for assessing the knockdown potential of the MBD3-specific miRNAs, a standard BEF cell line was used. To quickly validate which miRNA had the most potent knockdown activity, a transient (24 h) transfection approach was undertaken. Achieving a high transfection efficiency is particularly important for transient knockdown assays which is why we initially performed the MBD3 miRNA transfection using the Neon™ electroporation protocol. However, cell viability was severely compromised by electroporation resulting in approximately 50% cell death and a low transfection efficiency of only 20%. By comparison, subsequent transient transfection attempts using Lipofectamine® LTX resulted in only minimal cell death with comparable transfection efficiencies.

To observe protein knockdown, ICC staining for MBD3 was performed. No MBD3 knockdown was observed for any of the treatment groups even when focusing on the cells with the highest expression of GFP. As the *GFP* transcript is produced in cis with the pre-miRNA, these cells should have also been highly expressing the MBD3-specific miRNA and thus cells should have had reduced MBD3 expression. However, the intensity of the MBD3 stain was no different to the intensity of MBD3 in non-GFP positive cells.

We suspected that the reason why no MBD3 knockdown was observed on the protein level after transient transfection with MBD3-specific miRNAs was because MBD3 has a long protein half-life. If true, 24 hours of mRNA knockdown would not have been evident on the protein level as the existing MBD3 protein would not have been degraded within the time period. To support this hypothesis, a protein inhibition time course experiment was performed to estimate the half-life of MBD3. Cells were treated for between 0 - 112 hours with the fast-acting protein translation inhibitor, cycloheximide. ICC staining for MBD3 revealed that the protein was still present even after 112 hours of cycloheximide exposure. Quantification of MBD3 staining intensity was performed which revealed MBD3 has an approximate half-life of 48 hours. Because degradation of the BLOCK-iT^{TM} plasmid within the cytoplasm also occurs within 48 hours, it meant that a transient transfection approach was not going to be a feasible option for reducing MBD3 protein levels *in vitro*.

Given that the half-life of the *MBD3* transcript is 8.5 hours, a knockdown effect should have been detectable on the mRNA level. However, similarly to the *NANOG* qPCR assay, no significant difference in *MBD3* mRNA expression was detected between cells transfected with either one of the MBD3-specific miRNAs and the negative miRNA control even when normalised on GFP expression. Although not significant, the qPCR data do suggest that *MBD3* expression is reduced in MBD3 miRNA transfected cells. If the transfection efficiency were to improve, background *MBD3* expression from non-transfected cells could be reduced and a knockdown effect could be quantified more accurately.

4.3 Objective Three: Generation of Stable Knockdown Bovine Cell Lines

A separate objective of this project was to generate stable knockdown cell lines. The stable lines would then serve as donor cells for SCNT enabling knockdown embryos to be produced *in vitro* and the specific biological functions of bovine MBD3 and NANOG could thus be determined.

The successful generation of stable knockdown clones using the BLOCK-iT^{TM} miRNA expression kit has previously been demonstrated by other researchers, including a stable BLG knockdown within a bovine fetal fibroblast line (Jabed et

al., 2012). Selection of stable transfectants is made possible by the blasticidin resistance gene encoded on the miRNA expression plasmid and driven by the constitutively active EM7 promoter, a synthetic version of the T7 bacteriophage promoter. The nucleoside antibiotic blasticidin kills both prokaryotic and eukaryotic cells by inhibiting protein synthesis (Yamaguchi et al., 1965). Resistance to blasticidin is made possible by expression of the blasticidin S deaminase gene (bsd) (Kimura et al., 1994). Initially discovered in *Aspergillus terreus*, bsd converts blasticidin into a non-toxic deaminohydroxy derivative preventing protein synthesis inhibition (Izumi et al., 1991).

Multiple attempts to generate stable knockdown clones were conducted. Two different bovine fibroblast cells lines were used to transfect in the NANOG, MBD3, or control miRNA plasmids using either the Lipofectamine® LTX or Neon™ electroporation protocols. Transfection rates varied between the different protocols but were typically between 20 – 60% based on the number of GFP expressing cells. Approximately 24 hours after transfection, cells were split harshly onto fresh culture dishes and blasticidin selection was initiated the following day at a concentration of 10 µg/ml. On all attempts, both the non-transfected control cells and pMAX transfected cells all died within 2 to 4 days of blasticidin treatment suggesting they were not resistant. However, in the cells transfected with the miRNA expression plasmids, the GFP positive cells would not initially proliferate and would become overgrown by non-fluorescent blasticidin resistant cells. This occurred in all miRNA plasmids transfected including the negative and positive control plasmids supplied by the BLOCK-iT™ miRNA expression kit. Subsequent qPCR analysis of the blasticidin resistant non-fluorescent cells from the MBD3 miRNA dishes suggested that they were not expressing the miRNA plasmid as there was no difference in *MBD3* expression when compared to non-transfected controls.

It seemed as though blasticidin resistance was occurring following transfection with the miRNA expression constructs but this did not correlate with GFP expression. One possible explanation for this occurrence could be that these cells had indeed integrated the plasmid but the GFP and pre-miRNA sequences had become methylated and consequently silenced within the genome while the

blasticidin resistance gene remained switched on. However, it is unlikely that this phenomenon would have occurred for every single miRNA construct on every single stable transfection attempt.

Another possible explanation is promoter competition between the CMV promoter which drives expression of the GFP/miRNA transcript and the EM7 promoter which drives expression of the blasticidin resistance gene. After integration into the genome, access to transcription factors and RNA polymerase could have become biased to one of the plasmid promoters, in this case, EM7. The lower expression of the GFP/miRNA transcript could have offered a selective growth advantage over cells which did express the GFP/miRNA transcript which would explain why these non-fluorescent cells were able to overgrow the GFP positive cell population.

When cells reach complete confluence they either die or enter into a state of cellular quiescence (Gos et al., 2005). In this experiment, it appears the non-fluorescent cells were unable to become quiescent at full confluence and instead started to die and lift off the culture dish. Without the presence of the non-fluorescent cell population, the growth disadvantage of the GFP expressing cells was removed and these cells were then able to proliferate and form distinct cell colonies. However, after transfer to individual culture, the GFP positive clones all entered into a state of cellular senescence where they stopped proliferating. This failure to expand meant that no clonal knockdown cell lines were established and SCNT could not be performed to generate knockdown embryos.

One possibility that was not explored, but could be advantageous moving forward, is to apply fluorescence activated cell sorting (FACS) to cells 24 hours post-transfection. With the ability to sort heterogeneous cell populations according to their level of fluorescence, FACS would enable cells transfected with the miRNA expression plasmids that are GFP positive to be separated from non-GFP positive cells. Blasticidin selection could then be applied to only the GFP positive cells which may facilitate their proliferation as they would no longer have to wait for the non-fluorescent cell population to reach confluence and lift off. Previously, FACS coupled with selection media has proven to be an effective strategy for

generating high expression stable cell lines (Zhang et al., 2006). Using Lipofectamine®, Zhang et al. transfected Chinese hamster ovary (CHO) cells with a GFP expression plasmid followed by culture in selective growth media. By applying three rounds of FACS, the percentage of GFP positive cells increased eventually resulting in the establishment of high expressing cell lines. By comparison, non-FACS control cells experienced a rapid reduction in GFP positive cells and overall GFP induction was low.

4.4 Conclusions and Future Recommendations

In conclusion, we found that the BLOCK-iT^{TM} miRNA expression system was capable of efficiently knocking down NANOG protein expression by as much as 89%. Unfortunately, due to the longevity of the MBD3 protein, a knockdown effect was not apparent after transient miRNA expression. Frequent attempts were made to generate stable knockdown cell lines, a prerequisite for the generation of knockdown embryos by SCNT. Stably transfected GFP-miRNA expressing cells did not initially proliferate during blasticidin selection, becoming overgrown by non-fluorescent blasticidin resistant cells. Eventually, after three weeks of selection, we were able to isolate GFP-miRNA expressing clones. However, these clones failed to expand after transfer to individual culture. Future research efforts should be directed into understanding why the GFP positive cells do not initially proliferate under blasticidin selection after miRNA transfection. Further characterisation of the blasticidin resistant non-fluorescent cells would also be advantageous. For the BLOCK-iT^{TM} miRNA expression system to be effectively applied in bovine embryos, these issues will need to be resolved. The inclusion of FACS to sort the GFP positive cells from the non-fluorescent cells immediately prior to blasticidin selection is one option that should be trialled before abandoning the BLOCK-iT^{TM} miRNA expression system.

However, should FACS also fail to generate stable knockdown cell lines, an emerging system which could be explored as an alternative to miRNA-mediated silencing is the clustered regulatory interspaced short palindromic repeat (CRISPR)/Cas9 genome editing system. Initially discovered in bacteria as a strategy to defend against invading phages, the CRISPR/Cas9 system has now been exploited by scientists to enable precise modification of specific sites within

the genome (Barrangou1 et al., 2007, Hsu et al., 2014). Briefly, how this system works is that Cas9 is a nuclease capable of introducing double-strand breaks in DNA. Its specificity is determined by the inclusion of a guide RNA which in complex with Cas9, targets the nuclease to a complementary sequence within the genome. In an attempt to repair the double-strand break, the genome undergoes either non-homologous end joining or homology-directed repair which often lead to insertions or deletions within the sequence (Sander & Joung, 2014). In this way, gene knockout or knock-in phenotypes can be generated. Just recently, the CRISPR/Cas9 system was successfully used to specifically integrate a GFP transgene cassette into intron 1 of the *NANOG* gene locus in bovine iPSCs and embryos (Heo et al., 2015).

With rapid progress in the construction of large guide RNA libraries, it will soon be possible to design guide RNAs to target virtually any gene within an organism (Sander & Joung, 2014). Because of its simplicity, high efficiency, and versatility, the CRISPR/Cas9 system is set to revolutionise transgenic research and would be an ideal alternative system for investigating the biological functions of bovine NANOG and MBD3, as it can be applied directly to embryos circumventing the need to first create a stable cell line. Guide RNAs could be microinjected into bovine embryos at the one-cell stage. However, not all of these embryos will be successfully mutated by the CRISPR/Cas9 system. Therefore, an embryo screening assay would have to be developed to allow embryos with a biallelic knockout to be selected for. Once a knockout embryo is confirmed, the biological function of bovine NANOG and MBD3 could then be determined. Overall, this research will help to improve our current understanding of bovine pluripotency specification which will likely assist in the ultimate goal of establishing authentic livestock-derived ESCs.

References

Abad, M., Mosteiro, L., Pantoja, C., Cañamero, M., Rayon, T., Ors, I., … & Serrano, M. (2013). Reprogramming in vivo produces teratomas and iPS cells with totipotency features. *Nature, 502*(7471), 340-345.

Abranches, E., Guedes, A. M. V., Moravec, M., Maamar, H., Svoboda, P., Raj, A., & Henrique, D. (2014). Stochastic NANOG fluctuations allow mouse embryonic stem cells to explore pluripotency. *Development, 141*(14), 2770-2779.

Alberio, R., Croxall, N., & Allegrucci, C. (2010). Pig epiblast stem cells depend on activin/nodal signaling for pluripotency and self-renewal. *Stem Cells and Development, 19*(10), 1627-1636.

Alberts, B., Johnson, A., Lewis, J., Walter, P., Raff, M., & Roberts, K. (2002). Studying gene expression and function. In *Molecular Biology of the Cell (4th ed.)*. New York, NY: Garland Science.

Apostolou, E., & Hochedlinger, K. (2013). Chromatin dynamics during cellular reprogramming. *Nature, 502*(7472), 462-471.

Avillion, A. A., Nicolis, S. K., Pevny, L. H., Perez, L., Vivian, N., & Lovell-Badge, R. (2003). Multipotent cell lineages in early mouse development depend on SOX2 function. *Genes & Development, 17*(1), 126-140.

Azzam, T., & Dom, A. J. (2004). Current developments in gene transfection agents. *Current Drug Delivery, 1*(2), 165-193.

Barrangou, R., Fremaux, C., Deveau, H., Richards, M., Boyaval, P., Moineau, S., Romero, D. A., & Horvath, P. (2007). CRISPR provides acquired resistance against viruses in prokaryotes. *Science, 315*(5819), 1709-1712.

Bellinge, R. H. S., Liberles, D. A., Iaschi, S. P. A., O'Brien, P. A., Tay, G. K. (2005). Myostatin and its implications on animal breeding: a review. *Animal Genetics, 36*(1), 1-6.

Bi, C. M., Zhang, S. Q., Zhang, Y., Peng, S. Y., Wang, L., An, Z. X., Qi, A., & Lv, N. (2007). Immortlaization of bovine germ line stem cells by c-myc and hTERT. *Animal Reproduction Science, 100*(3-4), 371-378.

Blair, K., Wray, J., & Smith, A. (2011). The liberation of embryonic stem cells. *PLoS Genetics, 7*(4), e1002019.

Blomberg, L., Hashizume, K., & Viebahn, C. (2008). Blastocyst elongation, trophoblastic differentiation, and embryonic pattern formation. *Reproduction, 135*(2), 181-195.

Boland, M. J., Hazen, J. L., Nazor, K. L., Rodriguez, A. R., Gifford, W., Martin, H., … & Baldwin, K. K. (2009). Adult mice generated from induced pluripotent stem cells. *Nature, 461*(7260), 91-94.

Boyer, L. A., Lee, T. I., Cole, M. F., Johnstone, S. E., Levine, S. S., Zucker, J. P., … & Young, R. A. (2005). Core transcriptional regulatory circuitry in human embryonic stem cells. *Cell, 122*(6), 947-956.

Buchon, N., & Vaury, C. (2006). RNAi: a defensive RNA-silencing against viruses and transposable elements. *Heredity, 96*(2), 195-202.

Buecker, C., Chen, H. H., Polo, J. M., Daheron, L., Bu, L., Barakat, T. S., … & Geijsen, N. (2010). A murine ESC-like state facilitates transgenesis and homologous recombination in human pluripotent stem cells. *Cell Stem Cell, 6*(6), 535–546.

Burgess-Brown, N. A., Sharmas, S., Sobott, F., Loenarz, C., Oppermann, U., & Gileadi, O. (2008). Codon optimization can improve expression of human genes in *Escherichia coli*: A multi-gene study. *Protein Expression and Purifcation,59*(1), 94-102.

Cadiñanos, J., & Bradley, A. (2007). Generation of an inducible and optimized piggyBac transposon system. *Nucleic Acids Research, 35*(12), e87.

Campeau, P., Chapdelaine, P., Seigneurin-Venin, S., Massie, B., & Tremblay, J. P. (2001). Transfection of large plasmids in primary human myoblasts. *Gene Therapy, 8*(18), 1387-1394.

Capecchi, M. R. (2005). Gene targeting in mice: functional analysis of the mammalian genome for the twenty-first century. *Nature Reviews. Genetics, 6*(6), 507–512.

Chakraborty, S., Ji, H., Chen, J., Gersbach, C. A., Leong, K. W. (2014). Vector modifications to eliminate transposase expression following piggyBac-mediated transgenesis. *Scientific Reports, 4*(7403).

Chambers, I., Colby, D., Robertson, M., Nichols, J., Lee, S., Tweedie, S., & Smith, A. (2003). Functional expression cloning of Nanog, a pluripotency sustaining factor in embryonic stem cells. *Cell, 113*(5), 643-655.

Chambers, I., Silva, J., Colby, D., Nichols, J., Nijmeijer, B., Robertson, M., … & Smith, A. (2007). Nanog safeguards pluripotency and mediates germline development. *Nature, 450*(7173), 1230- 1234.

Chan, C. Y., Carmach, C. S., Long, D. D., Maliyekkel, A., Shao, Y., Roninson, I. B., & Ding, Y. (2009). A structural interpretation of the effect of GC-contenton efficiency of RNA interference. *BMC Bioinformatics, 10 Suppl 1*: 533.

Chesnoy, S., & Huang, L. (2000). Structure and function of lipid-DNA complexes for gene delivery. *Annual Review of Biophysics and Biomolecular Structure, 29*, 27-47.

Cockburn, K., & Rossant, J. (2010). Making the blastocyst: lessons from the mouse. *The Journal of Clinical Investigation, 120*(4), 995-1003.

Colosimo, A., Goncz, K. K., Holmes, A. R., Kunzelmann, K., Novelli, G., Malone, R. W., Bennett, M. J., & Gruenert, D. C. (2000). Transfer and expression of foreign genes in mammalian cells. *Biotechniques, 29*(2), 314-318.

Cowan, C. A., Atienza, J., Melton, D. A., & Eggan, K. (2005). Nuclear reprogramming of somatic cells after fusion with human embryonic stem cells. *Science, 309*(5739), 1369-1373.

Czechanski, A., Byers, C., Greenstein, I., Schrode, N., Donahue, L. R., Hadjantonakis, A. K., & Reinholdt, L. G. (2014). Derivation and characterization of mouse embryonic stem cells from permissive and nonpermissive strains. *Nature Protocols, 9*(3), 559 – 574.

De Miguel, M. P., Fuentes-Julián, S., & Alcaina, Y. (2010). Pluripotent stem cells: origins, maintenance and induction. *Stem Cell Reviews, 6*(4), 633-649.

Dhang, C. V. (1999). c-Myc target genes involved in cell growth, apoptosis, and metabolism. *Molecular and Cellular Biology, 19*(1), 1-11.

Di Micco, R., Fumagalli, M., & d'Adda di fagagna, F. (2006). Oligofection of siRNAs in senescent human fibroblasts. *Protocol Exchange*, doi:10.1038/nprot.2006.365

Ding, S., Wu, X., Li, G., Han, M., Zhuang, Y., & Xu, T. (2005). Efficient transposition of the piggyBac (PB) transposon in mammalian cells and mice. *Cell, 122*(3), 473-483.

Dos Santos, R. L., Tosti, L., Radzisheuskaya, A., Caballero, I. M., Kaji, K., Hendrich, B., & Silva, J. C. (2014). MBD3/NuRD facilitates induction of pluripotency in a context-dependent manner. *Cell Stem Cell, 15*(1), 102-110.

Drissi, R., Zindy, F., Roussel, M. F., & Cleveland, J. L. (2001). C-myc-mediated regulation of telomerase activity is disabled immortalized cells. *The Journal of Biological Chemistry, 276*(32), 29994-30001.

Eistetter, H. R. (1989). Pluripotent embryonal stem cell lines can be established from disaggregated mouse morulae. *Development, Growth & Differentiation, 31*(3), 275-282.

Evans, M. J., & Kaufman, M. H. (1981). Establishment in culture of pluripotential cells from mouse embryos. *Nature, 292*(5819), 154-156.

Evans, M. J., Notarianni, E., Laurie, S., & Moor, R. M. (1990). Derivation and preliminary characterization of pluripotent cell lines from porcine and bovine blastocyst. *Theriogenology, 33*(1), 125-128.

Fire, A., Xu, S., Montgomery, M. K., Kostas, S. A., Driver, S. E., & Mello, C. C. (1998). Potent and specific genetic interference by double-stranded RNA in Caenorhabditis elegans. *Nature, 391*(6669), 806-811.

Fisher, P. J., Hyndman, D. L., Bixley, M. J., Oback, F. C., Popovic, L., Berg, M. C., & Wells, D. N. (2012). Potential for genomic selection of bovine embryos. *Proceedings of the New Zealand Society of Animal Production, 72*, 156-158.

Food and Agriculture Organization of the United Nations. (2009). *The state of food and agriculture - Livestock in the balance*. Food and Agriculture Organization of the United Nations, Rome, Italy.

Fussengger, M., Morris, R. P., Fux, C., Rimann, M., von Stockar, B., Thompson, C. J., & Bailey, J. E. (2000). Streptogramin-based gene regulation systems for mammalian cells. *Nature Biotechnology, 18*(11), 1203-1208.

Gelato, K. A., & Fischle, W. (2008). Role of histone modifications in defining chromatin structure and function. *Biological Chemistry, 389*(4), 353-363.

George, J., & Tsutsumi, M. (2007). siRNA-mediated knockdown of connective tissue growth factor prevents N-nitrosodimethylamine-induced hepatic fibrosis in rats. *Gene Therapy, 14*(10), 790-803.

Gil, J., Kerai, P., Lleonart, M., Bernard, D., Cigudosa, J. C., Peters, G., Carnero, A., & Beach, D. (2005). Immortalisation of primary human prostate epithelial cells by c-myc. *Cancer Research, 65*(6), 2179-2185.

Glover, J. D., Taylor, L., Sherman, A., Zeiger-Poli, C., Sang, H. M., & McGrew, M. J. (2013). A novel piggybac transposon inducible expression system identifies a role for AKT signalling in primordial germ cell migration. *PLoS ONE, 8*(11), e77222.

Gos, M., Miloszewska, J., Swoboda, P., Trembacz, H., Skierski, J., & Janik, P. (2005). Cellular quiescence induced by contact inhibition or serum withdrawal in C3H10T1/2 cells. *Cell Proliferation, 38*(2), 107-116.

Gossen, M., & Bujard, H. (1992). Tight control of gene expression in mammalian cells by tetracycline-responsive promoters. *Proceedings of the National Academy of Sciences, USA, 89*(12), 5547-5551.

Hammond, S. M. (2005). Dicing and slicing: the core machinery of the RNA interference pathway. *FEBS Letters, 579*(26), 5822-5829.

Harris, D., Huang, B., & Oback, B. (2013). Inhibition of MAP2K and GSK3 signaling promotes bovine blastocyst development and epiblast-associated expression of pluripotency factors. *Biology of Reproduction, 88*(3), 74.

Hatano, S. Y., Tada, M., Kimura, H., Yamaguchi, S., Kono, T., Nakano, T., . . . & Tada, T. (2005). Pluripotential competence of cells associated with Nanog activity. *Mechanisms of Development, 122*(1), 67-79.

Hayashi, K., Ogushi, S., Kurimoto, K., Shimamotos, S., Ohta, H., & Saitou, M. (2012). Offspring from oocytes derived from in vitro primordial germ cell-like cells in mice. *Science, 338*(6109), 971–975.

Hayflick, L., & Moorhead, P. S. (1961). The serial cultivation of human diploid cell strains. *Experimental Cell Research, 25*, 585-621.

He, L., & Hannon, G. J. (2004). MicroRNAs: small RNAs with a big role in gene regulation. *Nature Review Genetics, 5*(7), 522-531.

Hendrich, B., Guy, J., Ramsahoye, B., Wilson, V. A., & Bird, A. (2001). Closely related proteins MBD2 and MBD3 play distinctive but interacting roles in mouse development. *Genes & Development, 15*(6), 710-723.

Henriksson, M., & Luscher, B. (1996). Proteins of the Myc network: essential regulators of cell growth and differentiation. *Advances in Cancer Research, 68*, 109-182.

Heo, Y. T., Quan, X., Xu, Y. N., Baek, S., Choi, H., Kim, N., & Kim, J. (2015). CRISPR/Cas9 nuclease-mediated gene knock-in in bovine-induced pluripotent cells. *Stem Cells and Development, 24*(3), 393-402.

Hernandes Gifford, J. A., & Gifford, C. A. (2013). Role of reproductive biotechnologies in enabling food security and sustainability. *Animal Frontiers, 3*(3), 14-19.

Howard, K. A., Paludan, S. R., Behlke, M. A., Besenbacher, F., Deleuran, B., & Kjems, J. (2008). Chitosan/siRNA nanoparticle-mediated TNF-α knockdown in peritoneal macrophages for anti-inflammatory treatment in a murine arthritis model. *Molecular Therapy, 17*(1), 162-168.

Hsu, P. D., Lander, E. S., & Zhang, F. (2014). Development and applications of CRISPR-Cas9 for genome engineering. *Cell, 157*(6), 1262-1278.

Invitrogen. (2008). *BLOCK-iT™ Pol II miR RNAi Expression Vector Kits: User Manual*. Retrieved November, 2013, from http://www.lifetechnologies.com

Ivanova, N., Dobrin, R., Lu, R., Kotenko, I., Levorse, J., DeCoste, C., … & Lemischka, I. R. (2006). Dissecting self-renewal in stem cells with RNA interference. *Nature, 442*(7102), 533-538.

Izumi, M., Miyazawa, H., Kamakura, T., Yamaguchi, I., Endo, T., & Hanaoka, F. (1991). Blasticidin S-resistance gene (bsr): a novel selectable marker for mammalian cells. *Experimental Cell Research, 197*(2), 229-233.

Jabed, A., Wagner, S., McCracken, J., Wells, D., & Laible, G. (2012). Targeted microRNA expression in dairy cattle directs production of β-lactoglobulin-free, high-casein milk. *Proceedings of the National Academy of Sciences USA, 109*(42), 16811-16816.

Kaji, K., Caballero, I. M., MacLeod, R., Nichols, J., Wilson, V. A., & Hendrich, B. (2006). The NuRD component Mbd3 is required for pluripotency of embryonic stem cells. *Nature Cell Biology, 8*(3), 285-292.

Kaji, K., Nichols, J., & Hendrich, B. (2007). Mbd3, a component of the NuRD co-repressor complex, is required for development of pluripotent cells. *Development, 134*(6), 1123-1132.

Keefer, C. L., Karatzas, C. N., Lazaris-Karatzas, A., Gagnon, I., Poulin, S., & Downey, B. R. (1996). Isolation and maintenance of putative embryonic stem cells derived from Nigerian Dwarf goat embryos. *Biology of Reproduction, 54*, abstr. 462.

Ketting, R. F. (2011). The many faces of RNAi. *Developmental Cell, 20*(2), 148-161.

Kim, D. H., & Rossi, J. J. (2007). Strategies for silencing human disease using RNA interference. *Nature Review Genetics, 8*(3), 173-184.

Kim, T. K., & Eberwine, J. H. (2010). Mammalian cell transfection: the present and the future. *Analytical and Bioanalytical Chemistry, 397*(8), 3173-3178.

Kim, Y. K., & Kim, V. N. (2007). Processing of intronic microRNAs. *The EMBO Journal, 26*(3). 775-783.

Kimura, M., Takatsuki, A., & Yamaguchi, I. (1994). Blasticidin S deaminase gene from Aspergillus terreus (BSD): a new drug resistance gene for transfection of mammalian cells. *Biochimica et Biophysica ACTA, 1219*(3), 653-659.

Kirchhof, N., Carnwath, J. W., Lemme, E., Anastassiadis, K., Schöler, H., & Niemann, H. (2000). Expression pattern of Oct-4 in preimplantation embryos of different species. *Biology of Reproduction, 63*(6), 1698-1705.

Kopp, J. L., Ormsbee, B. D., Desler, M., & Rizzino, A. (2008). Small increases in the level of Sox2 trigger the differentiation of mouse embryonic stem cells. *Stem Cells, 26*(4), 903-911.

Kuijk, E. W., Du Puy, L., van Tol, H. T., Oei, C. H., Haagsman, H. P., Colenbransder, B., & Roelen, B. A. (2008). Differences in early lineage segregation between mammals. *Developmental Dynamics, 237*(4), 918-927.

Kuijk, E. W., van Tol, L. T., Van de Velde, H., Wubbolts, R., Welling, M., Geijsen, N., & Roelen, B. A. (2012). The roles of FGF and MAP kinase signaling in the segregation of the epiblast and hypoblast cell lineages in bovine and human embryos. *Development, 139*(5), 871-882.

Kumar, L. D., & Clarke, A. R. (2007). Gene manipulation through the use of small interfering RNA (siRNA): from in vitro to in vivo applications. *Advanced Drug Delivery Reviews, 59*(2-3), 87-100.

Laible, G. (2009). Enhancing livestock through genetic engineering - recent advances and future prospects. *Comparative Immunology, Microbiology and Infectious Diseases 32*(2), 123–137.

Laible, G., & Alonso-González, L. (2009). Gene targeting from laboratory to livestock: current status and emerging concepts. *Biotechnology Journal, 4*(9), 1278-1292.

Li, Z., Michael, I. P., Zhou, D., Nagy, A., & Rini, J. M. (2013). Simple piggyBac transposon-based mammalian cell expression system for inducible protein production. *Proceedings of the National Academy of Sciences, USA, 110*(13), 5004-5009.

Li, M., Zhang, D., Hou, Y., Jiao, L., Zheng, X., & Wang, W. H. (2003). Isolation and culture of embryonic stem cells from porcine blastocysts. *Molecular Reproduction and Development, 65*(4), 429-434.

Liang, G., & Zhang, Y. (2013). Embryonic stem cell and induced pluripotent stem cell: an epigenetic perspective. *Cell Research, 23*(1), 49-69.

Loh, Y., Wu, Q., Chew, J., Vega, V. B., Zhang, W., Chen, X., … & Ng, H. (2006). The Oct4 and Nanog transcription network regulates pluripotency in mouse embryonic stem cells. *Nature Genetics, 38*(4), 431-440.

Lund, E., & Dahlberg, J. E. (2006). Substrate selectivity of exportin 5 and Dicer in the biogenesis of microRNAs. *Cold Spring Harbor Symposia on Quantitative Biology, 71*, 59-66.

Luo, M., Ling, T., Xie, W., Sun, H., Zhou, Y., Zhu, Q., … & Grummt, I. (2013). NuRD blocks reprogramming of mouse somatic cells into pluripotent cells. *Stem Cells, 31*(7), 1278-1286.

Macgregor, G. R., Nolan, G. P., Fiering, S., Roederer, M., & Herzenberg, L. A. (1991). Use of Escherichiu coli (E. coli) lacZ (β-Galactosidase) as a Reporter Gene. In E. J. Murray (Ed.), *Methods in Molecular Biology, Vol 7: Gene Transfer and Expression Protocols* (pp. 217-235). Clifton, NJ: The Human Press Inc.

MacRae, I. J., Ma, E., Zhou, M., Robinson, C. V., & Dounda, J. A. (2008). In vitro reconstitution of the human RISC-loading complex. *Proceedings of the National Academy of Science USA, 105*(2), 512-517.

Martin, G. R. (1981). Isolation of a pluripotent cell line from early mouse embryos cultured in medium conditioned by teratocarcinoma stem cells. *Proceedings of the National Academy of Sciences, USA, 78*(12), 7634-7638.

Masui, S., Nakatake, Y., Toyooka, Y., Shimosato, D., Yagi, R., Takahashi, K., … & Niwa, H. (2007). Pluripotency governed by Sox2 via regulation of Oct3/4 expression in mouse embryonic stem cells. *Nature Cell biology, 9*(6), 625-635.

McDonel, P., Costello, I., & Hendrich, B. (2008). Keeping things quiet: roles of NuRD and Sin3 co-repressor complexes during mammalian development. *The International Journal of Biochemistry & Cell Biology, 41*(1), 108-116.

McLean, Z., Meng, F., Henderson, H., Turner, P., & Oback, B. (2014). Increased MAP kinase inhibition enhances epiblast-specific gene expression in bovine blastocysts. *Biology of Reproduction, 91*(2), 49.

Menafra, R., & Stunnenberg, H. G. (2014). MBD2 and MBD3: elusive functions and mechanisms. *Frontiers in Genetics, 5*(428).

Meshorer, E., & Misteli, T. (2006). Chromatin in pluripotent embryonic stem cells and differentiation. *Nature Reviews. Molecular Cell Biology, 7*(7), 540-546.

Mitalipova, M., Beyhan, Z., & First, N. L. (2001). Pluripotency of bovine embryonic cell line derived from precompacting embryos. *Cloning, 3*(2), 59-67.

Mitsui, K., Tokuzawa, Y., Itoh, H., Segawa, K., Murakami, M., Takahahi, K., Maruyama, M., Maeda, M., & Yamanaka, S. (2003). The homeoprotein Nanog is required for maintenance of pluripotency in mouse epiblast and ES cells. *Cell, 113*(5), 631-642.

Muñoz, M., Díez, C., Caamaño, J. N., Jouneau, A., Hue, I., & Gómez, E. (2008). Embryonic stem cells in cattle. *Reproduction in Domestic Animals, 43*(Suppl 4), 32-37.

Murray, S. C., Eckhoff, P., Wood, L., & Paterson A. H. (2013). A proposal to use gamete cycling in vitro to improve crops and livestock. *Nature Biotechnology, 31*(10), 877-880.

Naldini, L., Blömer, U., Gallay, P., Ory, D., Mulligan, R., Gage, F. H., Verma, I. M., Trono, D. (1996). In vivo gene delivery and stable transduction of nondividing cells by a lentiviral vector. *Science, 272*(5259), 263-267.

Napoli, C., Lemieux, C., & Jorgesensen, R. (1990). Introduction of a chimeric chalcone synthase gene into petunia results in reversible co-suppression of homologous genes in trans. *The Plant Cell, 2*(4), 279-289.

Navarro, P., & Avner, P. (2009). When X-inactivation meets pluripotency: an intimate rendezvous. *FEBS Letters, 583*(11), 1721-1727.

Ng, K., Pullirsch, D., Leeb, M., Wutz, A. (2007). Xist and the order of silencing. *EMBO Reports, 8*(1), 34-39.

Nichols, J., Zevnik, B., Anastassiadis, K., Niwa, H., Klewe-Nebenius, D., Chambers, I., … & Smith, A. (1998). Formation of pluripotent stem cells in the mammalian embryo depends on the POU transcription factor Oct4. *Cell, 95*(3), 379-391.

Niwa, H., Burdon, T., Chambers, I., & Smith, A. (1998). Self-renewal of pluripotent embryonic stem cells is mediated via activation of STAT3. *Genes & Development, 12*(13), 2048-2060.

Niwa, H., Miyazaki, J., & Smith, A. G. (2000). Quantitative expression of Oct-3/4 defines differentiation, dedifferentiation or self-renewal of ES cells. *Nature Genetics, 24*(4), 372-376.

No, D., Yao, T. P., & Evans, R. M. (1996). Ecdysone-inducible gene expression in mammalian cells and transgenic mice. *Proceedings of the National Academy of Sciences, USA, 93*(8), 3346-3351.

Notarianni, E., Galli, C., Laurie, S., Moor, R. M., & Evans, M. J. (1991). Derivation of pluripotent, embryonic cell lines from the pig and sheep. *Journal of Reproduction and Fertility. Supplement, 43*, 255-260.

Novina, C. D., & Sharp, P. A. (2004). The RNAi revolution. *Nature, 430*(6996), 161-164.

Oback, B., & Huang, B. (2014). Pluripotent stem cells from livestock. In F. Calegari & C. Waskow (Eds.), *Stem Cells: From Basic Research to Therapy. Volume 2 - Tissue Homeostasis and Regeneration during Adulthood, Applications, Legislation and Ethics* (pp. 304–346). Boca Raton, FL: CRC Press.

Oh, J. H., Do, H. J., Yang, H. M., Moon, S. Y., Cha, K. Y., Chung, H. M., & Kim, J. H. (2005). Identification of a putative transactivation domain in human Nanog. *Experimental & Molecular Medicine, 37*(3), 250-254.

Palomares, L. A., Estrada-Mondaca, S., & Ramírez, O. T. (2004). Production of recombinant proteins: challenges and solutions. *Methods in Molecular Biology, 267*, 15-52.

Pan, G. J., & Pei, D. Q. (2003). Identification of two distinct transactivation domains in the pluripotency sustaining factor nanog. *Cell Research, 13*(6), 499-502.

Pan, G., & Thomson, J. A. (2007). Nanog and transcriptional networks in embryonic stem cell pluripotency. *Cell Research, 17*(1), 42-49.

Phillips, C. J. C. (2010). *Principles of Cattle Reproduction* (2nd ed.). Cambridge, UK: Cambridge University Press.

Prall, O. W., Rogan, E. M., Musgrove, E. A., Watts, C. K., & Sutherland, R. L. (1998). c-Myc or cyclin D1 mimics estrogen effects on cyclin E-Cdk2 activation and cell cycle re-entry. *Molecular and Cellular Biology, 18*(8), 4499-4508.

Rais, Y., Zviran, A., Geula, S., Gafni, O., Chomsky, E., Viukov, S., … & Hanna, J. H. (2013). Deterministic direct reprogramming of somatic cells to pluripotency. *Nature, 502*(7469), 65-70.

Recillas-Targa, F. (2006). Multiple strategies for gene transfer, expression, knockdown, and chromatin influence in mammalian cell lines and transgenic animals. *Molecular Biotechnology, 34*(3), 337-354.

Reynolds, N., Latos, P., Hynes-Allen, A., Loos, R., Leaford, D., O'Shaughnessy, A., … & Hendrich, B. (2012a). NuRD suppresses pluripotency gene expression to promote transcriptional heterogeneity and lineage commitment. *Cell Stem Cell, 10*(5), 583-594.

Reynolds, N., Salmon-Divon, M., Dvinge, H., Hynes-Allen, M., Balasooriya, G., Leaford, D., … & Hendrich, B. (2012b). NuRD-mediated deacetylation of H3K27 facilitates recruitment of Polycomb Repressive Complex 2 to direct gene repression. *The EMBO Journal*, *31*(3), 593-605.

Rossant, J., & Tam, P. P. L. (2009). Blastocyst lineage formation, early embryonic asymmetries and axis pattering in the mouse. *Development*, *136*(5), 701-713.

Saini, H. K., Griffiths-Jones, S., & Enright, A. J. (2007). Genomic analysis of human microRNA transcripts. *Proceedings of the National Academy of Science, USA*, *104*(45), 17719-17724.

Saito, S., Ugai, H., Sawai, K., (2002). Isolation of embryonic stem-like cells from equine blastocysts and their differentiation in vitro. *FEBS Letters*, *531*(3), 389-396.

Sander, J. D., & Joung, J. K. (2014). CRISPR-Cas systems for editing, regulating and targeting genomes. *Nature Biotechnology*, *32*(4), 347-355.

Saridey, S. K., Liu, L., Doherty, J. E., Kaja, A., Galvan, D. L., Fletcher, B. S., & Wilson, M. H. (2009). PiggyBac transposon-based inducible gene expression in vivo after somatic cell gene transfer. *Molecular Therapy*, *17*(12), 2115–2120.

Shigekawa, K., & Dower, W. J. (1998). Electroporation of eukaryotes and prokaryotes: a general approach to the introduction of macromolecules into cells. *Biotechniques*, *6*(8), 742-751.

Silva, J., Nichols, J., Theunissen, T. W., Guo, G., van Oosten, A. L., Barrandon, O., … & Smith, A. (2009). Nanog is the gateway to the pluripotent ground state. *Cell*, *138*(4), 722-737.

Silva, J., & Smith, A. (2008). Capturing pluripotency. *Cell*, *132*(4), 532-536.

Singh, A. M., Hamazaki, T., Hankowski, K. E., & Terada, N. (2007). A heterogeneous expression pattern for nanog in embryonic stem cells. *Stem Cells*, *25*(10), 2534-2542.

Singh, S., Narang, A. S., & Mahato, R. I. (2011). Subcellular fate and off-target effects of siRNA, shRNA, and miRNA. *Pharmaceutical Research*, *28*(12), 2996-3015.

Soutschek, J., Akinc, A., Bramlage, B., Charisse, K., Constien, R., Donoghue, M., … & Vornlocher, H. P. (2004). Therapeutic silencing of an endogenous gene by systemic administration of modified siRNAs. *Nature*, *432*(7014), 173-178.

Strelchenko, N., Verlinsky, O., Kukharenko, V., & Verlinsky, Y. (2004). Morula-derived human embryonic stem cells. *Reproductive Biomedicine Online*, *9*(6), 623-629.

Tada, M., Takahama, Y., Abe, K., Nakatsuji, N., & Tada, T. (2001). Nuclear reprogramming of somatic cells by in vitro hybridization with ES cells. *Current Biology*, *11*(19), 1553-1558.

Takahashi, K., & Yamanaka, S. (2006). Induction of pluripotent stem cells from mouse embryonic and adult fibroblast cultures by defined factors. *Cell*, *126*(4), 663-676.

Takaoka, K., & Hamada, H. (2012). Cell fate decisions and axis determination in the early mouse embryo. *Development*, *139*(1), 3-14.

Talbot, N. C., & Blomberg, L. A. (2008). The pursuit of ES cell lines of domesticated ungulates. *Stem Cell Research, 4*(3), 235-254.

Tarkowski, A. K., & Wroblewska, J. (1967). Development of blastomeres of mouse eggs isolated at the 4- and the 8-cell stage. *Journal of Embryology and Experimental Morphology, 18*(1), 155-180.

Tessanne, K., Golding, M. C., Long, C. R., Peoples, M. D., Hannon, G., & Westhusin, M. E. (2012). Production of transgenic calves expressing an shRNA targeting myostatin. *Molecular Reproduction and Development, 79*(3), 176-185.

Theunissen, T. W., Costa, Y., Radzisheuskaya, A., van Oosten, A. L., Lavial, F., Pain, B., … & Silva, J. C. R. (2011). Reprogramming capacity of Nanog is functionally conserved in vertebrates and resides in a unique homeodomain. *Development, 138*(22), 4853-4865.

Toyooka, Y., Shimosato, D., Murakami, K., Takahashi, K., & Niwa, H. (2008). Identification and characterization of subpopulations in undifferentiated ES cell culture. *Development, 135*(5), 909-918.

Tsukiyama, T., Asano, R., Kawaguchi, T., Kim, N., Yamada, M., Minami, N., Ohinata, Y., & Imai, H. (2011). Simple and efficient method for generation of induced pluripotent stem cells using piggyBac transposition of doxycycline-inducible factors and an EOS reporter system. *Genes to Cells, 16*(7), 815–825.

Van der Krol, A. R., Mur, L. A., Beld, M., Mol, J. N., & Stuitje, A. R. (1990). Flavonoid genes in petunia: addition of a limited number of gene copies may lead to a suppression of gene expression. *The Plant Cell, 2*(4), 291-299.

Vejlsted, M., Du, Y., Vajita, G., & Maddox-Hyttel, P. (2006). Post-hatching development of the porcine and bovine embryo – defining criteria for expected development in vivo and in vitro. *Theriogenology, 65*(1), 153-165.

Vinci, M. C. (2011). Sensing the environment: epigenetic regulation of gene expression. *Journal of Physical Chemistry & Biophysics, S3*, 1-6.

Wang, S. H., Tsai, M. S., Chiang, M. F., & Li, H. (2003). A novel NK-type homeobox gene, ENK (early embryo specific NK), preferentially expressed in embryonic stem cells. *Gene Expression Patterns, 3*(1), 99-103.

Wang, W., Lin, C., Lu, D., Ning, Z., Cox, T., Melvin, D., … & Liu, P. (2008). Chromosomal transposition of PiggyBac in mouse embryonic stem cells. *Proceedings of the National Academy of Sciences, USA, 105*(27), 9290-9295.

Wang, W., Yang, J., Liu, H., Lu, D., Chen, X., Zenonos, Z., Campos, L. S., Liu, P., … & Liu, P. (2011). Rapid and efficient reprogramming of somatic cells to induced pluripotent stem cells by retinoic acid receptor gamma and liver receptor homolog 1. *Proceedings of the National Academy of Sciences USA, 108*(45), 18283–18288.

Weber, W., Rimann, M., Spielmann, M., Keller, B., Daoud-El Baba, M., Aubel, D., Webber, C. C., & Fussenegger, M. (2004). Gas-inducible transgene expression in mammalian cells and mice. *Nature Biotechnology, 22*(11), 1440-1444.

Wells, D. N., Oback, B., & Laible, G. (2003). Cloning livestock: a return to embryonic cells. *Trends in Biotechnology, 21*(10), 428-432.

Wilson, R. C., & Dounda, J. A. (2013). Molecular mechanism of RNA interference. *Annual Review of Biophysics*, *42*, 217-239.

Wolpert, L., & Tickle, C. (2011). Evolution and development. In *Principles of Development (4th ed.)* (pp. 556-585). New York, NY: Oxford University Press.

Yamaguchi, H., Yamamoto, C., & Tanaka, N. (1965). Inhibition of protein synthesis by blasticidin S.I. Studies with cell-free systems from bacteria and mammalian cells. *Journal of Biochemistry (Tokyo)*, *57*, 667-677.

Ying, Q. L., Nichols, J., Chambers, I., & Smith, A. (2003). BMP induction of Id proteins suppresses differentiation and sustains embryonic stem cell self-renewal in collaboration with STAT3. *Cell*, *115*(3), 281-292.

Zauner, W., Kichler, A., Schmidt, W., Mechtler, K., & Wagner, E. (1997). Glycerol and polylysine synergize in their ability to rupture vesicular membranes: a mechanism for increased transferrin-polylysine-mediated gene transfer. *Experimental Cell Research*, *232*(1), 137-145.

Zhang, S., Liu, W., He, P., Gong, F., & Yang, D. (2006). Establishment of stable high expression cell line with green fluorescent protein and resistance genes. *Journal of Huazhong University of Science and Technology [Medical Sciences]*, *26*(3), 298-300.

Zhao, X. Y., Li, W., Lv, Z., Liu, L., Tong, M., Hai, T., … & Zhou, Q. (2009). iPS cells produce viable mice through tetraploid complementation. *Nature*, *461*(7260), 86-90.

Zhong, B., Zhang, Y., Yan, Y., Wang, Z., Ying, S., Huang, M., & Wang, F. (2014). MicroRNA-mediated myostatin silencing in caprine fetal fibroblasts. *PLoS ONE*, *9*(9), e107071.

Appendices

Appendix I. Plasmids

Table I. Commercial plasmids

Plasmid	Source
BLOCK-iT™ polII miR RNAi Plasmids	
pcDNA™6.2-GW/EmGFP-miR	Invitrogen (USA)
pcDNA™6.2-GW/EmGFP-miR-neg control	Invitrogen (USA)
pcDNA™1.2/V5-GW/*lac*Z control	Invitrogen (USA)
PB-CAG-rtTA	Wellcome Trust Sanger Institute (UK)
PB-TET-MKOS	Addgene (UK)
pCyL43	Wellcome Trust Sanger Institute (UK)
pEGFP-N1	Clontech Laboratories Inc. (USA)
pEF1α-Tet3G	Clontech Laboratories Inc. (USA)
pMAX	Lonza (Switzerland)
pTRE3G-mCherry	Clontech Laboratories Inc. (USA)
TOPO-TA	Invitrogen (USA)

Table II. Plasmids derived from commercial plasmids

Plasmid	Derived from
CMV-NANOG	pEGFP-N1
lacZ miRNA	pcDNA™6.2-GW/EmGFP-miR
NANOG miRNA 1	pcDNA™6.2-GW/EmGFP-miR
NANOG miRNA 2	pcDNA™6.2-GW/EmGFP-miR
NANOG miRNA 3	pcDNA™6.2-GW/EmGFP-miR
MBD3 miRNA 4	pcDNA™6.2-GW/EmGFP-miR
MBD3 miRNA 5	pcDNA™6.2-GW/EmGFP-miR
MBD3 miRNA 6	pcDNA™6.2-GW/EmGFP-miR
PB-TRE-NANOG	PB-TET-MKOS
pC-MYC	pTRE3G-mCherry

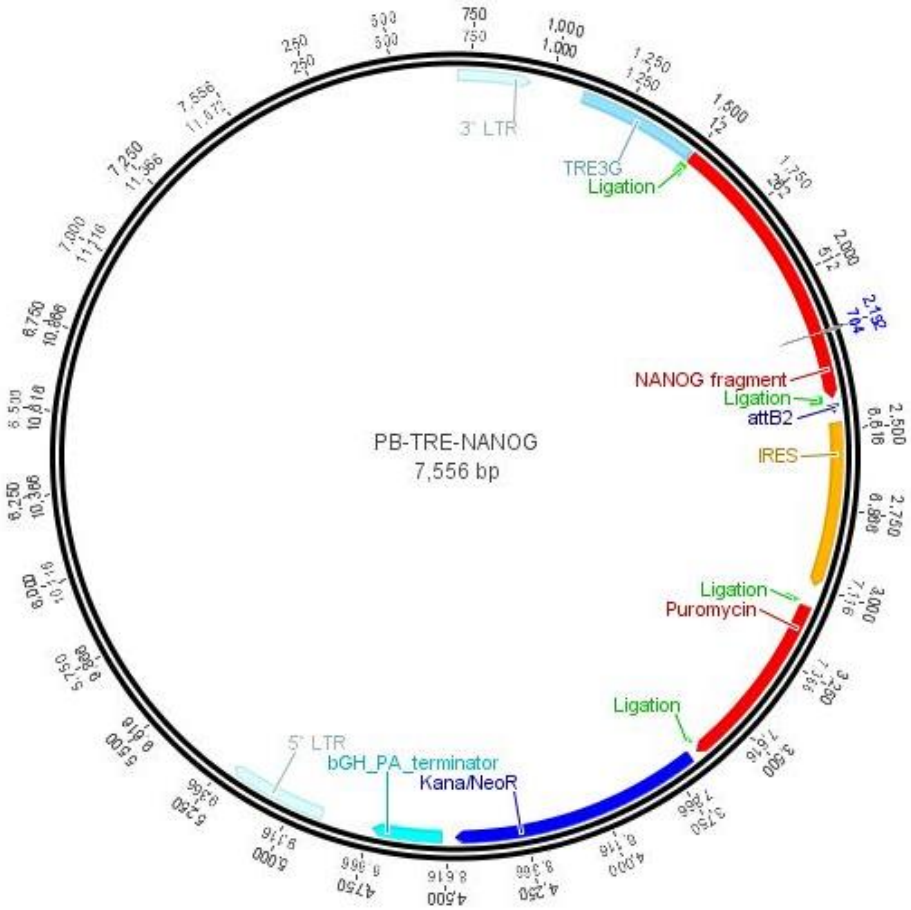

Fig. I. Plasmid Map of PB-TRE-NANOG

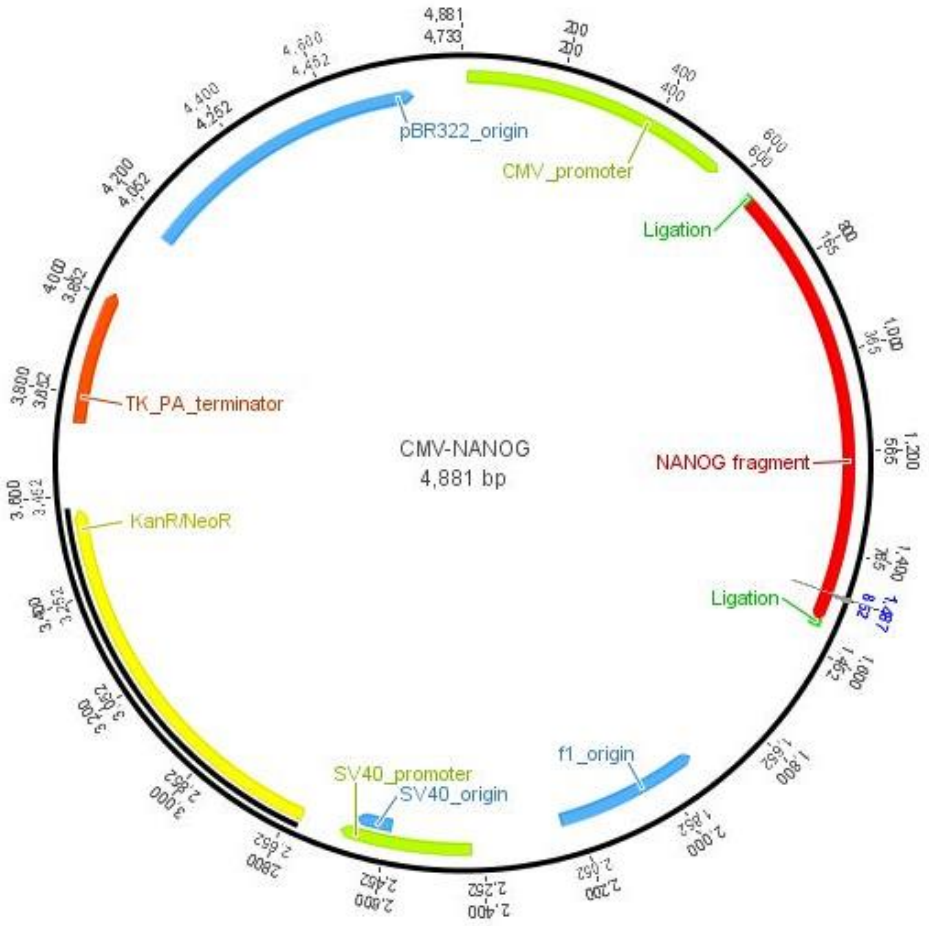

Fig. II. Plasmid Map of CMV-NANOG.

Appendix II. Oligonucleotide Sequences

Table III. MicroRNA oligonucleotides designed using RNAi designer (Invitrogen) and ordered from IDT except for the lacZ miRNA which was supplied with the Block-IT™ miRNA expression kit

miRNA	Target region	Start site	Sequence 5' to 3'
NANOG miRNA1	ORF	236	Top:TGCTGCATGGGTGAAGATTCCCTAGAGTTTTGGCCACTGACTGACTCTAGGGACTTCACCCATG Bottom:CCTGCATGGGTGAAGTCCCTAGAGTCAGTCAGTGGCCAAAACTCTAGGGAATCTTCACCCATGC
NANOG miRNA2	ORF	264	Top:TGCTGTTTGCAAGGACACGTAACTTTGTTTTGGCCACTGACTGACAAAGTTACGTCCTTGCAAA Bottom:CCTGTTTGCAAGGACGTAACTTTGTCAGTCAGTGGCCAAAACAAAGTTACGTGTCCTTGCAAAC
NANOG miRNA3	ORF	275	Top:TGCTGAGCAGATGACGTTTGCAAGGAGTTTTGGCCACTGACTGACTCCTTGCACGTCATCTGCT Bottom:CCTGAGCAGATGACGTGCAAGGAGTCAGTCAGTGGCCAAAACTCCTTGCAAACGTCATCTGCTC
MBD3 miRNA4	ORF	21	Top:TGCTGTTGCTTCGGAACTTCTTCCCGGTTTTGGCCACTGACTGACCGGGAAGATTCCGAAGCAA Bottom:CCTGTTGCTTCGGAATCTTCCCGGTCAGTCAGTGGCCAAAACCGGGAAGAAGTTCCGAAGCAAC
MBD3 miRNA5	ORF	95	Top:TGCTGTTAGCATCTTGCCCGTGCGGAGTTTTGGCCACTGACTGACTCCGCACGCAAGATGCTAA Bottom:CCTGTTAGCATCTTGCGTGCGGAGTCAGTCAGTGGCCAAAACTCCGCACGGGCAAGATGCTAAC
MBD3 miRNA6	ORF	107	Top:TGCTGTCACCTTGCTCATTAGCATCTGTTTTGGCCACTGACTGACAGATGCTAGAGCAAGGTGA Bottom:CCTGTCACCTTGCTCTAGCATCTGTCAGTCAGTGGCCAAAACAGATGCTAATGAGCAAGGTGAC
LacZ miRNA	ORF	2399	Top:TGCTGAAATCGCTGATTTGTGTAGTCGTTTTGGCCACTGACTGACGACTACACATCAGCGATTT Bottom:CCTGAAATCGCTGATGTGTAGTCGTCAGTCAGTGGCCAAAACGACTACACAAATCAGCGATTTC

Table IV. Bovine NANOG fragment that was cloned into PB-TRE-NANOG and CMV-NANOG plasmids

Full Sequence of NANOG fragment (with SalI and NotI cut sites)
ATT**GTCGAC**ATGAGTGTGGGCCCAGCTTGTCCCCAAAGCCTGCTTGGCCCCG AAGCATCCAACTCTAGGGAATCTTCACCCATGCCTGAAGAAAGTTACGTGTC CTTGCAAACGTCATCTGCTGACACCCTCGACACGGACACTGTCTCTCCTCTTC CCTCCTCCATGGATCTGCTTATTCAGGACAGTCCTGATTCTTCCACAAGCCCC AGAGTGAAACCACTGTCCCCGTCTGTGGAGGAGAGCACAGAGAAGGAAGAG ACGGTCCCGGTCAAGAAACAAAAGATTAGAACTGTGTTCTCGCAGACCCAGC TGTGTGTGCTCAATGACAGATTTCAGAGGCAGAAATACCTCAGTCTCCAGCA AATGCAAGAACTTTCCAACATCTTGAACCTCAGCTACAAGCAGGTGAAGACC TGGTTCCAGAACCAGAGAATGAAATGTAAGAAATGGCAGAAAAACAACTGG CCGAGGAATAGCAATGGCATGCCTCAGGGGCCAGCAATGGCAGAATACCCA GGCTTCTATTCCTACCACCAGGGGTGTTTGGTGAACTCTCCTGGAAACCTGCC CATGTGGGGTAACCAGACCTGGAATAACCCCACGTGGAGCAACCAGAGCTGG AACAGTCAGTCTTGGAGCAACCACTCCTGGAACAGTCAGGCCTGGTGCCCCC AAGCCTGGAATAACCAGCCTTGGAACAATCAGTTCAACAACTACATGGAGGA ATTCCTGCAGCCCGGGATCCAGCTCCAGCAGAATTCTCCCGTCTGTGATCTGG AGGCCACCCTGGGAACTGCTGGGGAAAATTATAACGTTATACAGCAAACTGT CAAGTATTTCAATTCCCAGCAGCAAATCACTGATTTATTCCCAAACTACCCTC TCAACATACAGCCTGAAGATTTGTAA**GCGGCCGC**ATA

Appendix III. Molecular Biology Reagents and Stocks

Table V. DNA and mRNA analysis reagents

Reagent	Source
1x TAE buffer	40mM tris base, 20mM acetic acid, 1mM EGTA in milliQ H_2O
1 Kb+ DNA Ladder™ (1 µg/µl)	Invitrogen (USA)
5x DNA loading buffer	30% glycerol, 1% orange G dye in milliQ H_2O
5x First-Strand Buffer [250mM Tris-HCl, 375mM KCl, 15mM $MgCl_2$]	Invitrogen (USA)
Agarose UltraPure™ Powder	Invitrogen (USA)
dATPs (10mM)	Invitrogen (USA)
dNTP mix (10mM)	Invitrogen (USA)
FastStart 10x buffer	Roche (Germany)
FastStart Taq DNA polymerase	Roche (Germany)
$MgCl_2$ (25mM)	Roche (Germany)
Random hexamer primers (50µM)	Roche (Germany)
RNaseOUT™ Recombinant Ribonuclease Inhibitor (40 U/µl)	Invitrogen (USA)
SuperScript™ III Reverse Transcriptase (200 U/µl)	Invitrogen (USA)
SYBR® Safe DNA Gel Stain	Invitrogen (USA)
T4 DNA ligase	Invitrogen (USA)
T4 DNA ligase buffer	Invitrogen (USA)
Takara Bio SYBR® Premix Ex Taq™ (Tli RNaseH Plus)	Clontech Laboratories Inc. (USA)

Table VI. Protein analysis reagents

Reagents	Source
Blocking solution	5% goat or donkey serum in PBS
Hoechst 33342 nuclear stain	Sigma Aldrich (Switzerland)
Quench solution	50mM NH_4Cl
PFA fixing solution, pH 7	4% depolymerised (w/v) PFA, 4% (w/v) sucrose, in PBS with phenol red indicator
ProLong® Diamond Antifade Mountant	Life Technologies (USA)
X-Gal staining solution, pH 7.5	20mM $K_3Fe(CN)_6$, 20mM $K_4Fe(CN)_6$, 2mM $MgSO_4$, 100mM Na_2HPO_4, 0.02% NP-40, 0.01% deoxycholic acid in milliQ H_2O

Table VII. Stock reagents

Reagent	Source
Acetic acid	Thermo Fisher Scientific (USA)
Deoxycholic acid	Sigma Aldrich (Switzerland)
Donkey Serum	GIBCO, Life Technologies (USA)
DMSO	Sigma Aldrich (Switzerland)
EDTA	Invitrogen (USA)
EGTA	Sigma Aldrich (Switzerland)
Ethanol	Thermo Fisher Scientific (USA)
Fetal Calf Serum	GIBCO, Life Technologies (USA)
Gelatin	Sigma Aldrich (Switzerland)
Goat Serum	GIBCO, Life Technologies (USA)
Glycerol	J.T. Baker® chemicals (USA)

Isopropanol	LabServ (Ireland)
KCl	Sigma Aldrich (Switzerland)
$K_3Fe(CN)_6$	BDH Ltd. (UK)
$K_4Fe(CN)_6$	Sigma Aldrich (Switzerland)
KH_2PO_4	Sigma Aldrich (Switzerland)
Methanol	Thermo Fisher Scientific (USA)
$MgCl_2$	J.T. Baker® chemicals (USA)
$MgSO_4$	Sigma Aldrich (Switzerland)
Nonidet® P 40 detergent	Sigma Aldrich (Switzerland)
Na_2HPO_4	Sigma Aldrich (Switzerland)
NaCl	J.T. Baker® chemicals (USA)
NP-40 detergent	Sigma Aldrich (Switzerland)
Orange G dye	Sigma Aldrich (Switzerland)
Ponceau-S	Sigma Aldrich (Switzerland)
SDS	Sigma Aldrich (Switzerland)
Tris base	J.T. Baker® chemicals (USA)
Triton X-100	Sigma Aldrich (Switzerland)
Tween	Bio-Rad (USA)

Appendix IV. Cell Culture Information

Table VIII. Bacterial cell culture reagents

Reagent	Source
Luria-Bertani (LB) broth (25g/L)	Invitrogen (USA)
LB agar	Invitrogen (USA)
SOC medium	Invitrogen (USA)

Table IX. Mammalian cell lines

Cell Line	Source
Bovine Embryonic Fibroblasts (BEFs)	Andria Green, AgResearch Ruakura
CCL44	ATCC (USA)
EF5-TET	Andria Green, AgResearch Ruakura
EOG-TET-NANOG	Andria Green, AgResearch Ruakura
HeLa	ATCC (USA)

Table X. Mammalian cell culture reagents

Reagent	Details	Source
Cryoprotectant Solution	FCS + 20% DMSO	Homemade
DMEM/F12 + GlutaMAX	2.438g/L Sodium bicarbonate, sodium pyruvate	GIBCO, Life Technologies (USA)
Doxycycline Hyclate	2 mg/ml stock	Sigma Aldrich (Switzerland)
Opti-MEM	2.4g/L Sodium bicarbonate, L-Glutamine	GIBCO, Life Technologies (USA)
10x PBS	80g NaCl, 2g KCl, 14.4g Na_2HPO_4, 2.4g KH_2PO_4 in 1L milliQ H_2O	Homemade
TrypLE™ Express	Used for lifting off fibroblast cells	GIBCO, Life Technologies (USA)
Trypsin-EDTA (0.25%), phenol red	Used for lifting off epithelial cells	GIBCO, Life Technologies (USA)

Table XI. Cell seeding density and media volume for various size tissue culture dishes

Tissue Culture Dish	Area (cm^2)	Seeding density	Volume of media
96-well	0.3	0.1×10^5	200 µl
48-well	0.7	0.3×10^5	400 µl
4-well/24-well	2	0.5×10^5	500 µl
12-well	4	1×10^5	1 ml
3cm/6-well	9.6	2×10^5	2 ml
6cm	28	5×10^5	5 ml
10cm	78.5	1×10^6	10 ml

Appendix V. Commercial Kits, Software, and Equipment

Table XII. Commercial kits

Kit	Source
BLOCK-iT™ Pol II miR RNAi Expression Vector Kit	Invitrogen (USA)
Lipofectamine® LTX with PLUS™ reagent	Invitrogen (USA)
Neon™ Transfection System	Invitrogen (USA)
PureLink® HiPure Plasmid Filter Maxiprep Kit	Invitrogen (USA)
PureLink® HiPure Plasmid Filter Miniprep Kit	Invitrogen (USA)
*RNA*Gem Tissue	ZyGEM (NZ)
TOPO-TA Cloning® Kit	Invitrogen (USA)
Wizard® SV Gel & PCR Clean-Up System	Promega (USA)

Table XIII. Software

Software	Source
BLAST	NCBI (USA)
BLOCK-iT™ RNAi Designer	Invitrogen (USA)
Chromas Lite	Technekysium pty ltd (Australia)
Geneious	Biomatter Ltd (NZ)
ImageJ	NIH (USA)
LightCycler®	Roche (Germany)
Microsoft Excel 2010	Microsoft (USA)
Quantity One	BioRad (USA)
Spot Basic	Spot Imaging Solutions (USA)

Table XIV. Equipment

Equipment	Manufacturer
Biofuge fresco centrifuge	Heraeus (Germany)
Biofuge primo centrifuge	Heraeus (Germany)
Clean bench fume hood	Pall Corporation (USA)
Dual-intensity transilluminator	UVP (USA)
Eppendorf centrifuge 5417C	Eppendorf (Germany)
Eppendorf Mastercycler gradient PCR machine	Eppendorf (Germany)
EVOS fluorescence microscope	AMG (USA)
Gel Doc 2000	Bio-Rad (USA)
Infors HT ecotron incubator (Bacterial culture)	Infors HT (Switzerland)
LC carousel centrifuge 2.0	Roche (Germany)
Leica DFC290 light microscope	Leica (Germany)
LightCycler 2.0	Roche (Germany)
Minispin plus centrifuge	Eppendorf (Germany)
Nanodrop ND-1000	Thermo Scientific (USA)
Neon™ transfection system	Invitrogen (USA)
Nikon TMS light microscope	Nikon (Japan)
Olympus BX50 fluorescent microscope	Olympus (Japan)
Sanyo incubator (Transformation plates)	Sanyo (Japan)
Sorvall RC5C Plus centrifuge	Thermo Scientific (USA)
Spot RT3 camera	Spot Imaging Solutions (USA)
Sub-cell gel tank	Bio-Rad (USA)
Thermo Forma series II water jacketed CO_2 incubator	Thermo Scientific (USA)